Università degli Studi di Padova

Sede Amministrativa: Università degli Studi di Padova

Dipartimento di Biologia

SCUOLA DI DOTTORATO DI RICERCA IN BIOCHIMICA E BIOTECNOLOGIE

INDIRIZZO IN BIOTECNOLOGIE

CICLO XXIII

A POSSIBLE ROLE OF SUPEROXIDE DISMUTASE 2 IN THE PATHOGENESIS OF PARKINSON DISEASE

Direttore della Scuola: Ch.mo Prof. Giuseppe Zanotti

Coordinatore d'indirizzo: Ch.mo Prof. Giorgio Valle

Supervisore: Ch.mo Prof. Mariano Beltramini

Dottorando: Elisa Belluzzi

Contents

Abstract **5**

Riassunto **9**

1. Introduction **13**

1.1 Parkinson's disease **13**

1.1.1 Clinical features and treatments 13

1.1.2 Nervous circuits implicated: the basal ganglia 15

1.2 Etiology of Parkinson disease 17

1.2.1. Genetic Parkinson disease 18

1.2. 2 Sporadic Parkinson: molecular mechanisms 21

1.3 Aim of the thesis 37

2. Materials and Methods **39**

2.1 Molecular Biology techniques for SOD2 cloning and Mutagenesis **39**

2.1.1 Expression Vector pET28a+ 39

2.1.2 Competent cells 41

2.1.3 Plasmid DNA extraction 42

2.1.4 DNA quantification 43

2.1.5 Agarose gel electrophoresis 43

2.1.6 Polymerase chain reaction (PCR) 44

2.1.7 DNA purification 46

2.1.8 DNA enzymatic restriction 46

2.1.9 Vector dephosphorylation 47

2.1.10 DNA Ligation 47

2.1.11 Bacterial transformation 48

2.1.12 Bacterial colonies screening 48

2.1.13 DNA sequencing 49

2.1.14 DNA mutagenesis 49

2.2 Biochemistry and biophysical techniques **51**

2.2.1 Cell growth for proteins expression **51**
2.2.2 Protein purification 51
2.2.3 Protein purification with Histidine-tag 52
2.2.4 Protein quantification 53
2.2.5 Protein concentration 53
2.2.5 Sodium dodecyl sulphate polyacrylamide gel electrophoresis (SDS-PAGE) 54
2.2.6 Native polyacrylamide gel electrophoresis (Native-PAGE) 55
2.2.7 Superoxide dismutase activity staining on native-PAGE 56
2.2.8 Determination of manganese concentration 57
2.2.9Reaction of dopamine quinones with superoxide dismutase 2 57
2.2.10 UV-visible spectroscopy of dopamine oxidation 58
2.2.11 Reversed-phase HPLC chromatography (RP-HPLC) and Mass Spectrometry analysis 58
2.2.12 Detection of quinoproteins by redox-cycling staining 59
2.2.13 Two-dimensional gel electrophoresis (2-DE or 2-D electrophoresis) 60
2.2.14 Superoxide dismutase enzymatic activity assays 61
2.2.15 Limited proteolysis 64
2.2.16 Circular dichroism (CD) 64
2.2.17 Radioactivity assay 65
3. Results 67
3.1 Cloning of the cDNA of Superoxide dismutase 2 67
3.2 SOD2 wild-type expression and purification 70
3.2.1 SOD2 expression and purification 70
3.2.2 His-tag SOD2 expression and purification 73
3.2.3 Protein characterization 76
3.3 Covalent modification of SOD2 induced by dopamine-quinones (DAQs) 78
3.3.1 UV-visible Spectroscopy 79
3.3.2 Reversed-phase HPLC and mass spectrometry analysis 81

3.3.3 Gel electrophoresis characterization of the interaction of SOD2 with DAQs 85
3.3.4 Superoxide dismutase enzymatic activity 89
3.4 Reactivity of SOD2 cysteines toward DAQs 95
3.4.1 Limited proteolysis 95
3.4.2 Site directed mutagenesis of cysteine residues of human SOD2 98
3.4.3 Interaction of SOD2 cysteine mutants with DAQs 101
3.5 Structural modifications induced by DAQs on SOD2 109
3.6 Protein crystallization optimization 112
4. Discussion and conclusion 115
Appendix 1 121
Appendix 2 123
1. Culture media 123
2. Bacteria strains of *Escherichia coli* 123
References 125

Abstract

Parkinson disease is the second most common neurodegenerative disorder after Alzheimer disease. Less than the 5% of the cases are associated with recessive or dominant Mendelian inheritance. It is characterized by tremor at rest, bradykinesia, postural instability and rigidity. The pathogenesis is still unknow but evidence suggests multifactorial mechanisms. In particular, mitochondrial dysfunction and oxidative stress are believed to have a central role in the pathology.

The hallmark of PD is the loss of dopaminergic neurons of substantia nigra pars compacta, hence dopamine may play an important role in the etiology due its metabolism. In fact, the cytosolic oxidation of dopamine may be very deleterious to neurons. This neurotransmitter, once synthesized, is sequestered in acid vesicles. However, mitochondrial dysfunction, in particular the inhibition of the complex I, causes ATP depletion, which can perturb the H^+-ATPase necessary to drive the dopamine into vesicles. The consequence will be a redistribution of the neurotransmitter in cytoplasm, where it can auto-oxidize spontaneously at alkaline pH yielding reactive dopamine quinones (DAQs) and reactive oxygen species (ROS) contributing to oxidative stress. DAQs are suggested to be involved in dopaminergic neurotoxicity because they can form adducts with cysteine residues exposed at the surface of proteins to generate 5-S-cysteinyl-DA. The covalent modification of proteins could lead to the impairment of their functional properties.

The cells have different mechanisms to protect from oxidative stress: catalase, glutathione peroxidise and superoxide dismutase (SOD). The function of SOD enzymes consists in the dismutation of superoxide anions to hydrogen peroxide and molecular oxygen. Among the three different isoforms of SOD, SOD2 is particularly important due its mitochondrial localization. Mitochondria are in fact the main source of superoxide anions.

The aim of this thesis is to investigate if SOD2 is a target of DAQs in vitro, the effects of this interaction on the enzymatic function of the protein and the residue/s target of DAQs.

The starting point was the cloning of the cDNA of the human SOD2 in the pET28a+ vector. Since *E.coli* present 3 different SOD that could potentially interfere with the purification, a second cloning was obtained, in which the cDNA was inserted downstream a cleavable His-tag. A protocol of SOD2 purification

was set up but a control purification, where the cells were transformed with empty vector, led to purify an endogenous SOD of *E.coli* demonstrating that a *E.coli* SOD co-purify with the human recombinant enzyme. To avoid the co-purification, a protocol of purification was optimized for the protein with the His-tag leading to obtain 40-60 mg of protein per 1 liter of culture.

The interaction between SOD2 and DAQs was investigated using different biochemical and biophysical techniques. Dopamine oxidation was induced by the addition of tyrosinase, which prevented the formation of radical species normally produced during dopamine auto-oxidation. It was verified that the protein did not interact with tyrosine residues of SOD2. The protein was incubated with dopamine at different ratio SOD2:dopamine in the presence of tyrosinase, following by UV-vis spectroscopy the formation of DAQs. The interaction of these products with the protein was studied by mass spectrometry analysis, which revealed the formations of new species whose molecular masses are compatible with the covalent modification of one cystiene residue with dopamine-o-quinone and with the indole 5,6 quinone. Other species were detected, however they were not attribuible to a specific DAQ, hence they might result from more complex interactions. Moreover, the presence of +287.8 Da product suggested the interaction of both the cystiene residues. SDS-PAGE analysis of the reaction products revealed the presence of the protein dimer and aggregates. Native-PAGE showed multiple bands and aggregates upon the interaction with DAQs. The multiple band profile was assigned to the combination of tetramers with monomers of SOD2 with different modifications (as demonstrated by mass analysis). This was supported by 2 dimensional gel, where at least 4 products of SOD2 with different isoelectric point appeared. Activity assay indicated inhibition of proten covalently modified by DAQs. Hence, pulse radiolysis measurements were performed to determine the kinetic parameters of the dismutation reaction. Data are currently under processing.

To identify the site of DAQs interaction, the cysteine residues were mutagenized obtaining the following mutated proteins: C140A, C196A and C140A/C196A. Incubation of the mutants incubated ^{14}[C]-labeled dopamine demonstrated that the cysteine 196 was the primary target of DAQs. This result was confirmed also by mass spectrometry. The enzymatic activity of the mutant C140A upon interaction of dopamine proved to be lower in comparison with the unmodified protein.

A weakly positive radioactivite signal was found also in association with the mutant C196A and the C140A/C196A suggesting secondary site of DAQs interaction. Since two covalent DAQ-derivatives were found by mass spectrometry after the incubation of the mutant C140A with dopamine, the

existence of a second site of interaction probably another nucleophilic residue is suggested.

Structural changes of SOD2 upon DAQs modification suggested protein precipitation and a possible change in tertiary structure. HFEPR spectra did not show any significant changes in metal coordination.

The results presented in this thesis demonstrate that SOD2 is covalently modified by DAQs in vitro. This suggests a possible role of SOD2 in the PD. The idea is that SOD2 can be covalently modified by DAQs in mitochondria. This would increase the oxidative stress in mitochondria, due to the decrease of dismutase activity of the target protein, ultimately determining mitochondrial dysfunction and contributing to the neuron cell death.

Riassunto

La malattia di Parkinson è la malattia neurologica degenerativa più diffusa dopo la malattia di Alzheimer. Meno del 5% dei casi presenta una correlazione genetica (ereditarietà autosomica dominante o recessiva). I sintomi principali caratteristici sono tremore a riposo, bradicinesia, instabilità posturale e rigidità. L'eziologia rimane ancora sconosciuta ma evidenze sperimentali suggeriscono che la malattia sia multifattoriale. In particolare due fattori, disfunzione mitocondriale e stress ossidativo, sembrano avere un ruolo chiave nella patogenesi.

La caratteristica della malattia di Parkinson è la perdita dei neuroni dopaminergici della substantia nigra pars compacta. Questo fa presupporre che la dopamina abbia un ruolo importante nell'eziologia attraverso il suo metabolismo. Infatti, l'ossidazione citosolica della dopamina può contribuire alla tossicità neuronale. Questo neurotrasmettitore, una volta sintetizzato, in condizioni normali è sequestrato nelle vescicole sinaptiche. Tuttavia, la disfunzione mitocondriale, in particolare l'inibizione a livello del complesso I riscontrata nella malattia di Parkinson, porta a causare una diminuzione dei livelli di ATP. Questo può influenzare il trasporto di dopamina nelle vescicole che è ATP-dipendente. La conseguenza sarebbe una ridistribuzione del neurotrasmettitore nel citoplasma, dove può auto-ossidarsi spontaneamente a pH alcalini producendo dopamino-chinoni (DAQs) e specie reattive dell'ossigeno (ROS) che contribuiscono allo stress ossidativo. E' stato suggerito che i DAQs possano essere coinvolti nella neurotossicità dei neuroni dopaminergici. Questo perchè possono interagire con le cisteine esposte sulla superficie di proteine generando 5-S-cisteinil-DA e la loro modificazione covalente da parte dei DAQs può compromettere la funzionalità e stabilità di queste proteine.

Le cellule possiedono differenti meccanismi per proteggersi dallo stress ossidativo: catalasi, glutatione perossidasi e superossido dismutasi (SOD). La funzione delle SOD consiste nel dismutare l'anione superossido a perossido d'idrogeno e ossigeno molecolare. Tra le tre isoforme di SOD presenti nell'uomo, la SOD2 è particolarmente importante a causa della sua localizzazione all'interno del mitocondrio.

Lo scopo di questa tesi è quello di investigare se la SOD2 sia un target dei DAQs in vitro, gli effetti di questa interazione sull'attività enzimatica della proteina e il/l residuo/i target dei DAQs.

Il punto di partenza è stato il clonaggio del cDNA della SOD2 umana nel vettore pET28a+. Dato che *E.coli* possiede tre differenti SOD che potrebbero

interferire con la purificazione, un secondo clonaggio è stato effettuato, clonando l'inserto a valle di un histidine-tag. È stato messo a punto un protocollo di purificazione della SOD2 ma la purificazione di controllo, dove le cellule erano state trasformate con il vettore senza l'inserto, ha portato alla purificazione di una SOD endogena di *coli*. Questo ha dimostrato che una SOD di *coli* co-purificava con l'enzima umano ricombinante. Per evitare questo, un protocollo di purificazione è stato ottimizzato con l'His-tag ottenendo 40-60 mg di proteina da un litro di coltura.

L'interazione tra la SOD2 e i DAQs è stata indagata utilizzando differenti tecniche biochimiche e biofisiche. L'ossidazione della dopamina è stata indotta dall'aggiunta di tirosinasi, che previene la formazione di specie radicaliche normalmente prodotte durante la sua auto-ossidazione. È stato verificato che la tirosinasi non interagisce con i residui tirosinici della proteina. La SOD2 è stata incubata con differenti rapporti SOD2:dopamina in presenza di tirosinasi, seguendo la formazione dei DAQs con spettroscopia UV-visibile. L'interazione di questi prodotti con la proteina è stata studiata tramite spettrometria di massa, che ha rilevato la formazione di nuove specie le cui masse erano compatibili con la modificazione covalente di una cisteina con il dopamino-o-chinone e con l'indolo 5,6 chinone. Altre specie sono state identificate ma non è stato possibile attribuirle ad uno specifico chinone, quindi queste potrebbero essere il risultato di interazioni più complesse. Inoltre, la presenza di una doppia modifica ha suggerito la possibile interazione di entrambe le cisteine della proteina. Analisi su SDS-PAGE dei prodotti di reazione ha mostrato la presenza di dimeri di proteina e aggregati. Native-PAGE ha rilevato un pattern di bande multiple e aggregati, dopo interazione con i chinoni. Il profilo delle bande multiple è stato attribuito alla combinazione monomeri di SOD2 con differenti modifiche (come dimostrato dalle analisi di spettrometria di massa) associati a formare tetrameri. Questo è supportato dal profilo nel gel bidimensionale, dove sono presenti 4 prodotti di SOD2 con differente punto isoelettrico. Il saggio enzimatico ha rilevato che la proteina modificata covalentemente dai DAQs risulta essere inibita. Misure di radiolisi pulsata sono state effettuate per determinare i parametri cinetici della reazione di dismutazione.

Per identificare i siti di interazione dei DAQs, le cisteine sono state mutagenizzate in alanine ottenendo i seguenti mutanti: C140A, C196A e C140A/C196A. L'incubazione dei mutanti con ^{14}[C]-dopamina ha dimostrato che il target primario dei DAQs è la cisteina 196. Questo risultato è stato confermato anche da analisi di spettrometria di massa. L'attività enzimatica del mutante 140 dopo interazione con DAQs risulta essere minore rispetto alla proteina non modificata.

Un debole segnale di radioattività è stato trovato anche in associazione con il mutante 196 e il doppio. Ciò suggerisce la presenze di un sito di interazione con i chinoni secondario. Dato che due modificazioni dovute a DAQs sono state trovate incubando il mutante C140A, si deduce che il secondo sito di interazione coinvolga un altro residuo nucleofilo.

Cambiamenti strutturali della SOD2 suggeriscono precipitazione della proteina un possibile cambiamento della struttura terziaria. Inoltre modificazioni rilevanti nella coordinazione del metallo non sono state rilevate mediante HFEPR.

I risultati presentati in questa tesi dimostrano che la SOD2 è un target dei DAQs in vitro suggerendo l'idea che la SOD2 possa essere coinvolta nella malattia di Parkinson. Una volta modificata dai DAQs, lo stress ossidativo aumenterebbe nei mitocondri, a causa della inibizione dell'attività dismutasica dell'enzima, determinando disfunzione mitocondriale e contribuendo alla morte neuronale.

1. Introduction

In the monograph "*An Essay of the Shaking Palsy*", James Parkinson (1755-1824) described for the first time a pathology on the basis of a clinical study carried out in 1817 on 6 patients (Parkinson, 1817). He reported: *"Involuntary tremulous motion, with lessened muscular power, in parts not in action and even when supported; with a propensity to bend the trunk forwards, and to pass from a walking to a running pace: the senses and intellect being uninjured*." In acknowledgment of James Parkinson's description, Jean Martin Charcot, the father of neurology, proposed that the syndrome should be called Parkinson's disease (Lees, 2009). Almost 200 years since the first description, many progress, mainly in the last 10 years, have been achieved in understanding the aetiopathogenesis of the disease but there are still "*missing pieces in the Parkinson's disease puzzle*" (Obeso et al., 2010).

1.1 Parkinson's disease

1.1.1 Clinical features and treatments

Parkinson' s disease (PD) is a progressive neurodegenerative disease and the most prevalent type of parkinsonism. Parkinsonism is used to define a clinical syndrome caused by lesions of the basal ganglia. PD is the second most common neurodegenerative disorder after Alzheimer's disease (AD). The incidence of the pathology increases markedly with age: from 20 cases per 100,000 individuals overall in average to 120/100,000 at age 70 (Dauer, 2003). The onset of PD is gradual and the earliest symptoms might be misinterpreted or unnoticed for a long time (Lees, 2009). The main clinical phenotype is parkinsonism that is resting tremor with a frequency of 4–6 Hz. Other motor symptoms are present: rigidity, bradykinesia (slowness of movements), akinesia (absence of normal unconscious movements), hypokinesia (reduction in movement amplitude) and impairment of postural instability reflex (Fahn, 2003).

Also non motor clinical manifestation appear such as micrographia, hypomimia (face without expression), hypophonia (decreased voice volume), dementia, sleep disorders insomnia, restless legs and periodic limb movements) autonomic and gastrointestinal symptoms (bladder disturbances, sexual dysfunctions, constipation, chewing and swallowing difficulties, drooling of saliva are common complaints (Chaudhuri et al., 2006).

The pathology is characterized by the death of dopaminergic neurons of substantia nigra pars compacta (SNpc) (fig. 1.1) accounting for the motor symptoms and in some cases the presence of Lewy bodies (LB) and Lewy neuritis (LN), described for the first time by Friederich Lewy in 1912. Lewy bodies are eosinophilic cytoplasmatic inclusions composed by insoluble aggregates of different proteins, mainly alpha synuclein (Spillantini et al., 1997) and ubiquitin (fig.1.2). Whether these inclusions are toxic or neuroprotective is still on debate (for a review on Lewy bodies see Shults, 2006).

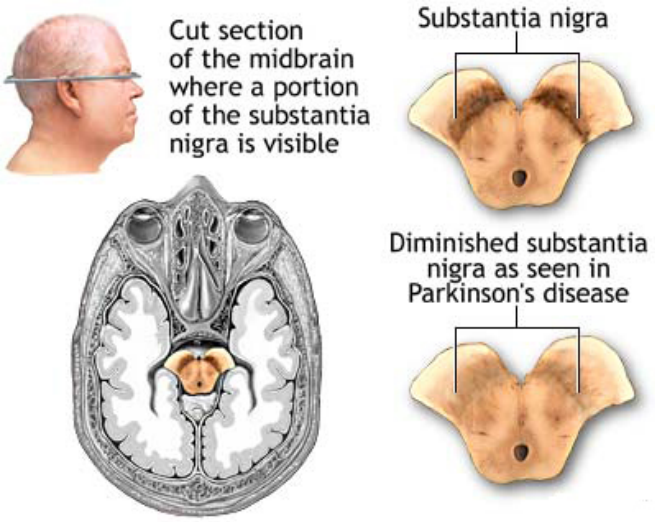

Figure 1.1. Degeneration of dopaminergic neurons in Parkinson disease.
The photograph on the top right-handed corner of the picture shows the normal pigmentation of the dopaminergic neurons of substantia nigra caused by the presence of neuromelanin. On the bottom right-handed corner is appreciable the neurodegeneration of dopaminergic neurons by the depigmentation in Parkinson disease.

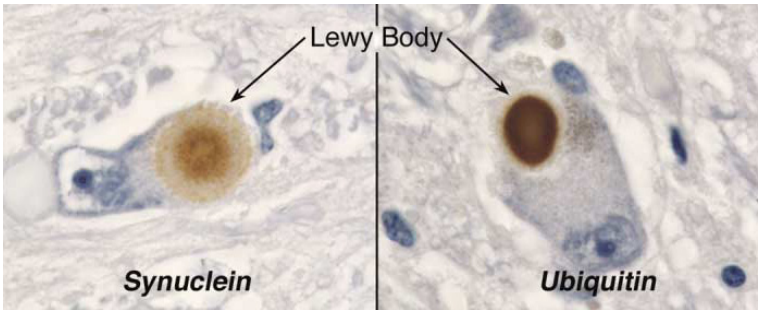

Figure 1.2. Immunohistochemical labeling of Lewy bodies.
On the right: immunostaining with an antibody against ubiquitin. On the left: immunostaining for α-synuclein. (Dauer and Przedborski, 2003).

Neurodegeneration occurs also in other regions: noradrenergic neurons in the locus caeruleus and serotoninergic neurons in the dorsal raphe nucleus (Braak et al., 2004; Shen and Cookson, 2004).

At the onset of the symptoms, the dopamine depletion is 80% and the 60% of SNpc neurons have already been lost. Hence, the therapeutic treatment of Parkinson's disease is based on the administration of dopaminergic drugs in order

to minimize the motor symptoms. These drugs are: dopamine agonists (such pramipexole and ropinerole) activating pre- and postsynaptic dopamine receptors: MAO-B (selegiline) and COMT inhibitors reducing dopamine catabolism; the precursor of dopamine levodopa (L-dopa). But the use of L-dopa after some years gives others motor complications: dyskinesias (involuntary movements) or wearing off (the return of the symptoms) (Schapira, 2009). Otherwise, a surgical treatment called deep brain stimulation (DBS) has replaced the older technique of lesioning specific brain's regions. DBS consists in the stimulation of specific brain's targets such for example the subthalamic nucleus, the internal segment of globus pallidus or the ventral intermediate nucleus of thalamus. This treatment improves the quality of life but do not slow down the progression of the pathology (Fahn, 2003).

1.1.2 Nervous circuits implicated: the basal ganglia

The basal ganglia consist of four nuclei: the striatum (composed by the putamen, the caudate nucleus and ventral striatum), the globus pallidus (divided in the internal and external segments), the substantia nigra (divided in pars reticulata and pars compacta) (fig.1.3).

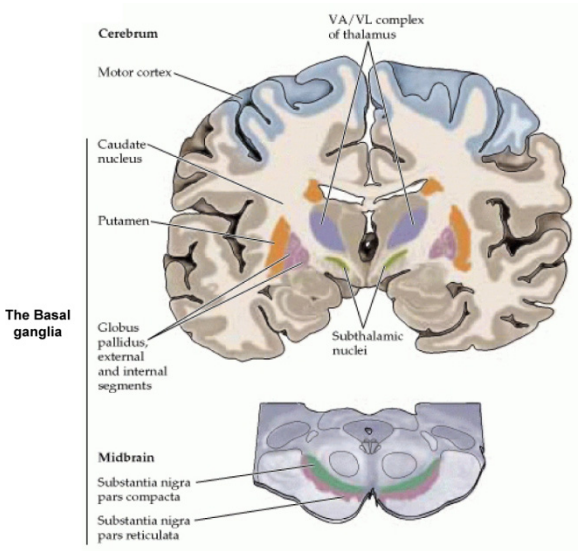

Figure 1.3. The structures involved in the basal ganglia circuit. *Adapted from (Dale Purves, 2001)*

The cerebral cortex projects (glutamatergic neurons) to the spiny neurons of striatum, which receives also excitatory projections from the thalamus and from brain stem (dopaminergic input from the midbrain and serotonergic projections from the raphe nuclei). The striatum projects to the substantia nigra pars reticolata and to the internal segment of the globus pallidus (GABAegic projections). The neurons of substantia nigra pars reticolata inhibit the superior colliculus, while those of the internal segment of globus pallidus inhibit two groups of neurons

present in the thalamus: the anterior ventral nucleus and the lateral ventral nucleus. Thalamus constantly stimulates the motor cortex via glutamatergic projections. In absence of movements, cortical neurons are silent but neurons of internal segment of globus pallidus and the substantia nigra pars reticulata are active and thus can inhibit the thalamic neurons. Otherwise, when the cortex neurons excite the striatum, they inhibit the downstream neurons, hence the thalamus is disinhibited and can excite motor cortex neurons facilitating the movement. This is the direct pathway of the basal ganglia, but there is another one called the indirect pathway (fig. 1.4) in which spiny neurons of striatum project first to the external segment of globus pallidus and from there to internal segment and to the subtalamic nucleus (GABAegic projections).

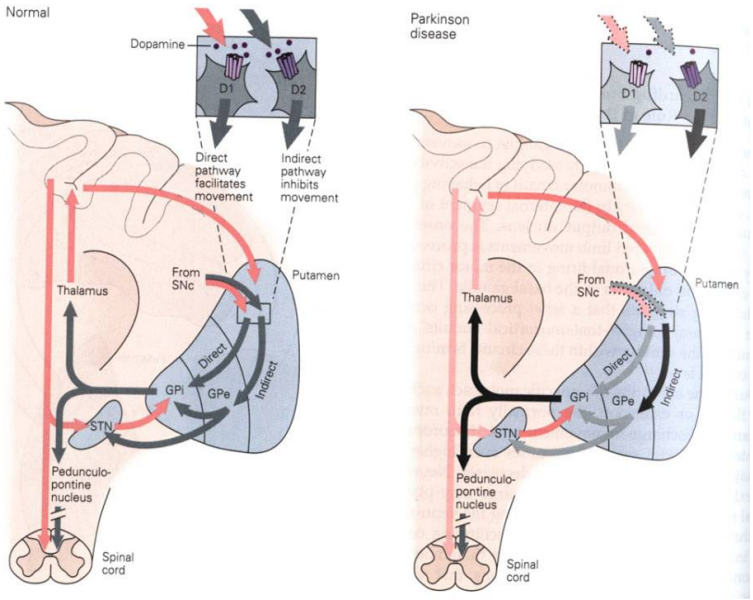

Figure 1.4. The basal ganglia-thalamocortical circuit under normal condition (on the left) and in Parkinson disease (on the right). *Excitatory connections are shown as pink arrows, while inhibitory connection as gray and black arrows. Abbreviations: Substantia nigra pars compacta (SNc), internal segment of globus pallidus (GPi), external segment globus pallidus (GPe), subthalamic nucleus (STN). Under normal condition the indirect and direct pathway modulated by dopaminergic neurons of SNc. In Parkinson disease the modulation of SNc is absent because of the neurodegeneration, hence there are activity changes in the circuit which lead to an increase of thalamus inhibition and difficult to start movements. The changes in activity are shown as changes in darkness of arrows: lighter arrows indicate a decrease in activity, while darker increased activity. (Eric R. Kandel, 2000)*

The subtalamic nucleus is connected to the internal segment of globus pallidus and to the pars reticolata via excitatory glutamatergic projections. Once the indirect pathway is activated by cortical projections, neurons of external segment of globus pallidus (normally active) are inhibited, thus the subtalamic nucleus is

disinhibited and stimulates (excitatory projection) the internal segment of globus pallidus. The final result is the inhibition of thalamus and the inhibition of the movement. In other words, the direct pathway provides a positive feedback whereas the indirect pathway a negative feedback in the neural circuit between the basal ganglia and the thalamus, which potentiate the inhibitory efficiency of the basal ganglia. On these two pathways neurons of substantia nigra pars compacta play an important role. Dopaminergic neurons of substantia nigra pars compacta project to the spiny neurons having a different effect on the two pathway: excitatory on the direct while inhibitory on the indirect. The reason is due to the presence of two dopamine types of dopaminergic receptors: D1 type receptor in the direct, while D2 receptor in the indirect (fig. 1.4) (Dale Purves, 2001; Eric R. Kandel, 2000). Both receptors are coupled to G-proteins, but D1 receptor activates adenylyl cyclase, while D2 inhibits adenylyl cyclase resulting in a different cellular response (for a review see Vallone et al., 2000). Even if there is a different action on the two pathways, dopaminergic input leads to the same effect that is the reduction of the inhibition of the thalamocortical circuit facilitating the movement.

In PD the loss of dopaminergic neurons causes an increase of the inhibition of the basal ganglia (fig. 1.4). Hence the activity output of the nuclei increases and this in turn increases inhibition of the thalamus, so the activation of cortical neurons (projecting to motor neurons) results more difficult leading to impaired movements (Dale Purves, 2001; Eric R. Kandel, 2000).

1.2 Etiology of Parkinson disease

The etiology of PD is still obscure, because multiple factors contribute to the disease: genetic predisposition, environmental toxins, oxidative stress, protein aggregation mitochondrial and proteasome dysfunction. Moreover, there are other risk factors associated with PD onset such as age. It has been reported that there is an inverse relationship between incidence of smoking and PD occurance (Nuti et al., 2004; Ritz et al., 2007) and between caffeine consumption and PD (Ascherio et al., 2001; Costa et al., 2010; Ross et al., 2000). A protective effect of nonsteroidal anti-inflammatory drugs (NSAIDs) have been proposed (Ton et al., 2006; Wahner et al., 2007) and it has been shown a combined effect of reduction of risk in individuals who were exposed to all three factors (Powers et al., 2008).
The discovery of genes involved in the pathology provided new opportunities to understand the molecular mechanism of PD. Less than the 5% of the PD cases are genetically linked, while the others are referred as sporadic or idiopathic. Positional cloning and linkage studies have led to the identification of several

genetic loci involved in PD. Among these, five genes have been clearly identified and associated with genetic PD: alpha synuclein (PARK1,PARK4), parkin (PARK2), Phosphatase and tensin homologue (PTEN)-induced putative kinase 1 (PARK6), DJ-1 (PARK7) and leucine-rich repeat kinase 2 (LRRK2) (PARK8) (reviewed by Thomas and Beal, 2007; Yang et al., 2009).

1.2.1. Genetic Parkinson disease

1.2.1.1 Alpha synuclein (PARK1 and 4)

Alpha synuclein was the first gene discovered to be linked to autosomal dominant PD. In particular three mutations (A30P, E46K, A53T), duplication and triplication of the gene have been associated with the pathology (Kruger et al., 1998; Polymeropoulos et al., 1997; Zarranz et al., 2004). The gene encodes for a small protein (14,5 kDa, 140 aminoacids) natively unfolded. Its function is still not known but it is suggested to be involved in vescicular neurotransmitter trafficking since it can bind to lipid vescicles acquiring alpha helix conformation. The protein can form oligomeric species and fibrils (for reviews on alpha synuclein see Auluck et al., 2010; Goedert, 2001; Lotharius and Brundin, 2002). Alpha synuclein is also the major component of Lewy bodies, the proteinaceous inclusions, found in patient's brains (fig. 1.2) reviewed by (Shults, 2006).

1.2.1.2 Parkin (PARK2)

Parkin is a E3 ubiquitin protein ligase (Shimura et al., 2000) of 465 aminoacids with a molecular weight of 52 kDa. Several mutations caused the pathology, accounting for almost 50% of cases of autosomal recessive juvenile PD. This protein is involved in the ubiquitin-proteasome system (UPS) where ubiquitin is firstly activated by E1 (activating enzyme), then is transferred to an E2 (conjugating system) that directly gives ubiquitin to the target protein. Otherwise, a third enzyme, E3 (ligating enzyme) such parkin is required to transfer ubiquitin from E2 to the target. So, a polyubiquitin chain is attached to the target protein and it recognized by the proteasome and degradated. Since ubiquitinated proteins are found in Lewy bodies, it is thought that the ubiquitin-proteasome system (UPS) may play an important role in the pathology (for a review see Tanaka et al., 2004).

1.2.1.3 Phosphatase and tensin homolog (PTEN)-induced kinase 1 (PINK1) (PARK6)

PINK 1 is a putative serine/threonine kinase (528 aminoacids) with mitochondrial localization, although a N-terminal processed form is present in the cytosol (Weihofen et al., 2008). Many mutations in this gene have been reported to be involved in the disease with autosomal recessive inheritance, all of these have effects on protein stability (Beilina et al., 2005). The physiological function of Pink1 is unknown but its localization and the presence of a kinase domain suggest that it may be involved in the phosphorilation of mitochondrial proteins such parkin as response to oxidative stress (Kim et al., 2008).

1.2.1.4 DJ-1 (PARK7)

DJ-1 encodes for a 189 aminoacid protein ubiquitously expressed and originally identified as a candidate oncogene (Nagakubo et al., 1997). As for PINK, a subset of mutations have been described causing the pathology (Bonifati et al., 2003), some of these disrupt the dimeric structure of the protein (Olzmann et al., 2004). Its function is not clear but it has been proposed to be involved in cellular response to oxidative stress, since it can translocate into the mitochondria in response to oxidative stress (reviewed in Lev et al., 2006)). In particular, it has been demonstrated that DJ-1 functions as a redox-sensitive molecular chaperone activated in an oxidizing environment (Shendelman et al., 2004). Moreover, DJ-1 exhibits a change in the isoeletric point (an acidic shift) after exposure to oxidative stress (Canet-Aviles et al., 2004)

1.2.1.5 Leucine-rich repeat kinase 2 (LRRK2) (PARK8)

LRRK2 is a complex multi domain kinase of 286 kDa (2527 aminoacids) forming dimers. The first mutation was reported in 2002 (Funayama et al., 2002) but in the last years several mutations were associated to PD. These mutations are spread throughout the gene and do not lead to a loss of enzymatic function (for a review see Mata et al., 2006). The disease appears to be dominant but the penetrance is incomplete (Latourelle et al., 2008). Lewy bodies are not always present. The pathology linked to LRRK2 mutations is pleomorphic, due to this fact it is thought that the protein might be implicated in multiple signaling pathway (Zimprich et al., 2004).

1.2.1.6 Other genes and genetic loci

Besides the 5 genes briefly listed above, other genes and genetic loci (see table 1) have been identified but their correlation with PD is not clear. These genes are: Ubiquitin Carboxyl-Terminal Hydroxylase (UCHL-1) (PARK5), ATP13A2 (PARK9), Omi/HtrA2 (PARK13). UCHL-1 protein is involved in the proteasome system, as it is catalyze the hydrolysis of polymeric ubiquitin chains. It's presence in Lewy bodies is controversial (for a review on UCH-L see Healy et al., 2004). One mutation (I93M) of UCHL-1 has been related to PD in a German family (Leroy et al., 1998) but if this mutation is really pathogenic remains still unclear because it has not been found in other families. A polymorphism (S18Y) has been found to be associated with a reduced risk for Parkinson's disease (Lincoln et al., 1999) but the role is controversial (Hutter et al., 2008; Ragland et al., 2009). Whether ATP13A2 is associated with PD is not so clear, there are contrasting studies (Di Fonzo et al., 2007; Vilarino-Guell et al., 2009). Omi/HtrA2 is a mitochondrial serine protease, that is found also in Lewy bodies. The mutation G399S and the A141S polymorphism were identified correlated with PD (Strauss et al., 2005) but another study performed on a larger population did not confirm such correlation (Ross et al., 2008). Additional genetic loci (Table 1) have been identified and yet are under validation and the respective genes are an active area of research.

Gene	Locus	Mutations and polymorphisms	Function	Neuropathology and clinical features	Age of onset	Inheritance	References
SNCA (alpha synuclein)	PARK1-4 4q21	A53T, E46K, A30P, gene duplication and triplication	unknow	Parkinsonism with autonomic dysfunction and dementia; and cognitive decline in E46K cases, rapid progression in A53T and triplication cases. Presence of Lewy bodies,	30-60	AD	(Kruger et al., 1998; Polymeropoulos et al., 1997; Zarranz et al., 2004)
Parkin	PARK2 (6q25.2-q27	Various mutations are reported	E3-ubiquitin ligase	Parkinsonism with slow progression. Absence of Lewy bodies	< 45 (range 16-72)	AR	(Kitada et al., 1998)
Unknow	PARK3 2q13	Unknow	unknow	Typical parkinsonism	60	AD	(Gasser et al., 1998)
UCHL-1	PARK5 4p14	I93M Polymorphism S18T	To catalyze the hydrolysis of polymeric ubiquitin chains	Typical parkinsonism	50	AD Polymorphism associated with risk of Sporadic pd?	(Leroy et al., 1998)
PINK1	PARK6 1p35-p36	Missense and exon-deletion mutations	mitochondrial kinase	Slow progression	20-40	AR	(Valente et al., 2004)
DJ-1	PARK7 1p36	L166P, delections and compound heterozygotes	Involved in the oxidative stress response	Slow progression, sometimes dystonia, psychiatric disturbance.	20-40	AR	(Bonifati et al., 2003)
LRRK2	PARK8 12p12	Many mutations are reported, in particular A1441C/G, Y1699C, G2019S and I2020T	Protein kinase	Parkinsonism, occasionally with dystonia, gaze palsy, dementia andamiotrophy. Variable presence of Lewy bodies,	40-80	AD but penetrance incomplete	(Paisan-Ruiz et al., 2004; Zimprich et al., 2004)
ATP13A2	PARK9 1p36	Homozygous/compound heterozygous delections	Possible ion pump	Parkinsonism with pyramidal degeneration, dementia and spasticity	<20	AR	(Di Fonzo et al., 2007; Vilarino-Guell et al., 2009)
Unknow	PARK10 1p32	Unknow	Unknow	Typical parkinsonism	Unknow	AD	(Hicks et al., 2002)
GIGYF2 (GRB10 interacting GYF protein 2)	PARK11 2q36-37		May act cooperatively with GRB10 to regulate tyrosine kinase receptor signaling, including IGF1 and insulin receptors	Typical parkinsonism	Unknow	AD	(Pankratz et al., 2003b), (Lautier et al., 2008)
Unknow	PARK12 Xq21-q25	Unknow	Unknow	Undetermined	Unknow	X-linked	(Pankratz et al., 2003a)
Omi/Htra2	PARK13 2p12	G399S, A141S polymorphism	Mitochondrial serine protease	Typical parkinsonism	49-77	AD Polymorphism associated with risk of Sporadic pd?	(Ross et al., 2008; Strauss et al., 2005)

Table 1.1. Genes and genetic loci linked to Parkinson's disease. AD = autosomal dominant, AR = autosomal recessive. Adapted from: (Farrer, 2006; Yang et al., 2009).

1.2. 2 Sporadic Parkinson: molecular mechanisms

PD is a multifactorial disease and the majority of the cases are sporadic. Most certainly, genetic predisposition and environmental toxins play an important role. In the last years, the use of PD models and studies on the inherited PD genes have been used to identify several pathogenic mechanisms involved also in sporadic PD: neuroinflammation, oxidative stress, mitochondrial and proteasomal dysfunction.

1.2.2.1 Protein aggregation and proteasomal dysfunction

The involvement of proteasomal dysfunction in PD was identified from the genes implicated in the pathology (UCHL-1 and parkin) and from the presence of ubiquitin in Lewy's bodies. Moreover, in sporadic PD brains the activity of the ubiquitin-proteasome system (UPS) is decreased and this could be deleterious for the cell because of the increase of misfolded and aggregate proteins, which normally are cleared by UPS, contributing to the formation of Lewy bodies (for a review see Xie et al., 2010). However, recently it has been debated if protein aggregation (for a review on protein aggregation see Robinson, 2008) is toxic favoring PD or protective preventing the formation of species more toxic such oligomeric forms of alpha synuclein (Dawson and Dawson, 2003; Shin et al., 2009).

1.2.2.2 Neuroinflammation: microglia mediated-neurotoxicity

In 1990s McGeer and collaborators suggested for the first time the involvement of neuroinflammation in PD, in particular they found activated microglia cells within the substantia nigra of PD patients (McGeer et al., 1988). Microglia cells are resting ramified immune cells of the brain, once activated their morphology changes into amoeboid. They can exert antimicrobial activity similar to macrophages, as well as cell toxicity due to the release of toxic oxygen and nitrogen species creating an oxidative environment (see 1.2.2.4). They can release proinflammatory cytokines such as TNFα, which would activate death pathways (for a review see Hirsch and Hunot, 2009). It is worth mentioning that currently the conditions defining whether microglia activation is toxic or beneficial to neuronal survival are not well understood. However it is suggested that stimuli can overactivate or dysregulate microglia (microgliosis), causing neurotoxic effects probably due to overproduction of superoxide, nitric oxide and TNFα. Microglia cells can be over/activated by a wide range of stimuli such as neuromelanin, rotenone, MPTP, 6-hydroxydopamine (6-OHDA) and alpha synuclein (for reviews see Block et al., 2007; Whitton, 2007).

1.2.2.3 Mitochondrial dysfunction

Several evidence suggests the involvement of mitochondrial dysfunction in the pathogenesis of PD. First of all the products of PD-associated genes have important direct or indirect effects on mitochondrial morphology, function and oxidative stress (fig. 1.5) (reviewed by Henchcliffe and Beal, 2008). In particular studies on Parkin and PINK1 have provided insights in the importance of

mitochondria and oxidative stress. These proteins seem to have the role to maintain mitochondrial integrity in oxidative stress conditions. *Drosophila melanogaster* knockout of parkin results in mitochondrial abnormalities and apoptosis and knockout *Droshophila* for PINK1 leads to a similar phenotype. Interestingly, parkin can rescue the loss of PINK1 but not the contrary, so PINK1 might be genetically upstream of parkin. Moreover mammalian cell culture studies support a common pathway between these two proteins with the output key being mitophagy (reviewed by Cookson, 2010; Cookson and Bandmann, 2010).

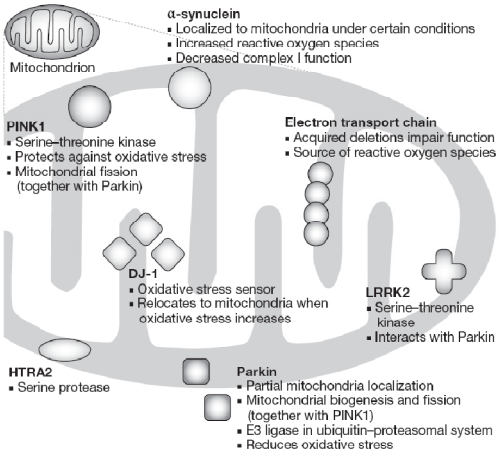

Figure 1.5. PD genes associated with mitochondria and oxidative stress (Henchcliffe and Beal, 2008).

In 1989 a mitochondrial defect of complex I was first identified in substantia nigra from PD patients (Schapira et al., 1990; Schapira et al., 1989). Over the years the study of complex I deficiency was deepened showing that there is about a 35% complex I deficiency in dopaminergic neurons of PD (Mann et al., 1994). The cause of this deficiency is not understood (Greenamyre et al., 2001). Complex I impairment seems to be relevant to the pathology, since complex I inhibitors reproduce PD. In cells ATP depletion will impair the ubiquitin proteasomal system causing an increase of misfolded/unfolded proteins not degradated (see 1.2.2.1) and the abnormal release of dopamine from the intracellular stores to cytoplasm, where dopamine can auto-oxidize (see 1.2.2.5).

Since the 7 subunits out of 43 of complex I are encoded by mitochondrial DNA (mtDNA), several research groups have investigated their possible mutations to verify a correlation with PD; however, until now no mutations have been consistently correlated (reviewed by Schapira, 2008). In contrast, mutations in the mitochondrial polymerase subunit γ (POLG) leads to clinical parkinsonism associated with multiple mtDNA deletions (Luoma et al., 2004).

Linked to mitochondrial dysfunction, in particular to complex I inhibition are the environmental toxins. The involvement of environmental toxins as cause

of PD was originated from the discovery that pesticides such as paraquat and rotenone and toxins such as 1-methyl-4-phenyl-1,2,3,6-tetrahydropyridine (MPTP) provoke a motor disorder indistinguishable from PD. The effect of MPTP appeared accidentally in heroin abusers in the 1980s, where this toxin was used as additive. MPTP is able to cross the blood-brain barrier and can be oxidized by MAO-B to $MPDP^+$ in glial cells. Then $MPDP^+$ deprotonates to MPP^+, which is the active toxic specie (fig. 1.6) (Kopin, 1987).

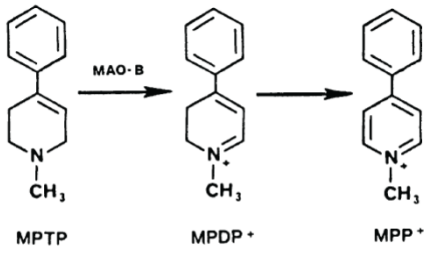

Figure 1.6. The molecular structure of MPTP. *MPTP is oxidized to $MPDP^+$ by MAO-B and $MPDP^+$, which deprotonates to MPP^+ (Kopin, 1987).*

The specific targets of MPP^+, a polar molecule, are the dopaminergic neurons, since it binds to the dopamine amino transporter (DAT) and enters in the neurons where it can follow three different ways: (i) it can interact with enzymes in cystoplasm, (ii) it can be sequestered in synaptic vesicles by the vesicular amino transporters (VMAT2) or (iii) it can go inside mitochondria (fig. 1.7). In mitochondria MPP^+ is able to block the electron transport chain inhibiting the activity of complex III, IV and I, leading to a decreased ATP production and an increased production of reactive oxygen species. The current hypothesis is that the cell death might be due to a combination of oxidative stress and ATP depletion (reviewed by (Smeyne and Jackson-Lewis, 2005).

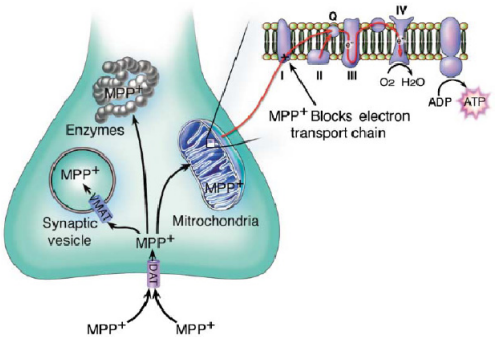

Figure 1.7. MPP+ intracellular pathways. *MPP+ can enter in dopaminergic neurons by DAT. Once in the cells, it can react with enzymes, enter in synaptic vescicles or in mitochondria. In mitochondria it block the complex I, III and VI leading to ATP depletion and oxidative stress (Dauer and Przedborski, 2003).*

Moreover, oxidative stress and ATP depletion are connected to the opening of the permeability transition pore leading to the collapse of the membrane potential, which results in mitochondria swelling and release of pro-apoptotic factors (such cytochrome c), hence activation of apoptotic pathway by the caspase cascade reviewed by Abou-Sleiman et al., 2006; Henchcliffe and Beal, 2008).

1.2.2.4. Oxidative stress

Oxidative stress has been observed in several neurodegenerative disorders such as amyotrophic lateral sclerosis, Alzheimer disease and PD. In particular, in PD extensive oxidative damage to proteins, lipids and DNA has been demonstrated. The issue is that it is not possible to discern if oxidative stress is the cause or the consequence of neuronal death (reviewed by Andreassen et al., 2001; Ischiropoulos and Beckman, 2003; Jenner, 2003). The sources of oxidative stress in dopaminergic neurons of PD patients rise from several factors: the complex I deficiency in mitochondria (see 1.2.2.3); the inflammatory response of microglia (see 1.2.2.2) activated by cellular damage, which produces superoxide anions and nitric oxide; from the pathway of dopamine auto-oxidation (Andersen, 2004). Oxidative stress is the result of the over production of reactive oxygen species (ROS), such as superoxide anion ($O_2^{\cdot-}$), hydrogen peroxide (H_2O_2) and hydroxyl radical ($OH^{\cdot}$) (fig. 1.7). Besides ROS, recently the involvement of reactive nitrogen species (RNS) (fig. 1.7) in PD has been highlighted. In particular peroxynitrite ($ONOO^-$), which is produced by the reaction of superoxide anions with $NO^{\cdot}$, is able to covalently modify proteins affecting their physiological function by tyrosine nitration or cysteine nitrosylation (rewieved by Danielson and Andersen, 2008; Reynolds et al., 2007; Tsang and Chung, 2009). Moreover, NO and $ONOO^-$ have been reported to inhibit the complex I (reviewed by Navarro and Boveris, 2009).

The target of ROS are lipids, proteins and DNA. Proteins can be oxidized, fragmented and carbonylated by ROS affecting the protein function (Berlett and Stadtman, 1997). Radicals can attack the double bond of unsaturated fatty acids generating highly reactive lipid peroxy radicals, which are able to attack on other unsatured lipid in a chain propagating reaction. Lipid damage, in turn, leads to loss of membrane integrity and increase permeability to ions such as calcium promoting cell toxicity (Andreassen et al., 2001). ROS are able to react with DNA causing not only strand breaks but also more than 20 different modifications, many of these induce mutagenesis, affect DNA replication and transcription. The most studied is 8-oxo-2'deoxyguanosine, used as DNA oxidative stress marker (Cooke et al., 2003).

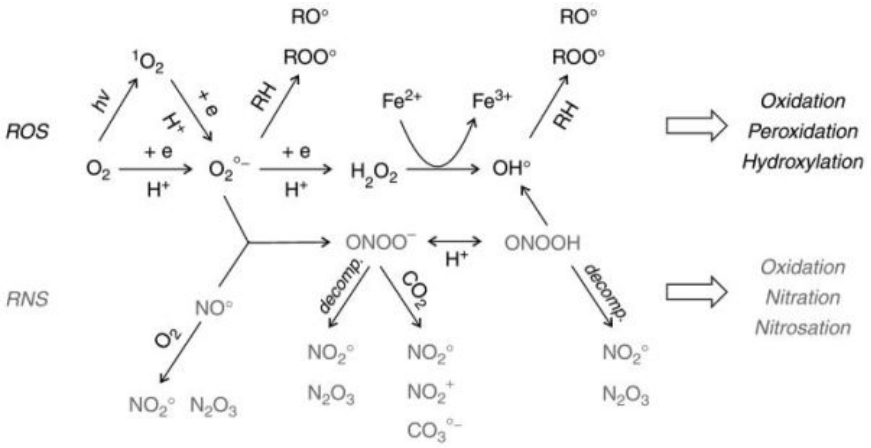

Figure 1.7. Reactive oxygen species (ROS) and reactive nitrogen species (RNS) derived from the conversion of molecular oxygen to superoxide anion and from oxide nitric. Adapted from: *(Amatore and Arbault, 2007)*

Moreover oxidative stress triggers intracellular signaling pathway, such as calcium signaling, leading to cell death by apoptosis. It has been demonstrated that oxidative stress causes an increase of calcium concentration because of the abnormal influx from endoplasmic reticulum and from the extracellular environment. In cytoplasm the excess of calcium disregulates the phosphorilation/dephosphorilation of proteins and signal transduction pathways.
Moreover, as consequence of calcium high concentrations, mitochondria increase the import of this ion disrupting the normal metabolism and activating the apopstosis pathway. Besides mitochondria, also nuclei import calcium, which regulates genes controlling apoptosis (Ermak and Davies, 2002). Thus, it is clear that oxidative stress plays an important role in the cycle events, which lead to neurodegeration acting on the multiple pathways already described (fig. 1.8).

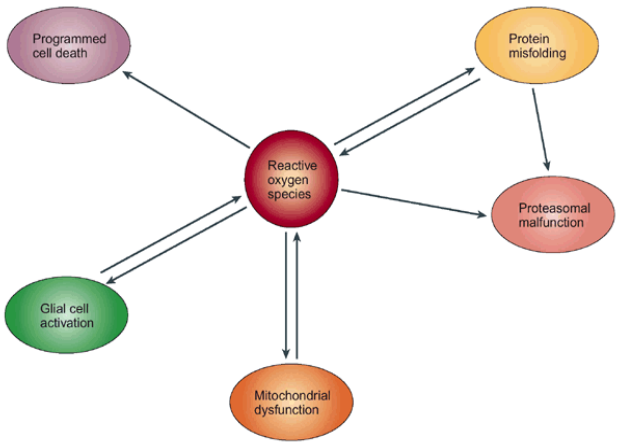

Figure 1.8. ROS plays an important role in neurodegeneration. *(Andersen, 2004)*

1.2.2.5 Dopamine

Since the neurodegeneration in PD affect mainly the dopaminergic neurons of substantia nigra pars compacta, it has been suggested a possible central role of dopamine due its metabolism linked with oxidative stress (reviewed by Hastings, 2009). The synthesis of dopamine starts form the amino acid tyrosine, which is converted to L-dopa by tyrosine hydroxylase, then L-dopa is decarboxylated to dopamine by aromatic aminoacid decarboxylase (fig. 1.9). Once synthesized, dopamine is safely stored by low pH in synaptic vesicles at millimolar concentration where it is transported in an ATP-dependent process by the vesicular monoamine transporter-2 (VMAT2). The dopamine metabolism and storage is highly controlled in dopaminergic neurons to avoid the cytoplasmic accumulation of the neurotransmitter. If dopamine vesicular storage is disrupted by ATP depletion or by α-synuclein (see 1.2.1.1), dopamine will be released in cytoplasm where can be metabolized following the two different pathways. In cytoplasm dopamine can be oxidized by monoamino oxidase located on the outer surface of mitochondria and by aldehyde dehydrogenase forming the dihydroxyphenylacetic acid (DOPAC) and hydrogen peroxide. The DOPAC production is not toxic for the cell but the concomitant hydrogen peroxide produced can be scavenged by GSH, catalase or react with Fe^{2+} to form hydroxyl radical (OH•) by Fenton reaction increasing oxidative stress (fig. 1.9) (Hastings, 2009; Lotharius and Brundin, 2002; Sulzer and Zecca, 2000).

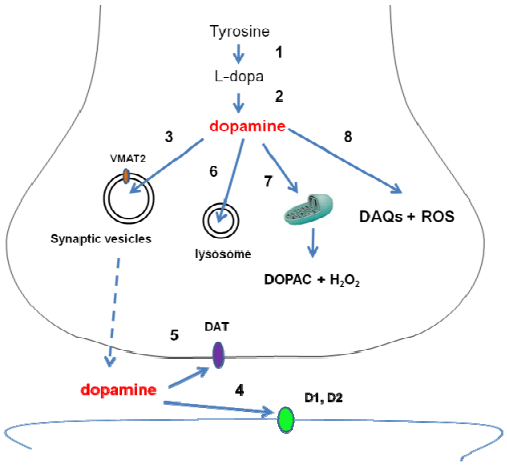

Figure 1.9. Dopamine metabolism. *Tyrosine is converted to L-dopa by tyrosine hydrohylase (1), which is decarboxylated by aromatic aminoacid decarboxylase producing dopamine (2). Dopamine can be sequestered in synaptic vesicles by VMAT2 (3) which released the neurotransmitter in the synaptic cleft in response to the action potential, where it can interact with D1 or D2 receptors (4) or it can be re-uptaken in the presynaptic neuron by the dopamine transporter (DAT) (5). Dopamine can also be sequestered in lysosome (6) or can react with monoamino oxidise on mitochondria and aldehyde dehydrogenase producing DOPAC and hydrogen peroxide (7). In alternative dopamine can auto-oxidize to give rise to dopamine quinones and ROS (8).*

Alternatively, dopamine can auto-oxidize spontaneously to produce dopamine quinones (DAQs) and reactive oxygen species (fig. 1.10). Dopamine oxidizes producing dopamine-o-quinone (DQ), which cyclizes to leukoaminoachrome. The latter oxidizes to aminochrome (AC) rearranging to 5,6-dihydroxindole (DHI). The oxidation of DHI leads to indole-5,6-quinone (IQ), which polymerases to neuromelanin (Graham, 1978; Hastings, 1995; Tse et al., 1976). The function of neuromelanin is still debated and it is currently under investigation its possible role in PD (reviewed by Zecca et al., 2006; Zucca et al., 2004).

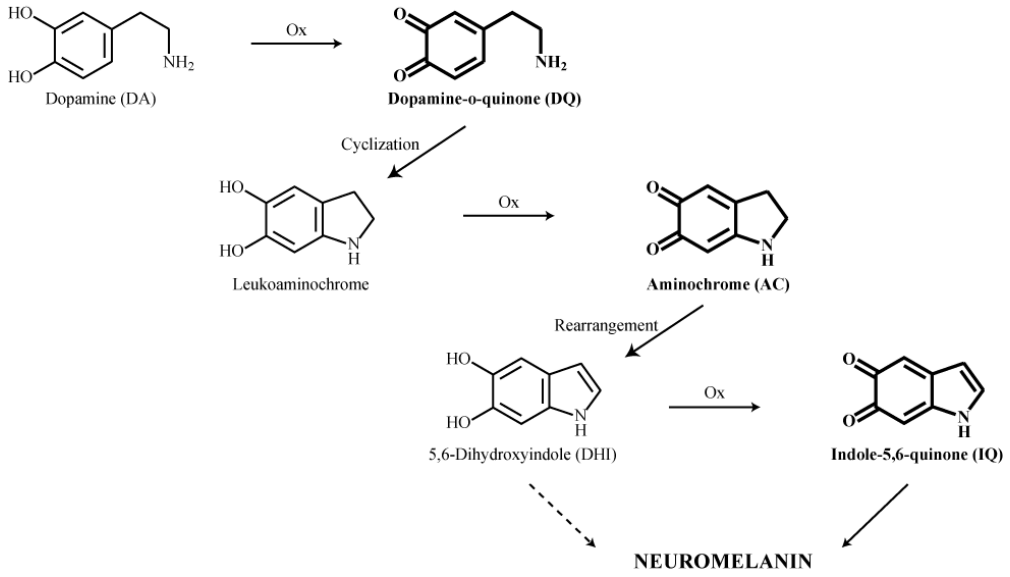

Figure 1.10. The dopamine auto-oxidation pathway. *Dopamine oxidizes to dopamine-o-quinone (DQ), which cyclizes to leukoaminochrome. Upon oxidation leukoaminochrome is converted in aminochrome (AC), which rearranges to 5,6.dihydroxyindole (DHI). DHI can be oxidized to indole-5,6-quinone (IQ) and polymerase to neuromelanin. Adapted from:(Bisaglia et al., 2007).*

The oxidation of dopamine is facilitated by the presence of metal ions such iron, copper and manganese (reviewed by Sulzer and Zecca, 2000), and by the presence of peroxynitrite (LaVoie and Hastings, 1999). Since DAQs are electron-deficients, they will react with GSH leading to the depletion of this antioxidant defense (Bisaglia et. al., 2010). Otherwise DAQs can react with other cellular nucleophiles, such cysteine residues of proteins. In particular, it has been demonstrated that DQ is more likely to react with cysteine residue than to undergo to cyclization producing 5-cysteinil-dopamine (fig. 1.11) (Tse et al., 1976).

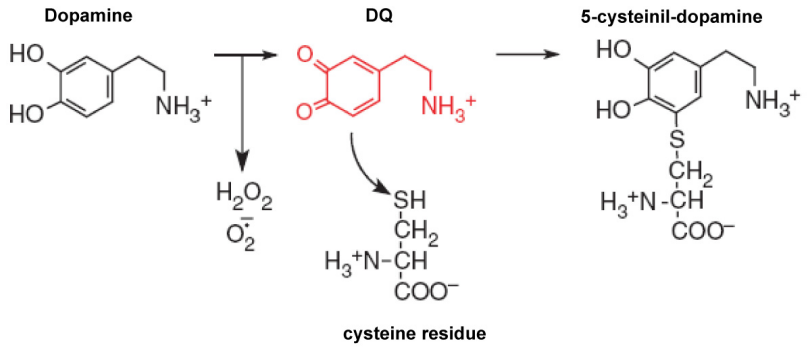

Figure 1.11. Scheme of the oxidation of dopamine (DA) to DQ and the irreversible chemical reaction between the DQ and the cysteine residue. *Adapted from (LaVoie et al., 2005).*

The covalent modification of cysteine residues exposed on the surfaces of proteins would impair their physiological function, since this aminoacid is often found at the active site. Hence the cysteine adducts formed would alter or inhibit the enzymatic activity or the stability of the protein causing cytotoxicity and increasing misfolded proteins (Asanuma et al., 2003). Several products of PD-genes have been shown to be DAQs target such DJ-1, UCH-L1, parkin and α-synuclein (Bisaglia et al., 2007; Bisaglia et al., 2010b; LaVoie et al., 2005; Van Laar et al., 2008; Van Laar et al., 2009). Moreover DAQs covalently modifies tyrosine hydroxylase, the rate limiting enzyme in dopamine biosynthesis, inhibiting its activity (Kuhn et al., 1999; Xu et al., 1998). It has been demonstrated that dopamine oxidation can affect mitochondria opening the permeability transition pore and inhibiting the respiratory chain inducing oxidative stress (Berman and Hastings, 1999). DAQs can also interact with GSH, which is depleted in PD, decreasing the antioxidant cell defenses (Bisaglia et al., 2010a).

To summarize, the auto-oxydation of dopamine could be deleterious for cell affecting different pathways and leading to the death of the neuron (fig. 1.12).

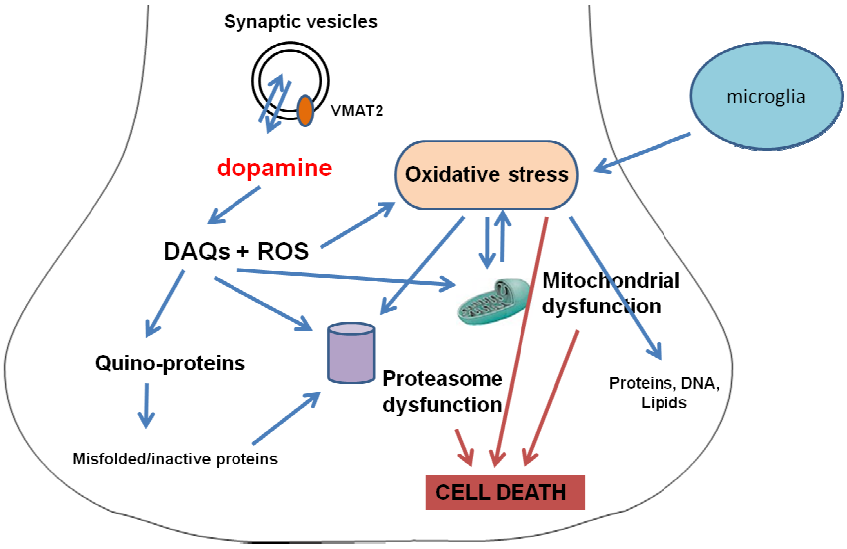

Figure 1.12. The involvement of dopamine auto-oxidation in oxidative stress in PD. *Dopamine auto-oxidation produces DAQs and ROS, DAQs can react with proteins leading to inactivation/misfolding. DAQs can affect proteasome function and increase oxidative stress, which can produce DNA, proteins and lipids damage. Oxidative stress is increased by complex I deficiency and inflammation from microglia activation. Proteasome dysfunction, mitochondrial dysfunction and oxidative stress lead to the death of the cell.*

1.2.2.6 Antioxidant cellular defense

Oxidative stress is a condition resulted from the imbalance between the antioxidant defense mechanisms of cells and the excessive formation of ROS/RNS (reviewed by Berg et al., 2004) (fig. 1.13).

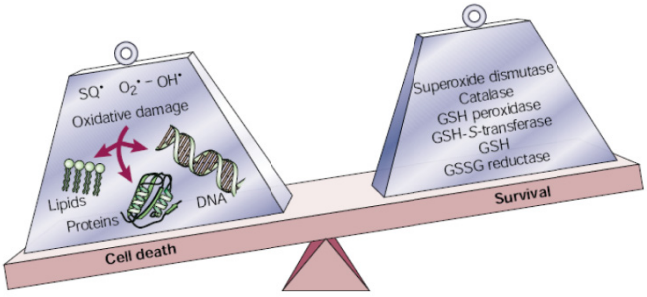

Figure 1.13. Oxidative stress results form a imbalance of the scavenging mechanisms of the cell *(Lotharius and Brundin, 2002).*

Cells have evolved several defense mechanism against reactive species: enzymes such superoxide dismutase, catalase, glutathione peroxidase, glutathione-s-transferase, glutathione reductase and antioxidant molecules such ascorbic acid and glutathione (Andersen, 2004). Glutathione is particularly interesting because it has been found depleted in substantia nigra of PD patiens in association with a decrease activity of glutathione reductase (Barker et al., 1996). Among the

antioxidant enzymes, superoxide dismutases (SOD), catalyzing the dismutation of superoxide anions into molecular oxygen and hydrogen peroxide (fig. 1.14), are particularly important. Three isoforms of SOD exist in mammalian cells with different localization: SOD1in cytoplasm, SOD2 in mitochondria and SOD3 in the extracellular fluid (reviewed by Zelko et al., 2002).

$$2O_2^{\bullet -} + 2H^+ \longrightarrow H_2O_2 + O_2$$

Figure 1.14. Dismutation reaction of superoxide anion catalyzed by SODs.

1.2.2.7 Superoxide dismutase 1 (SOD1)

Superoxide dismutase 1 is copper-zinc enzyme of 32 kDa composed by two identical subunits related by a two-fold axis. It is localized predominantly in the cytosol, but also in peroxisomes, nucleus and in the mitochondrial intermembrane space. The two subunits are related by a two-fold symmetry axis. Each monomer is made by 153 aminoacids and is foldedforms a greek key β-barrel motif of eight antiparallel β-strands and two important loops building the active site channel: the electrostatic and the zinc loop. The first one guides and accelerates the substrate to the active site whereas the function of the zinc loop (containing a intra-subunit disulfide bridge) is tethering the dimer interface. The catalytic copper ion and the structural zinc ion are localized outside the β-barrel in the active site channel of every subunit (fig.1.15).

A) ***B)***

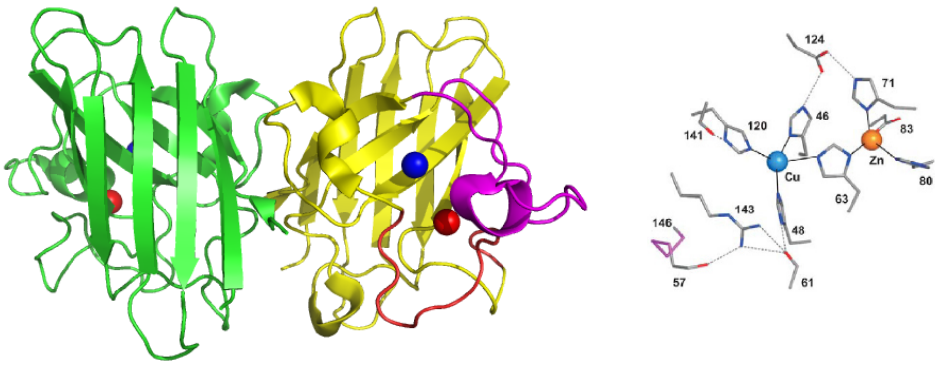

Figure 1.15. Dimeric structure of SOD1. *A) One monomer is displayed in green, while the other in yellow. Zinc and copper ions are shown, respectly, as red and blue spheres. In magenta is depiced the electrostatic loop and in red the zinc loop (PDB structure: 1PU0). B) network of protein active site (Valentine et al., 2005).*

The active protein requires disulfide bridge formation, dimerization and metals acquisition. The latter is helped out by a molecular chaperone called copper chaperone for SOD1 (CCS).
The catalysis mechanism is a two step process:

$$\text{Step 1:} \quad O_2^{\cdot-} + Cu^{2+}\text{ZnSOD} \rightarrow O_2 + Cu^{+}\text{ZnSOD}$$

$$\text{Step 2:} \quad O_2^{\cdot-} + Cu^{+}\text{ZnSOD} \rightarrow H_2O_2 + Cu^{2+}\text{ZnSOD}$$

One molecule of superoxide anion first reduces the cupric ion Cu(II) to form dioxygen (step 1) and then a second molecule of substrate reoxidizes the cuprous ion Cu(I) to form hydrogen peroxide (step 2) (reviewed by Abreu and Cabelli, 2010; Valentine et al., 2005).
Over 100 mutations (http://alsod.iop.kcl.ac.uk/als/), distributed throughout the gene, in this enzyme have been linked with approximately 20% of familial amyotrophic lateral sclerosis (fSLA) cases. SLA is a neurodegenerative disease characterized by the death of large motor neurons in the cerebral cortex and spinal cord leading to progressive paralysis and death typically within 1-5 years (Banci et al., 2008; Gros-Louis et al., 2006). The mechanism of toxicity is probably due to the gain of toxic function. The idea is that the mutations causes an increase of the propensity of SOD1 to oligomerize with itself or other proteins forming aggregates founded in the motor neurons. The reason of toxicity of the aggregates remains to be understood (Shaw and Valentine, 2007).

1.2.2.8 Superoxide dismutase 2 (SOD2)

Superoxide dismutase 2 (SOD2) is encoded by a nuclear gene located in chromosome 6q25 but, once synthesized in cytoplasm, it is imported in mitochondria with a cleavable N-terminal mitochondrial targeting sequence of 24 aminoacids (Wispe et al., 1989). A polymorphism on the mitochondrial targeting sequence encoding for one alanine into a valine (A-9V) affects the importing of the protein in mitochondria decreasing the percentage of active protein in the matrix. The possible correlation of this polymorphism with human diseases is under investigation (Sutton et al., 2003).

SOD2 is made up of 198 aminoacids, which constitute a monomer of 22 kDa. These aminoacids associate forming seven α-helices and three strands of antiparallel ß-sheets (fig. 1.16).

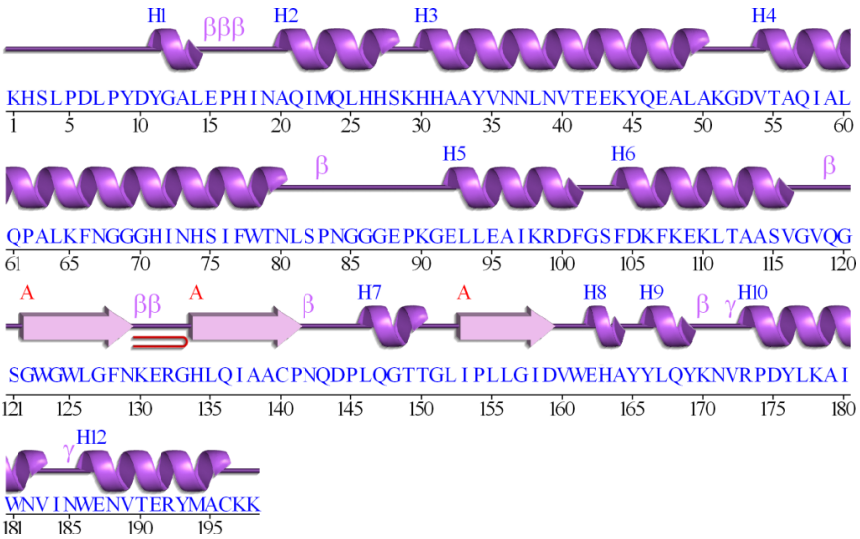

Figure 1.16. Primary and secondary structure of SOD2.
α-helices are labelled as H1, H2, H3, H4, H5 and H6, while the strand by their sheets A. β indicates beta turn, γ gamma turn and beta hairpin motifs.

The momoners associate forming a homotetramer, which is built up through a dimer of dimers creating two four-helix bundles, as suggested by the crystal structure and equilibrium sedimentation studies (fig. 1.17) (Borgstahl et al., 1992; Matsuda et al., 1990). Another polymorphism is I58T, which causes packing defects because of it destabilize the tetramerization interface (Borgstahl et al., 1996).

Figure 1.17. SOD2 homotetrameric structure. *Each monomer is highlighted by a different color and manganese ions are depicted as red spheres. (pdb ref.: 1n0j). Picture created with PyMOL.*

Each monomer presents an active site where a manganese ion is bound in a trigonal bipyramidal geometry by three histidine residues (His 26, His 74, His 163, one aspartic acid (Asp 159) and one solvent molecule (fig. 1.18). The water

molecule cycles between the OH^- when bound to the oxidized manganese and H_2O bounded to the reduced manganese as indicated enclosed in parenthesis in the proposed mechanism of catalysis.

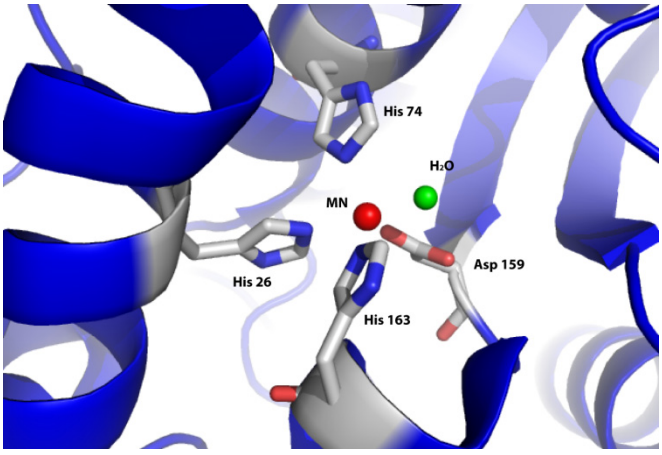

Figure 1.18. Trigonal bipyramidal geometry of the active site of SOD2. *The side chains of three histidine residues (His74, His26 and His163) and one aspartic acid (Asp159) bind a manganese ion (in red) in conjunction with a molecule of water showed as a green sphere. (pdb ref.: 1n0j). Picture created with PyMOL.*

The active site is extended by a hydrogen bond network called second sphere of manganese coordination. The solvent molecule bound to the metal forms a hydrogen bond with the N_ε of Gln 143. The side chain of Gln 143 forms an hydrogen bond with the Tyr 34. A water molecule mediates the hydrogen bonding between Tyr 34 and His 30. The latter residue completes the network binding the Tyr 166 of an adjacent subunit. Any modification of these residues results in decreasing the enzymatic activity, hence this hydrogen bond network is fundamental for the catalysis and for stability of the enzyme as demonstrated by several studies (reviewed by Abreu and Cabelli, 2010; Perry et al., 2010).

The mechanism of dismutation is based on cycling between the oxidized state (Mn^{3+}) and the reduced state (Mn^{2+}) of the metal as for the other SODs. The fundamental difference is that the simple first order reaction of substrate disappearance is not observed on a fast time scale at small concentration of protein. At sufficiently high ratio of [superoxide anion] : [SOD2], instead there is a "burst phase" and a "zero-order" phase. This observation led to the proposed mechanism in which reduced manganese has been suggested to react with the substrate through two concomitant pathways forming a $Mn^{3+}SOD\text{-}O_2^{2-}$ complex called the inhibited complex.

The simplest proposed mechanism is the following:

$$Mn^{3+}SOD(OH^-) + O_2^{\cdot -} + (H^+) \rightarrow Mn^{2+}SOD(H_2O) + O_2 \quad \mathbf{k1}$$

$$Mn^{2+}SOD(H_2O) + O_2^{\cdot -} + (H^+) \rightarrow M^{3+}SOD(H_2O) + H_2O_2 \quad \mathbf{k2}$$

$$Mn^{2+}SOD(H_2O) + O_2^{\cdot -} \rightarrow M^{3+}SOD(H_2O)\text{-}O_2^{2-} \quad \mathbf{k3}$$

$$Mn^{3+}SOD(H_2O)\text{-}O_2^{2-} + (H^+) \rightarrow Mn^{3+}SOD(OH^-) + H_2O_2 \quad \mathbf{k4}$$

The mechanism proposed above represent a special case, suitable to fit the kinetic data, of the more complex mechanism for manganese SOD catalysis proposed by Bull, where the $Mn^{3+}SOD\text{-}O_2^{2-}$ complex can form a ”dead-end”complex (Abreu and Cabelli, 2010; Bull et al., 1991; Hsu et al., 1996).
A way supporting the simplest mechanism is to study the reduction and oxidation of manganese directly through pulse radiolysis at high concentration of protein. $Mn^{3+}SOD$ presents a absorption band at 480nm, hence the decrease of absorbance (between 350-600nm) can be followed upon rapid generation of a substoichiometric concentration of superoxide. In the presence of high concentration of SOD with reduced manganese, it can be observed a transient absorbing at 420nm, which is attributed to $Mn^{3+}SOD\text{-}O_2^{2-}$ complex as well as the $Mn^{3+}SOD$, with the concomitant formation of Mn^{3+} at 480nm (Abreu and Cabelli, 2010).

1.2.2.9 Superoxide dismutase 3 (SOD3)

Superoxide dismutase 3 (SOD3) or extracellular Superoxide dismutase (EC-SOD) is a hydrophobic glycoprotein localized outside cells in the extracellular matrix where it prevents the cell and tissue damage initiated by extracellularly produced ROS (Marklund et al., 1982; Oury et al., 1994). It is a homotetramer of 135 kDa and every subunits has a molecular weight of 30 kDa. The two dimers are linked together by a disulfide bridge forming the tetramer. At the carboxy-terminus is present an unique 9-amino acid heparing-binding domain referred as the extracellular matrix (ECM)-binding region, which enables the binding of the protein to negatively charged heparan sulphate proteoglycans and type I collagen on cell surface (Olsen et al., 2004). Every monomer binds one copper and one zinc ions, both are required for the enzymatic activity. In this case the copper atom is delivered by a copper chaperone: antioxidant-1 protein (Atox1). Interestingly the monomer could fold in two distinct ways with different disulfide bridge patterns and only one retains enzymatic activity (fig. 1.19). Hence, it is theoretically possible to produce five different tetramers with 0, 25, 50, 75 or 100% enzymatic activity (Petersen et al., 2003; Petersen et al., 2007).

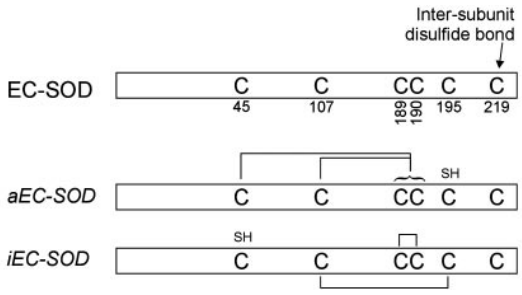

Figure 1.19. scheme of cysteinyl residues in SOD3 and relative disulfide bridges of the active (aEC-SOD) and the inactive form (iEC-SOD).

The partial crystal structure was solved last year revealing that the monomer has a fold identical to that of the β-barrel structure of SOD1 (fig.1.20). The dimer is formed through an interface similar to that of SOD1 as well as the structural core containing the two ion site, thus providing an explanation of similar turnover rates for the enzymatic activity (Antonyuk et al., 2009).

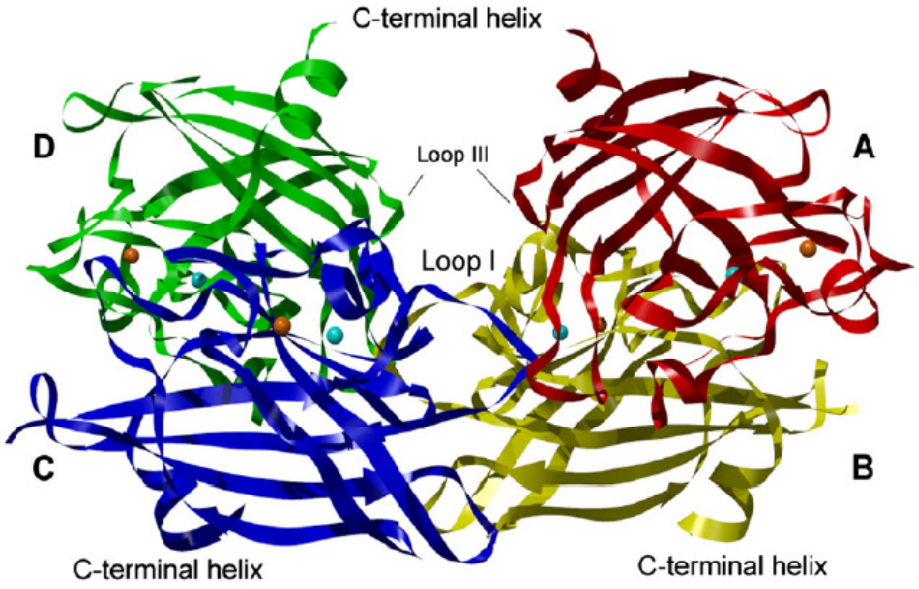

Figure 1.20. tetrameric SOD3. *The structure shows the subunits (A, B, C and D) with different colors, the C-terminus, the Cu in cyan and Zn in orange. The two loops involved in the tetrameric interface (Antonyuk et al., 2009).*

1.3 Aim of the thesis

The importance of superoxide dismutase 2 as antioxidant defense of the cell is demonstrated by the fact that mice without SOD2, obtained by recombinant homology, are not vital (Lebovitz et al., 1996; Li et al., 1995). Since dopaminergic neurons of substantia nigra pars compacta in PD are particularly affected by oxidative stress is clear that the role of SOD2 is crucial. Moreover the deficiency at the complex I with the consequence of an increase of superoxide anions production in mitochondria. Our hypothesis is that SOD2 could be a target of DAQs. The human protein contains two cysteine residues, potentially target of dopamine quinones, are present in each monomer: cysteine 140 and 196 (fig. 1.21). Cysteine 140 is localized on a ß-sheet and appears to be buried in the structure, while the 196 is located on an α-helix exposed to the solvent (Matsuda et al., 1990).

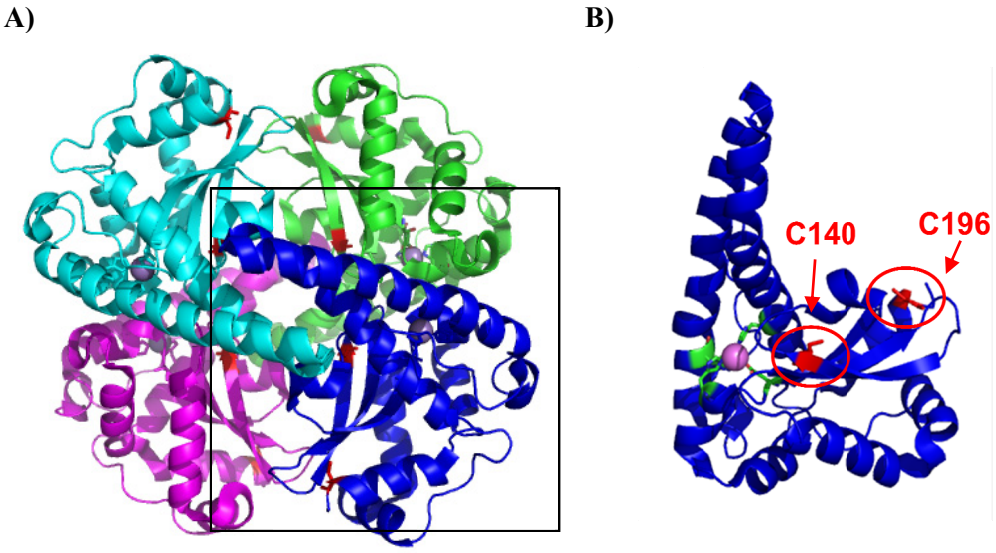

Figure 1.21. The hometrameric structure of SOD2 (A) and one monomer enlarged(B). *Manganese ions are depicted as violet spheres and the positions of cysteine residues 140 and 196 are highlighted in red.(pdb ref.: 1n0j). Pictures created with PyMOL.*

The aim of this thesis is first of all to investigate if SOD2 is covalently modified by DAQs in vitro. Then, the effects of the modification will be characterized. In particular, the enzymatic activity will be assayed to understand if the DAQ bound to the protein will cause an inhibition of the activity. In the PD contest, it is clear that a decrease of the enzymatic activity of SOD2 would exacerbate the oxidative stress condition in mitochondria leading to dysfunction and the death of the neuron. The structural changes will be studied in relation to the eventually change

in activity. Finally, the site/s of DAQs interaction will be investigated and its/their correlation with the enzymatic activity.

2. Materials and Methods

2.1 Molecular Biology techniques for SOD2 cloning and Mutagenesis

The composition of culture media and details on the *Escherichia coli* strains used in this work are described in Appendix 2.

2.1.1 Expression Vector pET28a+

The pET vector series is one of the most powerful system developed by Studier and colleagues in 1990s for protein expression and purification in *Escherichia coli* (Rosenberg et al., 1987; Studier and Moffatt, 1986; Studier et al., 1990). Starting from the first pET vector, many other were implemented in order to achieve best results. The system is so efficient that, when induced, almost all the cell's resources are converted to the expression of the gene target. The protein target can comprise more than the 50% of the cellular total proteins just few hours after induction. The cDNA of the target protein is cloned in the pET vector under the strong control of the bacteriophage T7 promoter. So, the expression of the target protein mRNA requires the T7 RNA polymerase, which is inserted in the host chromosome of *E.coli* under the control of the *lac* promoter. Hence, the T7 RNA polymerase can be trascripted only after addition of the inducer, Isopropil β-D-1-tiogalattopiranoside (IPTG) (fig. 2.1). To provide complete inhibition of the transcription, a lacI gene codyfing for the lac repressor has been inserted in the chromosomal host and in many pET vectors. The *lac* repressor is able to bind to the *lac* operator, which has been insert after the T7 promoter and after the *lac* promoter blocking the trascription.

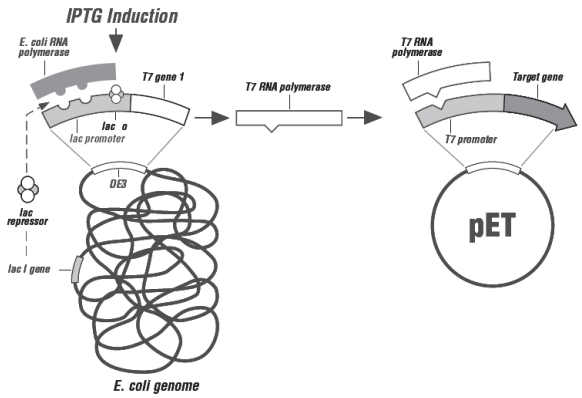

Figure 2.1. The pET expression system.
The chromosomal host carry the gene for the lacI gene and T7 RNA polymerase under the control of the lac promoter and lac operator. The pET vector carries a copy of the lacI gene and presents the gene target under the control of the T7 promoter and lac operator. The transcription of both T7 RNA polymerase and the gene target is blocked by the lac repressor (codified by lacI gene). After induction, the repressor is released from the operator and the transcription can start.

The pET28a+ vector (Novagen)

To express and purify the wild-type and mutated proteins the pET28a+ vector (Novagen) has been chosen. This vector is a low copy (15-20 copies per cell) plasmid of 5469bp, whose features are summarized in fig 2.2 and table 2.1.

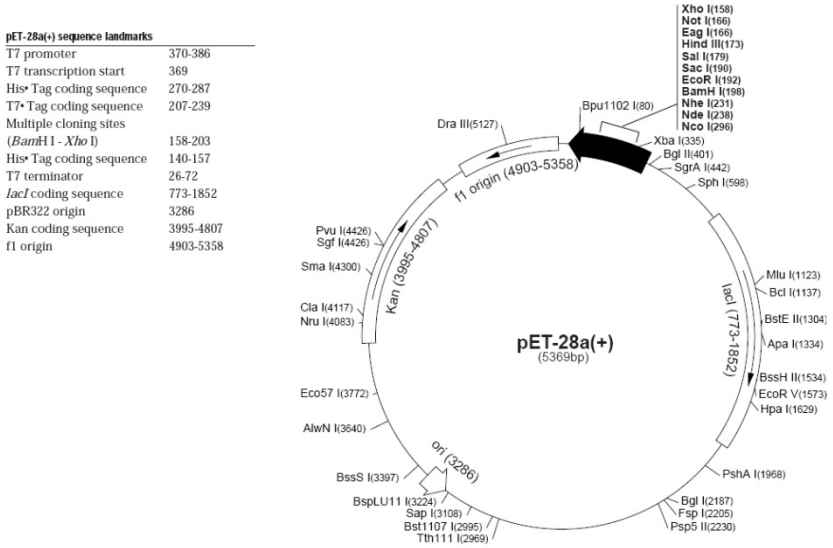

Figure 2.2. the pET28a+ expression vector.

Feature	Description
T7 RNA polymerase promoter (370-386bp)	It is the promoter upstream of the cDNA of the protein target, recognized by the T7 RNA polymerase
T7 transcription start (369bp)	The start of the transcription
Multiple cloning site (polylinker) (*Bam*H I - *Xho* I)(158-203 bp)	Segment of DNA containing many restriction sites allowing the cloning of the cDNA of the protein target.
N-terminal His•Tag coding sequence (140-157 bp)	Histidine – tag, a tag used to purify the target protein
C-terminal His•Tag coding sequence (270-287 bp)	A tag used to purify the target protein
T7•Tag coding sequence (207-239 bp)	A tag of 11 aminoacids localized in the multiple cloning site
Universal primer T7 forward and T7 terminator	Primers which can be used to perform PCR of the cDNA of the target protein or sequencing
lacI coding sequence (773-1852 bp)	The gene codified for the lac repressor which bound to the *lac* operator enabling the transcription.
pBR322 origin (3286 bp)	A colE1 origin, which maintains the low the number of plasmid copy inside the cell
kanamycin resistance coding sequence (3995-4807 bp)	The gene codified for beta-lattamase, a periplasmic enzyme, which can disrupt the B-lactam ring of kanamycin allowing the clone selection
f1 origin (4903-5358bp)	To produce a single-strand plasmid
Thrombin site	Site of thrombin cleavage which enables to eliminate the His-tag

Table 2.1. Main features of pET28a+.

2.1.2 Competent cells

Competence is defined as the ability of a cell to take up extracellular DNA and bacteria exhibiting this capability are referred to as "competent". *Escherichia coli,* the gram negative bacterium used in this work, cannot normally take up foreign DNA (is not naturally competent). Two different protocols were used to artificially induce competence in these cells: rubidium chloride treatment in the case of DH5α cells and calcium chloride treatment with BL21 cells.

2.1.2.1 DH5α rubidium chloride competent cells

A colony of DH5α *Escherichia coli* strain was picked up from a LB plate and it was inoculated in 100 ml of LB broth. The flask was shaked at 37 °C until the optical density OD_{600} reached values between 0.22 to 0.50. Then, the cells were chilled on ice for 20 minutes. and all further steps were carried out at 4°C and using pre-chilled solutions and supplies. The cells sedimented by centrifugation for 7 minutes at 7500g and and the pellet was resuspended in 20ml of TB I (composition is described below) and kept on ice for 5 minutes. The cells were centrifuged again for 7 minutes at 7500 g, the pellet resuspended in 2ml of TBII and incubated 15 minutes in wet ice. The cell were dispensed 100µl into microcentrifuge tubes, snap freezed with liquid nitrogen and stored at -80°C.

Buffer composition:

TB I: rubidium chloride 100mM, manganese chloride 50mM, potassium acetate 30mM, calcium chloride 10mM and glycerol 15% v/v.
Adjust to pH 5.8 with acetic acid 0.2M and filter 0.45µm.

TB II: calcium chloride 75mM, rubidium chloride 10mM, MOPS 10mM and glycerol 15% v/v . Adjust pH to 6.5 with KOH and filter 0.45µm.

2.1.2.2 BL21 Calcium chloride competent cells

A colony was picked up from a LB plate and inoculated in 5ml LB starter culture. The culture was shaked overnight at 37°C. Then, it was re-inoculated (typically 1ml in 100 ml) in fresh medium and grown at 37°C shaking until an OD_{600}nm of 0.3 was reached. The culture was cooled in ice for 15 minutes. After this point, it is important work in cold room (4°C) and pre-chill buffers and all supplies. The cells were harvested by centrifugation for 5 minutes at 4000 g and the pellet resuspended in ½ of initial volume with calcium chloride 0.1M

(typically 50ml) and kept in ice for 30 minutes. The cells were centrifuged again at 4000 g for 5 minutes and the pellet was resuspended in 1/50 of the initial volume with a solution of calcium chloride 0.1M and 25% glycerol. The competence starts after 1 hour of ice incubation and increases with time until 24 hours. After 24 hours cells are stored at -80°C.

The competence of cells was tested for each preparation using 1 µg of DNA and the efficiency obtained was between 10^7- and 10^9 cfu (colony-forming unit)/ 1 µg of DNA.

2.1.3 Plasmid DNA extraction

To extract and purify plasmid DNA from *E.coli* cells, small-scale purifications of plasmid DNA (minipreps) were performed. One colony was picked from a LB plate and inoculated in 10 ml (for low copy number vectors such pET28a+) or 5 ml LB (for high copy plasmid such pCMV-Sport6) with kanamycin 25µg/ml. After overnight shaking at 37 °C, the cells were centrifuged at 3000 g for 5 minutes. The LB broth was discarded and the cells were gently resuspended in 250 µl of Cell Resuspension Solution, an isotonic buffer (see below). Cell Lysis Solution (250 µl), containing SDS to disrupt the cell and NaOH to denaturate DNA, was added. At interval of 5 min each, the following solutions (composition described below) were added: 10µl of Alkaline Protease Solution to inactivate endonucleases; 350µl of Neutralization Solution to neutralize the pH. The lysate was centrifugated at 14000 g for 10 minutes to separate the DNA in the supernatant from the lipids, proteins and genomic DNA of the cells. The supernatant, was loaded into the spin column , a chromatographic anion exchange column (Promega Wizard® Plus SV *Minipreps* DNA Purification System kit). The DNA binds to the column and after two step of wash with Column Wash Solution, the DNA was eluted in sterile H_2O mQ pH 8.4.

Buffer composition:

Cell Resuspension Solution: Tris(hydroxymethyl)aminomethane (Tris-HCl) (pH 7.5), 50mM Ethylenediaminetetraacetic acid (EDTA) 10mM, RNase A 100µg/ml.

Cell Lysis Solution: sodium hydroxide 0.2M and sodium dodecyl sulphate (SDS) 1%.

Neutralization Solution: potassium acetate (pH 4.8) 1.32M.

Column Wash Solution: potassium acetate 80mM, Tris-HCl (pH 7.5) 8.3mM, EDTA 40µM and ethanol 55%.

2.1.4 DNA quantification

DNA quantification is necessary to ascertain the approximate quantity of DNA obtained for further analysis. Two methods were used: spectrophotometric analysis and gel electrophoresis. The first one consists in measuring the absorbance of DNA solution at 260nm, where DNA shows an absorption maxima. Since an absorbance of 1 corresponds to a concentration of 50 ng of double-stranded DNA in solution, the concentration of DNA in solution can be easily calculated using the following formula:

$$\text{ng/µl of dsDNA} = \left(A_{260nm} \times c\right) \times \textit{dilution factor}$$

Moreover, the purity of the sample, in terms of proteins contamination, can be calculated from the ratio of OD_{260}/OD_{280}. A pure DNA preparation has a value around 1,8.

The second method with gel electrophoresis (see 2.1.7) consists in the comparison on the transilluminator of the sample with standard DNA (plasmids or PCRs, depending of the type of the sample) previous quantified. This method is very sensitive, since it allows to quantify down to few nanograms of DNA.

2.1.5 Agarose gel electrophoresis

Agarose (Applichem) was dissolved in the suitable electrophoresis buffer TAE 1X containing ethidium bromide 0.025 µg/ml. Agarose concentrations were 1% for DNA plasmids of 5-6 kbp and 2% to analyze DNA fragments of 0,1-1 kbp. The mixture was heated in a microwave oven until completely melted, then was poured into a casting tray containing a sample comb. Once the gel has cooled at room temperature, the comb was removed and the gel placed into an electrophoresis cell, filled with TAE 1X buffer. Before loading the DNA samples into the wells with a micropipette, it was necessary mix the samples with loading dye (Promega), a colored loading buffer containing glycerol, which enables to tack the running of the gel and avoid the sample's diffusion from the wells. Beside to DNA samples, an appropriate molecular weight standard, the 100bp or 1kbp DNA ladder (fig. 2.3), was loaded in order to identify the size of DNA samples by comparison with the fragments of known size. At this point, a current field, between 50-100 volts depending on the gel size, was applied to gel until the bromophenol blue front of the loading dye was migrated about 70-80% toward the positive pole. At the end of the running, the gel was placed on a UV trans-illuminator to visualize the DNA due to the presence of the DNA intercalator

ethidium bromide, which can be excited at around 300 nm emitting to 590 nm revealing the presence of DNA.

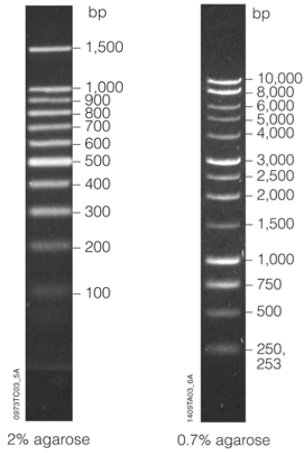

Figure 2.3: DNA ladders (Promega), **molecular weight standards.**
A) 100bp DNA ladder*. Eleven fragments that range in size from 100bp to 1,000bp in 100bp increments with an additional band at 1,500bp. The 500bp fragment is present at increased intensity for easy identification with a concentration of 30ng/µl.*

B) 1kbp DNA ladder. *Thirteen fragments with sizes ranging from 250bp to 10,000bp. The 1,000bp and 3,000bp fragments have increased intensity relative to the other bands for easy identification. All other fragments are of equal intensity.*

Buffer composition:

TAE 1X: Tris-Acetate 40mM, EDTA 1mM, pH 8.3.

Loading dye 6X (Promega): orange G 0.4%, bromophenol blue 0.03%, xylene cyanol FF 0.03%, Ficoll® 400 15%, Tris-HCl (pH 7.5) 10mM and EDTA 50mM (pH 8.0).

2.1.6 Polymerase chain reaction (PCR)

The polymerase chain reaction is a powerful technique which allows to obtain *in vitro* millions copies of target DNA segments between two regions of known sequence starting from few copies of such target DNA. A variant was used to insert restriction sites at the termini of the SOD2 cDNA using engineering primers carrying the sequence recognized by the restriction enzymes. Five additional cycles, the mutagenic phase, (before the 25) have to be performed with a low temperature of annealing allowing the primers to anneal. So, the amplification will generate fragment with two different restriction sites at the termini that will be useful for the cloning in the pET28a+ vector.

In the following table (table 2.2) the used primers are listed with the their melting temperature:

Primer	Nucleotide number	Tm (°C) *
FOR-NdeI 5'-CTGGGCTCC**CATATG**AAGCACAGC-3'	24	62
FOR-NcoI 5'-ATCTGGGCT**CCATGG**GAAGCACAG-3'	26	64,8
REV-XhoI 5'-CCACGATCGTTATG**CTGATC**ATACCC-3'	25	60,8

Table 2.2: primers (Sigma) used to insert restriction site at the termini of SOD2 cDNA for the cloning in pET28a+ vector. *The restriction site are in bold and underlined. * The temperature of melting was calculated using IDT SciTools Oligo Analyzer 3.1.*

The reaction mix used was:

DNA (400pg/µl) pCDNA	1 µl
dNTPs (10 mM)	1 µl
Pfu (Promega, 3u/µl)	1 µl
Buffer 10X (Promega)	5 µl
Primer FOR-NdeI or FOR-NcoI (10 mM)	2,5 µl
Primer REVpET-XhoI (10 mM)	2,5 µl
sterile H_2O mQ	37,58 µl
	50 µl

The PCR program carried out by the thermocycler *My Cycler thermal cycler* (BIO-RAD) was the following:

- Denaturation, 1 minute at 95°C
- Amplification:

  Denaturation, 1 minute at 95°C
  Annealing, 30 seconds at 42-43°C
  Amplification, 1 minute at 72°C
  } Mutagenic phase, 5 cycles

  Denaturation, 30 seconds at 95°C
  Annealing, 30 seconds at 60°C
  Amplification, 1 minute at 72°C
  } Amplification phase, 25 cycles

- Amplification, 10 minutes at 72°C

All the PCR products were analyzed on agarose gel electrophoresis (see 2.1.7) and purified (see 2.1.9).

2.1.7 DNA purification

DNA purification was achieved using the kit Wizard ® SV Gel and PCR Clean-Up System (Promega). The kit is based on the ability of the DNA to bind to silica membrane of the minicolumn in the presence of chaotropic salts. It consists in the addition of an equal volume of Membrane Binding Solution (guanidine isothiocyanate 4.5M, potassium acetate 0.5M, pH 5.0) to the DNA sample and the loading into the SV minicolumn. After two wash steps with Membrane Wash Solution (potassium acetate 10mM (pH 5.0), ethanol 80%, EDTA 16.7µM (pH 8.0)), the DNA was eluted with H_2O mQ pH 8,4.

2.1.8 DNA enzymatic restriction

DNA enzymatic restriction was carried out with the enzymes summarized in Table 2.3, together with the specific nucleotide sequence recognized by them.

Name of the enzyme	Recognition site
NcoI	C / C A T G G G G T A C / C
NdeI	C A / T A T G G T A T / A C
XhoI	C / T C G A G G A G C T / C

Table 2.3. Restriction enzymes used

The experimental protocols for DNA digestion with the different restriction enzymes are summarized below.

PCRs fragments digestions:

DNA (75ng/µl)	15 µl	DNA (50ng/µl)	15 µl
NdeI (Promega, 10u/µl)	0,2 µl	*NcoI* (Promega, 10u/µl)	0,2 µl
XhoI (Promega, 10u/µl)	0,2 µl	*XhoI* (Promega, 10u/µl)	0,2 µl
Buffer D 10X (Promega)	2 µl	Buffer D 10X (Promega)	2 µl
sterile H_2O mQ	2,6 µl	sterile H_2O mQ	2,6 µl
	20 µl		20 µl

pET28a+ digestions:

DNA (250ng/µl)	8 µl	DNA (250ng/µl)	8 µl
NdeI (Promega, 10u/µl)	1 µl	*NcoI* (Promega, 10u/µl)	1 µl
XhoI (Promega, 10u/µl)	1 µl	*XhoI* (Promega, 10u/µl)	1 µl
Buffer D 10X (Promega)	2 µl	Buffer D 10X (Promega)	2 µl
sterile H_2O mQ	8 µl	sterile H_2O mQ	8 µl
	20 µl		20 µl

All the reactions are kept at 37°C for 1-2 hours.

To verify the result of digestion small aliquots of restricted DNA were loaded on gel electrophoresis and then restricted DNA was purify (see 2.1.8 DNA purification) to eliminate the endonucleases.

2.1.9 Vector dephosphorylation

The dephosphorylation, consisting in the removalof the of 5´-phosphate groups from both termini of the linear, double-stranded pET28a+ vector, was carried out before ligation in order to prevent the vector recircularization (self-ligation). The restricted linearized vector in NEBuffer 3 1X (Tris-HCl 50mM, sodium chloride 100mM, magnesium chloride 10mM and dithiothreitol 1mM) was incubated with calf intestine phosphatase (NEB biolabs, 0.5 unit/µg vector DNA) for 60 minutes at 37°C. The treatment was repeated twice to ensure a better result. After each dephosphorylation, the DNA vector was purified (see 2.1.7).

2.1.10 DNA Ligation

The ligation was applied in order to insert the digested PCR products into the pET28a+ vector restricted and dephosphorylated. To extimate best amounts of vector and inserts, the following formula was used:

$$\text{ng insert} = \frac{100 \text{ ng Vector x bp of insert}}{\text{bp vector}}$$

The ligation reaction was carried out for 3 hours at room temperature in the following medium:

pET28a+ DNA vector (30ng/µl)	2 µl
Insert (*NdeI-XhoI* or *NcoI-XhoI*) (30ng/µl)	3 µl
T4 DNA ligase (Promega, 3u/µl)	1 µl
Buffer 10X (Promega)	1 µl
sterile H_2O mQ	3 µl
	10 µl

As negative control of the ligation, a reaction of autoligation was performed in the presence of the vector without the insert to estimate the yield of vector self-ligation. At the end of the ligation, *E.coli* DH5α were transformed.

Buffer composition:

10X Reaction Buffer: Tris-HCl 300mM (pH 7.8), magnesium chloride 100mM, dithiothreitol 100mM and adenosine triphosphate 10mM.

2.1.11 Bacterial transformation

For bacterial transformation an aliquot of 100 µl frozen competent cells (see 2.1.4) were defrost on ice. After that, the DNA sample was added and cells were kept 20 minutes on ice. The cells were incubated for 90s at 42°C (thermal shock) and placed 2 minutes on ice. A volume of 900 µl of SOC medium (see appendix 2) was added and the cells were further incubated shaking at 37°C for 45-60 minutes. This step allows the expression and translation of the antiobiotic resistence. At the end, the cells were plated out on LB agar plates containing kanamycin to select the cells with the vector on the basis of their acquired resistance to kanamycin (25 µg/ml) LB agar plates were kept overnight at 37°C.

2.1.12 Bacterial colonies screening

After the trasformation with the ligation and overnight growth at 37°C, the kanamycin resistant colonies have been screened to select those that have incorporated the insert. For this purpose, the bacterial colonies were picked up, dispensed in Eppendorf tubes with 10 µl of sterile H_2O mQ and kept for 10 minutes at 95°C. A volume of 1 µl of this solution would be the template for a PCR using the T7 universal primers located next to the cloning site.

The PCR reaction was set up as indicated below:

Colony DNA	1 µl
Go Taq polymerase (Promega, 3u/µl)	0,25 µl
Buffer 5X (Promega)	5 µl
sterile H_2O mQ	14,25 µl
dNTPs (10 mM)	0,5 µl
Magnesium chloride	1,5 µl
Primer T7 FOR (10 mM)	1,25 µl
Primer T7 REV (10 mM)	1,25 µl
	25 µl

The program executed by the thermocycler My Cycler thermal cycler (BIO-RAD) was:

Initial denaturation, 1 minute at 95°C
Denaturation, 30 seconds at 95°C
Annealing, 30 seconds at 60°C } 25 cycles
Amplification, 1 minute at 72°C
Final amplification, 1 minute at 72°C

For the positive colonies identified by analyzing the PCR results on agarose gel electrophoresis, miniprep cultures in the presence of kanamycin (25 µg/ml) were set up to extract the vector.

2.1.13 DNA sequencing

The pET28a+ vector containing the insert was dried at 65°C and sequenced at the BMR Genomics (spin-off University of Padova) to verify the exact sequence.

2.1.14 DNA mutagenesis

In order to obtain the mutants of the protein, site directed mutagenic PCR was applied. This PCR variant enables to make point mutations directly on the double-stranded DNA vector using the Pfu DNA polymerase. The procedure involves the amplification of one or two primers, complementary to the opposite strands of the vector and containing the desidered mutation, which are extended

during the PCR cycling leading to the generation of entire new mutated vectors. The primers used for the mutagenesis are listed below in table 2.4.

Mutagenic Primers	Nucleotide number	Tm (°C) *
C140A 5'-CTTACAAATTGCTGCTGCTCCAAATCAAGATCCA-3'	34	62,1
FOR- C196A 5'-CTGAAAGATACATGGCTGCCAAAAAGTAAACCACGATCG-3'	39	63,9
REV- C196A 5'-CGATCGTGGTTTACTTTTTGGCAGCCATGTATCTTTCAG-3'	39	63,9

Table 2.3: primers (Sigma) used to mutagenize the cDNA of SOD2
** The temperature of melting was calculated using IDT SciTools Oligo Analyzer 3.1.*

The mix of site direct mutagenesis was set up as indicated below:

C140A direct mutagenesis

DNA pET28a+ SOD2 (150ng/ µl)	2 µl
Pfu polymerase (Promega, 3u/µl)	1 µl
Buffer (Promega) 10X	5 µl
Primer C140A (10 µM)	5 µl
dNTPs (10 mM)	1 µl
sterile H2O mQ	36 µl
	50 µl

C196A direct mutagenesis

DNA pET28a+ SOD2 (40ng/ µl)	1 µl
Pfu polymerase (Promega, 3u/µl)	1 µl
Buffer (Promega) 10X	5 µl
Primer FOR- C196A (10 µM)	2 µl
Primer REV- C196A (10 µM)	2 µl
dNTPs (10 mM)	1 µl
sterile H2O mQ	38 µl
	50 µl

The site direct mutagenesis PCR program carried out by the thermocycler *My Cycler thermal cycler* (BIO-RAD) was the following:

C140A direct mutagenesis

- Initial denaturation, 1 minute at 95°C
- Vector amplification:
  - Denaturation, 30 seconds at 95°C
  - Annealing, 1 minute at 55°C
  - Amplification, 6 minutes at 72°C

  } 18 cycles
- Amplification, 5 minutes at 72°C

C196A direct mutagenesis

- Initial denaturation, 1 minute at 95°C
- Vector amplification:
  - Denaturation, 30 seconds at 95°C
  - Annealing, 1 minute at 55°C
  - Amplification, 6 minutes at 72°C

  } 12 cycles
- Amplification, 5 minutes at 72°C

The obtained PCR products were treated with 1 µl of the enzyme DpnI (NEB biolabs 20U/µl), an endonuclease specific for fully methylated and hemimethylated DNA. It recognizes the sequence 5´-G^{m6}ATC-3´degradating the DNA template, since the mutation-containing synthesized DNA did not have any methylations. After 90 minutes at 37°C, 2 µl of the DNA was used to transform bacterial cells (see 2.1.11). Once obtained the colonies, the mutation containing DNA was isolated (see 2.1.3) and sequenced (see 2.1.13).

2.2 Biochemistry and biophysical techniques

2.2.1 Cell growth for proteins expression

The BL21 DE3 cells were transformed (see 2.1.11) with the pET28a+ vector containing the cDNA of SOD2 wt or mutants (with or without Histidine-tag). The day after the transformation, several colonies were picked up and grown shaking at 37°C in 500 ml of LB medium with kanamycin (25 μg/ml). When an OD_{600nm} of 0,6 was reached corresponding to the logarithmic phase of bacterial growth, $MnCl_2$ was added to a final concentration of 3,65 mM and the protein expression was induced with 0,1 mM IPTG. Before and at the end of the induction, aliquots of culture were withdrawn in order to analyze the protein expression on SDS-PAGE (see 2.2.5). After overnight IPTG induction, the cells were harvested by centrifugation at 3800 g for 10 minutes at 4°C . The cells were gently resuspended in Tris-HCl 50 mM pH 7,8, or PBS buffer 1X (sodium chloride 137mM, potassum chloride 2.7mM, sodium phosphate dibasic10mM and potassium phosphate monobasic 2mM) in case of histidine-tagged proteins, and harvested again to completely eliminate LB traces. At this point the aliquots of pellet corresponding to 250 ml of culture can be stored at – 20°C or the protein can be purified.

2.2.2 Protein purification

Cells were disrupted by sonication using a Omni Sonic ruptor 400 sonicator (Omni International) The pellet corresponding to 250 ml of protein expression culture was resuspended in Tris-HCl 50mM pH 7.8 in the presence of a cocktail of protease inhibitors (Protease Inhibitor Cocktail for use with bacterial cell extracts, Sigma) and phenylmethanesulfonylfluoride (PMSF) 1mM. The cells were sonicated on ice with 20-25 repetitive cycles of 30 seconds with short burst and 30 second interval between each sonication cycle. Cell debris were sedimented at 15000 g for 30 minutes at 4°C and the supernatant containing the proteins was collected.

The supernatant after sonication was heated at 60°C for 40 minutes to precipitate most of contaminant proteins. The precipitated was removed by centrifugation at 5000 g for 10 minutes. The supernatant was brought first to 45% and then to 90% saturation with ammonium sulphate. Each step involved stirring for 20 min at 4°C, followed by centrifugation at 10000 g for 15 minutes to pellet the precipitated proteins. Excess salt was removed by dialsysi against 1 liter of Tris-HCl 50mM pH 7.8 with cut-off of 14000 Dalton for 2 hours. This procedure

was repeated for 3 times. After the dialysis of sample, anionic IEX was performed using a RESOUCE Q 6ml column (GE Healthcare) to purify wild-type SOD2. In the case of SOD2, the protein did not bind to the anion exchanger, hence it eluted in the flow through, while all the other proteins were retained by the stationary phase. The contaminants proteins were eluted using 500mM NaCl in Tris-HCl 50mM pH 7.8.

2.2.3 Protein purification with Histidine-tag

A pellet of 250 ml culture of histidine-tagged wild-type or mutant SOD2 was resuspended in 20 ml of PBS 1X and sonicated (see 2.2.2 for sonication protocol). The protein was purified by Immobilized metal ion affinity chromatography (IMAC). The column used was the HiTrap IMAC FF of 1 ml (GE Healthcare) with 37 μm sepharose chelating beads as matrix functionalized with Ni^{2+} ions. The metal was loaded into the column pumping a solution of 0,1 M NiSO4 with a syringe and the metal excess was washed with 15 of H_2O mQ. After sonication the 20 ml of sample was loaded into the IMAC column enabling to separate the majority of contaminat proteins, which are not able to bind to the metal and elutes immediately, from the bounded SOD2 protein. The SOD2 protein was eluted using a linear imidazole (a competitor for the binding to the ion) gradient 0-500 mM in 20 minutes. To eliminate the imidazole from the PBS buffer containing the protein, the sample was dialyzed in PBS.

Every 5-7 protein purifications, the metal ions were stripped with 10 ml of 0,5 M sodium chloride, 50 mM EDTA pH 7,4; the column was washed first with 10 ml of PBS 1X 500 mM imidazole, then with 10 ml of H_2O mQ water and recharged.

The N-terminal histidine tag of the protein was removed by thrombin, a serine protease which recognizes the aminoacid consensus sequence Leu-Val-Pro-Arg-Gly-Ser (placed between the tag and protein) cleaving the peptide bond between arginine and glicine. The purified protein in PBS 1X was kept 16 hours at room temperature in the presence of 3 units of thrombin (GE healthcare) per mg of protein.

A step of batch purification was applied after the cleavage of the histidine tag. This step allows to remove the histidine-tag peptide and also the uncut histidine-tag fused protein. The HIS-Select® Cobalt Affinity Gel (Sigma) was used (1 ml for 15 mg of protein). Before mixing the gel with the sample, the former was washed with 2 volumes of H_2O mQ to remove the ethanol and equilibrated with PBS 1X buffer. The sample was incubated for 30 minutes with the affinity gel shaking and then centrifuged at 5000 g for 2 minutes to spun down

the gel. The sample was filtered (0.22 μm) to remove all the beads and quantified (see 2.2.4).

The affinity gel was recovered eluting the histidine tag and uncut histidine tag fused protein with 3 volumes of PBS 1X pH 7.4 imidazole 500 mM and the beads were centrifuged at 5000 g for 2 minutes. The procedure was repeated for a second time and after that the affinity gel was washed with H_2O mQ and stored at 4°C in the presence of ethanol 30% to avoid bacteria proliferation.

2.2.4 Protein quantification

The purified protein was quantified with a spectrophotomer (Agilent 8453 UV-Visible spectrophotometer) measuring the absorbance at 280 nm using the Lambert-Beer law, with a molar extinction coefficient of 42846 $M^{-1} \cdot cm^{-1}$. The molar extinction coefficient was determined using the Edeloch method {Gill, 1989 #2199}. The absorbance spectra of the protein at the same concentration were measured in the presence of guanidinium chloride 6 M or buffer Tris-HCl 50 mM pH 7.8. The extinction coefficient in the presence of guanidinium chloride 6M ($\varepsilon_{denatured}$) was calculated with a program tool (ProtParam). Since the protein concentration is the same, rearranging the Lambert-Beer law, the following formula has been used to obtain the extinction coefficient for the native protein:

$$\varepsilon_{native} = \frac{\mathrm{Abs}_{\ native} \cdot \varepsilon_{denaturated}}{\mathrm{Abs}_{denaturated}}$$

2.2.5 Protein concentration

When necessary, the purified protein was concentrated using Vivaspin 20 concentrator (Sigma) with a molecular cut-off of 5000 Dalton allowing the buffer to be pulled away to the bottom of the 50 ml falcon tubes. The Vivaspin was centrifuged at 2000 g until the optimal protein concentration was achieved. This procedure was used also to change the buffer PBS 1X to Tris-HCl 50mM pH 7.8.

2.2.5 Sodium dodecyl sulphate polyacrylamide gel electrophoresis (SDS-PAGE)

Proteins can be separated according to their size in polyacrilamyde gels in the presence of sodium dodecyl sulphate (SDS) applying an electric field. SDS-PAGE was carried out using stacking and resolving or running gels.

The resolving and the stacking gel were prepared as indicated below in table 2.4.

Resolving gel:	***Stacking gel:***
Acrylamide solution* 13%	Acrylamide solution* 5%
Tris-HCl 0.375 M pH 8.8	Tris-HCl 0.125 M pH 6.8
SDS 0.1%	SDS 0.1%
APS 0.1%	APS 0.1%
TEMED 0.008%	TEMED 0.1%

Table 2.4. Resolving and stacking composition.
*The acrylamide solution is composed by acrylamide:bis-acrylamide ratio 29:1.

Before loading the samples on the wells of the gel, they were boiled 10 minutes to denature the proteins in the presence of the Laemmli buffer (Tris-HCl 50mM pH 6.8, SDS 2%, DTT 100mM, bromophenol blue 0,1%, glycerol 10%). The sample were spun down, loaded into the gel and a potential of 100 volts was applied. Once the proteins had entered in the resolving gel the potential was increased to 150 – 200 volts. The running buffer used was: Tris-HCl 25mM, glycine 192mM, SDS 0.1%, pH 8.3.The low molecular weights marker (GE healthcare) (fig. 2.3) was loaded in each gel as reference.

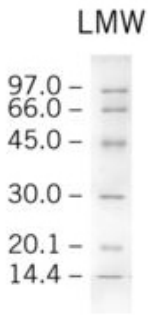

Figure 2.3 Low molecular weights (GE Healthcare).

Protein	***Molecular weight***
rabbit muscle phosphorylase b	*97 kDa*
bovine serum albumin	*66 kDa*
chicken egg white albumin	*45 kDa*
bovine erythrocyte carbonic anhydrase	*30 kDa*
soybean trypsin inhibitor	*20,1 kDa*
bovine milk α-Lactalbumin	*14,4 kDa*

After run, the gel was stained with Coomassie solution (Coomassie Brillant Blue R250 0,25% (w/v), ethanol 45 % (v/v) and acetic acid 10% (v/v)) and destained

(isopropanol 10% (v/v), acetic acid 10% (v/v)). After the staining the gel was stored in a solution of 10% acetic acid. Alternatively, when necessary to increase the sensitivity, silver staining was applied according to the protocol described in table 2.5.

Solution	Composition	Incubation time for 1,5 mm gel
Silver staining fixing solution	ethanol 40% acetic acid 10%	30 minutes
Sensitizing solution	ethanol 30% sodium acetate anhydrous 6.8% sodium thiosulfate pentahydrate 0.2% glutaraldehyde 25%	30 minutes
Wash H_2O mQ		3 X 10 minutes
Silver solution	Silver nitrate 0.0025%	30 minutes
Wash H_2O mQ		2 X 1 minute
Developing solution	Sodium Carbonate Anhydrous 2.5% Formaldehyde 40%	15-20 minutes *
Stopping solution	EDTA 1.5%	10 minutes
Wash H_2O mQ		3 X 5 minutes

Table 2.5. silver staining protocol.
** The gel is incubated in the developing solution until the brown bands appear.*

After the silver staining the gel was stored in the preserving solution (ethanol 30% and glycerol 4%).

2.2.6 Native polyacrylamide gel electrophoresis (Native-PAGE)

Native-PAGE is a gel electrophoresis performed in non-denaturing conditions so proteins retain their higher-order structure. The samples are not boiled but only mixed with native Laemmli buffer, which does not contain DTT and SDS. Hence the migration of a protein in a Native-PAGE is depending on its intrinsic charge and its hydrodynamic size. The choice of the buffer is very important because it affects the charge of the protein, it is indicated to use a buffer with a pH higher that the isoelectric point of the protein. This because the protein will be negative charged and would migrate toward the positive pole (as in the SDS-PAGE).

For Native-PAGE linear gradient gels were prepared from 5 % to 12.5 % to achieve a best resolution of the proteins. The gel was obtained mixing the light and the heavy solution (table 2.6) by a gel marker connected to a peristaltic pump. The stacking gel here was composed by the light solution. The electrophoresis was carried out at 80 volts at 4°C to avoid possible protein's denaturation caused by heating.

Light solution:	***High solution:***
Acrylamide solution* 5%	Acrylamide solution* 12.5 %
Tris-HCl 0,375M pH 8.8	Tris-HCl 0,375M pH 8.8
-	Sucrose 40%
APS 0.044%	APS 0.09%
TEMED 0.035%	TEMED 0.035%

Table 2.6. Heavy and light solution composition.
*The acrylamide solution is composed by acrylamide:bis-acrylamide ratio 29:1.

Buffer composition

Running buffer: Tris 0.025M, Glicina 0.25M, pH 8.8.
Native laemmli buffer 1X: Tris-HCl 50mM pH 8.8, bromophenol blue 0.1%, sucrose 10%.

2.2.7 Superoxide dismutase activity staining on native-PAGE

Proteins separated with native-PAGE retain their higher-order structure and enzymatic activity. An activity staining on Native-PAGE can be used to locate superoxide dismutase activity. The method developed by Beauchamp and Fridovich {Beauchamp, 1971 #2134} is based on the photochemical production of superoxide anions by riboflavin and TEMED, which reacts with nitroblue tetrazolium (NBT) producing insoluble blue formazan. SOD bands will appear colorless against a dark blue background of the gel caused by the precipitation of blue formazan.

The protocol consisted in soaking in dark conditions the native gel in NBT solution 2,45 mM for 20 minutes, then was kept 15 minutes in dark in buffer potassium phosphate 36 mM pH 7.8 containing TEMED 28 mM, riboflavin $2.8x10^{-5}$ M. At this point the gel was illuminated to catalyze the photochemical reaction until the colourless bands corresponding to SOD activity appeared on a dark blue background.

2.2.8 Determination of manganese concentration

Superoxide dismutase 2 is a manganese containing enzyme, hence the quantification of the metal content after the purification is important. The manganese quantification was performed in collaboration with Prof. Carlo Barbante at the University of Venezia with an inductively coupled plasma-mass spectrometer (ICP-MS) (7500, Agilent Technologies). An internal calibration standard curve was performed: a manganese standard solution was added at different concentrations to protein sample with a fixed concentration. Once the manganese was quantified, the intercept value obtained from the internal standard was corresponding to the count per second (that is the number manganese atoms detected in a second) of manganese bounded to the protein. The ratio between this number and the slope of the internal standard curve will give the manganese concentration in ppb.

2.2.9Reaction of dopamine quinones with superoxide dismutase 2

The interaction between dopamine quinones and wild type superoxide dismutase 2 were performed at different ratio of dopamine:SOD2 from 1:1 to 1:5, where at ratio 1:1 there is one dopamine quinone for one monomer of SOD2. In the case of SOD2 mutants the ratio used was halved. To induce dopamine oxidation, tyrosine was added to the buffer. In the table 2.7 are indicated the concentration used. The reaction were kept for 1 hour at 25 °C.

When it was necessary, to the reactions of SOD2:dopamine 1:1, 1:2 and 1:3, after one hours of incubation, dopamine at the same initial ratio was added and the reactions were kept for another hour at 25°C. The procedure was repeated for 5 times giving raised to the reactions called (1:1)x5, (1:2)x5 and (1:3)x5.

Ratio dopamine:SOD2 1:1	**Ratio dopamine:SOD2 1:2**
Dopamine 40µM	Dopamine 40µM
Buffer Tris-HCl 50mM pH 7.8	Buffer Tris-HCl 50mM pH 7.8
Tyrosinase (Sigma) 2.,5 units	Tyrosinase (Sigma) 2.5 units
SOD2 40µM	SOD2 80µM
Ratio dopamine:SOD2 1:3	**Ratio dopamine:SOD2 1:5**
Dopamine 40µM	Dopamine 40µM
Buffer Tris-HCl 50mM pH 7.8	Buffer Tris-HCl 50mM pH 7,8
Tyrosinase (Sigma) 2.5 units	Tyrosinase (Sigma) 2.5 units
SOD2 120µM	SOD2 200µM

Table 2.7 Interaction between dopamine quinones and superoxide dismutase 2 at different ratio in 100 µl.

2.2.10 UV-visible spectroscopy of dopamine oxidation

Dopamine oxidation in the presence or absence of superoxide dismutase 2 was monitored with a spectrophotomer (diode array Agilent 8453 UV-visible). The experiment were performed in buffer Tris-HCl 50 mM pH 7.8 and spectra were recorded at 25°C every 5 minutes for an hour. The reaction were performed in a total volume of 100 µl as indicated below in table 2.8.

Dopamine oxidation	***Dopamine oxidation:SOD2 (ratio 1:1)***
Dopamine 40 µM	Dopamine 40µM
Buffer Tris-HCl 50 mM pH 7,8	Buffer Tris-HCl 50 mM pH 7.8
Tyrosinase (Sigma) 2,5 units	Tyrosinase (Sigma) 2.5 units
	SOD2 40µM

Table 2.8. Reaction mixtures of dopamine oxidation in the presence or absence of SOD2 for UV-visible spectroscopy kinetics.

2.2.11 Reversed-phase HPLC chromatography (RP-HPLC) and Mass Spectrometry analysis

Reversed phase is another type of chromatography where the separation mechanism in depends on the hydrophobic binding interaction between the protein present in the mobile phase and the immobilized hydrophobic ligand of the stationary phase. The column was connected to High Performance Liquid Chromatography (HPLC) (Agilent) The column used was a Jupiter 5µ C4 300 Å, 150 x 4,60 mm (Phenomenex) with a stationary phased composed by hydrophobic alkyl chains ($-CH_2-CH_2-CH_2-CH_3$) that interact with the analyte. The proteins were loaded into the column in mobile phase A (H_2O mQ, trifluoroacetic acid (TFA) 001%). To elute the proteins a linear gradient of mobile phase B contains high concentration of acetonitrile, the organic solvent (modifier), is usually applied. Mobile phase B (HPLC grade Acetonitrile (Carlo Erba), TFA 0085 %**)** decreases the polarity of the solvent increasing the hydrophobicity, so bounded proteins can desorb from the stationary phase according to their individual hydrophobicity. In the case of SOD2, the elution was achieved with a linear gradient of mobile phase B from 43 to 48% in ten minutes.

The run method used at flow of 0.6ml/min was the following:

Time	% of mobile phase B
0	5
5	5
10	43
20	48
22	95
27	95
28	5
32	5
38	5

The eluted proteins were collected and analyzed by Patrizia Polverino De Laureto (CRIBI, University of Padova) with a Q-Tof Micro (Micromass, Manchester, UK) Mass spectrometer.

2.2.12 Detection of quinoproteins by redox-cycling staining

The method for detection of quinoproteins was developed by Paz (Paz et al., 1991) and is based on the oxidation of glycine by quinones at an alkaline pH producing superoxide. The superoxide reacts with nitroblue tetrazolium reducing it to blue formazan, which precipitates allowing the detection of quinones bounded on proteins on a nitrocellulose membrane.

The protocol of quinoproteins staining required the separation of protein with SDS-PAGE (see 2.2.5), then the proteins were immobilized by electroblotting on a nitrocellulose membrane. The gel and the nitrocellulose membrane (Whatman) were pressed together between buffer-wetted filter papers forming the sandwich, which was placed in the mini tank submerged of transfer buffer (Tris-HCl 25mM pH 8.3, glycine 192mM, methanol 20% (v/v) and SDS 0.1% (w/v)). The running takes 90 minutes at 50 volts or overnight at 30 volts at 4°C to dissipate the heat generated during the transfer. After the blotting, the nitrocellulose membrane was stained with an anionic dye, Ponceau (Ponceau S 0.1% (w/v) in 5% acetic acid), to visualize all the proteins, then the dye was washed away with H_2O mQ. The membrane was soaked in NBT solution (NBT 0.24mM in potassium glycinate 2M, pH 10) for 45 minutes in dark condition resulting in a blue-purple stain of quinoprotein bands and no staining of other proteins. The nitrocellulose was washed and stored in sodium borate 0.1M, pH 10, at 4 °C.

2.2.13 Two-dimensional gel electrophoresis (2-DE or 2-D electrophoresis)

This technique separate proteins in two steps, according to two independent properties. The first-dimension is isoelectric focusing (IEF), which separates proteins according to their isoelectric points (pI); the second-dimension is polyacrylamide gel electrophoresis and separates proteins according to their molecular weights (MW). At the end of the protocol, proteins are stained and each spot on the resulting two-dimensional gel corresponds to a single protein species in the sample.

The IEF is performed on an immobilized pH gradient, hence, when an electric field is applied, the protein will migrate in the pH gradient where its net charge is zero. The immobilized pH gradient is formed using a gradient of basic and acidic buffering groups called immobilines, which are covalently incorporated into a polyacrylamide gel casted onto a plastic support. The sample composition is critical for IEF, it is important to prepare a sample with low salt concentration because high conductive solutions will interfere with the isoelettric focusing. For this reason 70 µg of SOD2 in buffer Tris-HCl 50 mM pH 7.8 and 70 µg of SOD2 after the reaction at ratio 1:1 with dopamine were precipitated over night at -20°C with ice-cold acetone at 80%. The proteins were spun down at 15000 g for 10 minutes and resuspended in 250 µl of rehydratation buffer (Urea 8 M, Thiourea 2M, alkyl amidosulfobetaine ASB-14 1 %, IPG BUFFER (pH 3-10) 0.5 % and bromophenol blue 0.0002% (w/v). Just prior the use 3-[(3-cholamidopropyl)dimethylammonio]-1-propanesulfonate CHAPS 2 % and DTT 20 mM were added).The resuspended sample was placed in the ceramic strip holder on which the Immobiline DryStrip gels 3-10 pH of 13cm length (GE Healthcare) with gel-side down. The strip was overlayed with Immobiline DryStrip Cover Fluid (GE Healthcare) to minimize evaporation. The strip holder was placed on a Ettan IPGphor II (GE Healthcare) and the following IEF program was run:

Step	Voltage (V)	Step duration
1 - rehydratation	30	11 hours
2 - focusing	200	1 hour
3 - focusing	200 to 3500	30 minutes
4 - focusing	3500	3 hours
5 - focusing	3500 to 8000	30 minutes
6 - focusing	8000	4 hours

The running conditions were the following: temperature 20 °C; current 50 μA per strip. The resolving gel of the second dimension was prepared as indicated below:

Resolving gel:
Acrylamide solution* 12%
Tris-HCl 0,375M pH 8.8
Urea 8M
APS 0.1%
TEMED 0.008%

*The acrylamide solution is composed by acrylamide:bis-acrylamide ratio 37,5:1.

After IEF to gel equilibration the Immobiline DryStrip gel was equilibrated in SDS equilibration buffer (Tris-Cl 50mM, pH 8.8, urea 6M, glycerol 30% (v/v), SDS 2% (w/v). Just prior the use DTT 140 mM) for 20 minutes and then in the same buffer with iodoacetamide 135mM and bromophenol blue 0.002% (w/v) in absence of DTT for 20 minutes. The strip was loaded onto the top of the prepared gel in an hot solution of superior buffer with agar 3%. Then the gel was inserted in the electrophoresis apparatus, the superior tank was filled with superior buffer (Tris-HCl 25mM pH 8.3, glycine 192mM, SDS 0.1%) and the electrophoresis apparatus was immerged in the inferior buffer (Tris-HCl 25mM pH 8.3, glycine 192mM) in the tank. The electrophoresis separation was carried at 5 mA for an hour, then the intensity of the current was increased at 12 mA over night.

After the electrophoresis the gel was soaked for at least 3 hours in colloidal Coomassie staining solution (blue brilliant Coomassie G-250 0.1% (w/v), methanol 25% (v/v), acetic acid 5% (v/v)). After staining, the gel was immersed in destaining solution (methanol 5% (v/v), acetic acid 7.5% (v/v)) until the stained spots were visible on a colorless background. The 2-DE can be stored in acetic acid 5% (v/v).

2.2.14 Superoxide dismutase enzymatic activity assays

Superoxide enzymatic activity assays require a source of superoxide anions and a system for detecting it. Two types of enzymatic assays have been performed: the first one was pyrogallol assay, an indirect assay and the second one was pulse radiolysis, a indirect assay.

2.2.14.1 Indirect assay: pyrogallol assay

Pyrogallol solution was prepared in dark condition because the molecule is photosensitive. A volume of 8 ml of water and 30 mg of pyrogallol mixed anaerobically in a glass tonometer to prevent to prevent pyrogallol auto-oxidation. The exact concentration of pyrogallol was checked spectrophotometrically measuring the absorbance at 267 nm and based on the molar extinction coefficient 1290,8 $M^{-1} \cdot cm^{-1}$. The enzymatic assay is based on the dismutation of superoxide that is formed during the auto-oxidation of pyrogallol and that is responsible for the further oxidation of the molecule. Thus, the assay was performed in 3 ml of air equilibraterd buffer Tris-HCl 50mM pH 8,2 in the presence of EDTA 1mM and catalase (Sigma) 1 μM. When an aliquot of anaerobic pyrogallol stock solution was added to the assay medium, to yield a final concentration of 0,2 mM the auto-oxidation started and was followed by mesuring the absorbance at 420 nm with a diode array Agilent 8453 UV-visible spectrophotometer for 130 seconds. Each measurement was repeated three times and data were elaborated between 60 and 120 seconds because the reaction is linear in this range. In the case of superoxide dismutase one unit is defined as the amount of enzyme required to inhibit the auto-oxidation of pyrogallol by the 50 %. The percentage of inhibition and the units of SOD were calculated according to {McCord, 1999 #2202}:

$$\% \text{ inhibition} = \frac{|\text{blank slope} - \text{sample slope}|}{\text{blank slope}} \text{ X } 100$$

$$\text{Units of SOD} = \frac{\% \text{ inhibition}}{(100 - \% \text{ inhibition})}$$

2.2.14.2 Direct assay: pulse radiolysis

This assay involves the direct production of superoxide anions by pulse radiolysis. Pulse radiolysis experiments were performed in collaboration with Dr. Diane Cabelli at the Brookhaven national laboratory, NY using a 2Me Van der Graaf accelerator in order to produce electrons which are pulsed in solution causing the production of superoxide anions. The electrons were pulsed in a

cuvette cointaing the protein in buffer Tris-HCl 45mM pH 7.8 in the presence of 200 mM sodium formate as hydroxyl radical scavenger. Once electrons are pulsed in the water solution the following species appear:

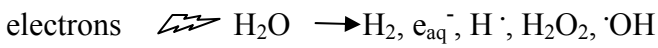

In a solution containing formate and molecular oxygen the primary radicals (OH, e_{aq}^- and H) are converted to O_2^- by the principal following reactions:

$$e_{aq}^- + O_2 \rightarrow \mathbf{O_2^{\cdot -}}$$

$$H^{\cdot} + O_2 \rightarrow HO_2^{\cdot}$$

$$OH + HCO_2^- \rightarrow H_2O + CO_2^-$$

$$CO_2^- + O_2 \rightarrow CO_2 + \mathbf{O_2^{\cdot -}}$$

$$O_2^{\cdot -} + H^+ \leftrightarrow HO_2^+ \text{ , pK = 4,8}$$

The total amount of O_2^- generated during pulse-radiolysis was established using the KSCN dosimeter assuming that $(SCN)_2^-$ has a *G* value of 6,13 and $\varepsilon_{472\ nm}$ = 7590 M^1cm^{-1}. Rates were measured by two methods: the first generating substoichiometric O_2^- concentrations and following the disappearance or appearance of Mn^{3+} SOD at 350-650 nm as Mn^{3+} SOD has an absorbance maximum at 480 nm with an extinction coefficient of 800 M^{-1} cm^{-1}; the second following the disappearance of O_2^- at 260 nm under catalytic conditions. The concentration of proteins used for first method was about 100 µM while for the second was about 1 µM. To elaborate and compare the data between the wild-type, the mutants and the dopamine treated samples manganese concentration of each sample was determined with atomic absorption. Data were fitted using the Numerical Integration of Chemical Kinetics program in PRWIN (by H. Schwarz, BNL) and assuming the dismutation mechanism reported in the introduction (1.2.2.8).

2.2.15 Limited proteolysis

SOD2 (50µg) and SOD2:dopamine at ratio 1:1 (50µg) were incubated in HCl 10mM in the presence of pepsin:protein 1:1000 for 45 minutes in total volume of 400µl. The reaction was blocked by the addition of ammonia 3% 250µl. Just prior to load the reactions products obtained on a C18 Jupiter 5µ 300A column 250x4.60 mm 5 micron (Phenomenex) connected to a HPLC system (Agilent), 350µl of TFA 5% were added to the sample. Mobile phase A and B are the same used for the separations of proteins with C4 column (see 2.2.11). The run method used at flow of 0.8ml/min was the following:

Time	% of mobile phase B
0	0
5	0
20	20
35	25
60	50
62	95
65	95
70	0

The eluted protein peptides were collected and analyzed by Patrizia Polverino De Laureto (CRIBI, University of Padova) with a Q-Tof Micro (Micromass, Manchester, UK) Mass spectrometer.

2.2.16 Circular dichroism (CD)

The CD measurements were recorded on a JASCO J-715 (Tokyo, Japan) spectropolarimeter in buffer Tris-HCl 50mM pH 7.8. In the case of the reactions of SOD2 with dopamine (performed as indicated in 2.2.9) a CD spectrum was recorded before starting the incubation with dopamine and tyrosinase. The signal-to-noise ratio was improved by accumulating four scans with a scanning speed of 10nm/min for each sample and the final spectra were obtained by subtracting the appropriate background. Far-UV CD spectra (190-260 nm) were performed in 200 µl of total volume using a 0,1 mm pathlength quartz cell and a protein concentration of 10 µM. Near-UV CD spectra (260-320 nm) were performed in 500 µl of total volume using a 1 cm pathlength quartz cell and a protein concentration of 17 µM. The CD signal was normalized for the pathlength of the cell and the protein concentration. In particular CD data are presented in terms of ellipticity [θ] ($deg \cdot cm^2 \cdot dmol^{-1}$). The mean residue ellipticity [θ] was calculated with the following formula: $[\theta] = (\theta_{obs}/10) \cdot (MRW \times l \times c)$, where θ_{obs} is the

observed ellipticity in deg at a specific λ, MRW is the mean residue molecular weight (molecular weight of the protein divided by the number of peptide bonds), *l* the optical pathlength in cm and *c* the protein concentration in $mg \cdot mL^{-1}$.

2.2.17 Radioactivity assay

The reactions were performed in a total volume of 20 µl in buffer Tris-HCl 50mM pH 7.8 in the presence of ^{14}[C]-dopamine (Sigma, 50µCi/µmol) and kept for 1 hour at 25°C. Different ratio of protein dopamine were analyzed such as 1:1 and 1:2 for the wildtype and the same ratio halved for the mutants, as indicated below:

	1:1	**1:0,5**		
	Wild-type	**C140A**	**C196A**	**C140A/C196A**
Protein	100 µM	100 µM	100 µM	100 µM
Dopamine	50 µM			
^{14}[C]-Dopamine	50 µM	50 µM	50 µM	50 µM
Tyrosinase	0,75 units	0,75 units	0,75 units	0,75 units

	1:2	**1:1**		
	Wild-type	**C140A**	**C196A**	**C140A/C196A**
Protein	100 µM	100 µM	100 µM	100 µM
Dopamine	100 µM			
^{14}[C]-Dopamine	100 µM	100 µM	100 µM	100 µM
Tyrosinase	1,5 units	1,5 units	1,5 units	1,5 units

The reaction products (2 or 4 µl of each reaction) were separated by 13% SDS-PAGE and stained with coomassie (see 2.2.5). After staining the gel was soaked 30 minutes in Amplify™ Fluorographic Reagent (GE Healthcare) to increase the detection efficiency. It was dried on a vacuum gel drying rack and radioactivity was detected by autoradiography: the dried gel was kept at -70 °C with preflashed HyperFilm MP (GE Healthcare) for 12 hours or 60 hours to detect the ^{14}[C]-dopamine.

3. Results

3.1 Cloning of the cDNA of Superoxide dismutase 2

The cDNA of superoxide dismutase 2 was purchased from ImaGenes GmbH (Berlin, Germany), cloned between the *SalI* e *NotI* restriction sites in the pCMV-Spot6 vector (fig.3.1).

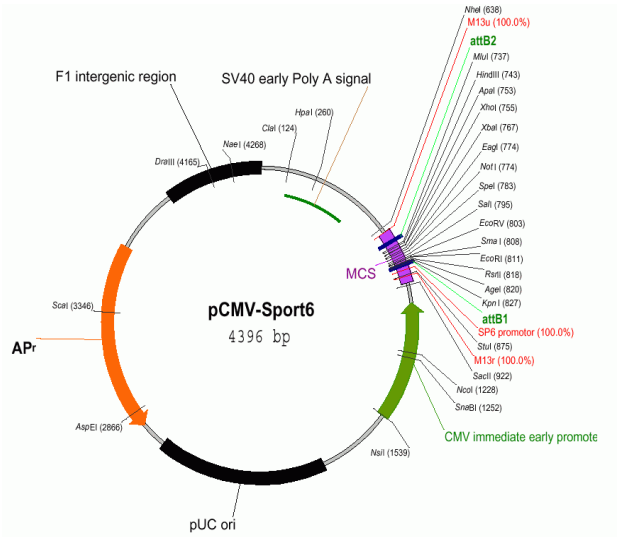

Figure 3. 1. Scheme of the pCMV-Sport6 vector containing the cDNA sequence of SOD2 inserted between the SalI and NotI restriction sites.
The cDNA of SOD2 comes from the library NIH_MGC_68 of human lung carcinoma.

Since the pCMV-Sport6 is a vector not suitable for expression of proteins in *E.coli*, it was necessary to clone the cDNA of SOD2 in another vector, the pET28a+. To this aim, the cDNA was amplified using a variant of PCR, which enables the insertion of restriction sites at the protein sequence termini useful for the pET28a+ cloning. The restriction site chosen for the cloning were *NcoI* and *XhoI*, corresponding to the primers FOR-NcoI and REV-XhoI. It was decided to perform another cloning of SOD2, a cloning allowing to obtain the histidine tag (His-tag) at the N-terminal of protein. The rational of two cloning was to circumvent a potential interference of endogenous SOD's *E.coli* in the purification of the protein without the tag. The His-tag would allow a rapid and simple one step purification with an IMAC column and it can be easily removed after the purification.

Since the multiple cloning site of pET28a+ (fig. 3.2) provides the His-tag sequence downstream of the *NcoI* restriction site, it was enough to choose a restriction site downstream the tag, that is *NdeI*. Therefore, it was performed a second PCR with the primer FOR-NdeI and REV-XhoI to insert the NdeI and XhoI sites. All FOR primers were projected on the SOD2 sequence, excluding the mitochondrial signal sequence.

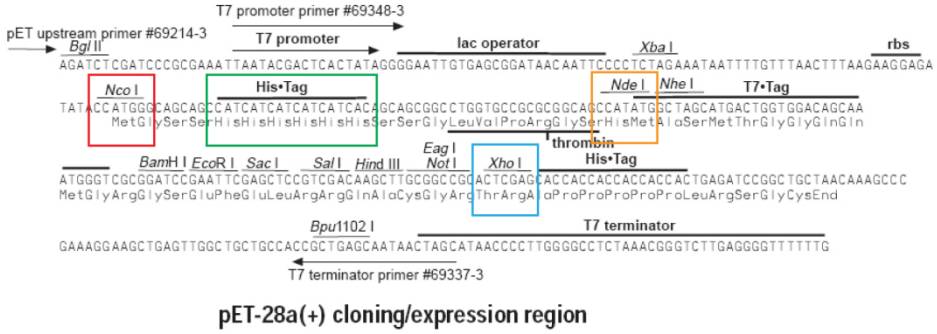

Figure 3.2. The multiple cloning site of pET28a+.
The first cloning was based on the NcoI (in red) and XhoI (in blue) site with the purpose to eliminate the tag. A second cloning included the histidine-tag highlighted in green and was based on the NdeI (in orange) and XhoI (in blue) restriction sites.

The first temperature of annealing used for the two PCRs was 45°C (fig. 3.3). Since this temperature did not allow to obtain the amplification of the cDNA for the cloning with the sites NcoI and XhoI, the temperature was decrease to 43°C to enable the annealing of the primers obtaining the amplification of both PCR inserts. The dimension of the PCR fragments were: 639bp for the insert amplified with primers FOR-NdeI and REV-XhoI; 641bp for the other obtained with primers FOR-NcoI e REV-XhoI, hence in gel electrophoresis the PCR products were comprised between 600bp and 700bp (fig. 3.3). The PCR products were digested with the appropriate restriction enzymes, purified and quantified with electrophoresis on agarose gel.

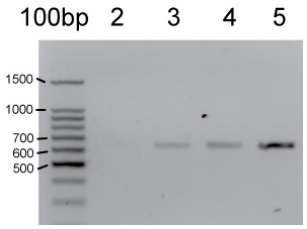

Figure 3.3. Gel electrophoresis of SOD2 PCR products obtained from the SOD2 cDNA inserted in the pCMV-Sport6 vector.
First lane: 100bp molecular weight marker; lanes 2 and 4: PCR product for the cloning with NcoI – XhoI; lanes 3 and 5: PCR product for the cloning with NdeI – XhoI. For every PCR two melting temperatures were tested: 45°C (lanes 2 and 3) and 43°C (lanes 4 and 5).

The pET28a+ vector was restricted with *NdeI-XhoI* and with *NcoI-XhoI* to obtain cohesive ends with the PCR inserts for the two cloning (fig. 3.4).

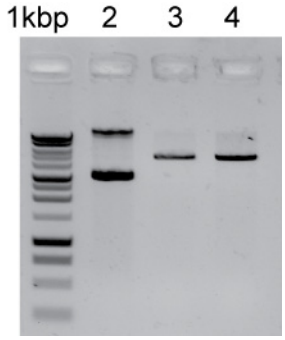

Figure 3.4. Gel electrophoresis of the enzymatic restrictions of pET28a+ vector.
First lane: 1kbp molecular weight marker; lane 2: pET28a+ not restricted as control; lane 3: the vector digested with NdeI and XhoI enzymes; lane 4: the restriction with NcoI and XhoI enzymes.

The vector was dephosphorylated two times to prevent its recircularization during the ligation and quantified. The ligation was performed using a ratio pET28a+ vector:insert 1:3 for the two cloning. Besides the ligation, the autoligation, which consist in the incubation of the digested vector without the insert, was prepared as negative control. Then, the ligation products were used to transform the chemically competent DH5α cells. The presence of kanamycin on the agar LB plates enabled the growth of the cells, which had taken the pET28a+. The results of the ligation are listed in table 3.1.

	Cloning NcoI-XhoI	**Cloning NdeI-XhoI**
Autoligation	0 colonies	0 colonies
Ligation 1:3 (vector:insert)	12 colonies	15 colonies

Table 3.1. Number of colonies grown after the bacterial transformation for the two cloning.

The absence of bacterial colonies on the plates of autoligation (table 3.1) was a positive indication of the cloning outcome. However to be certain of the presence of the insert inside the pET28a+ vector, a PCR colonies screening was performed. For the screening the universal T7 primers were used because their complementary sequences are located at the ends of the multiple cloning site of pET28a+ (fig. 3.2); hence, the PCR will amplify, if present, the insert. The calculated expected lengths of the PCR products were: 806bp for the insert NdeI-XhoI and 749bp for NcoI-XhoI. To verify the presence of the insert, the screening PCR products were analyzed in a gel electrophoresis (fig.3.5).

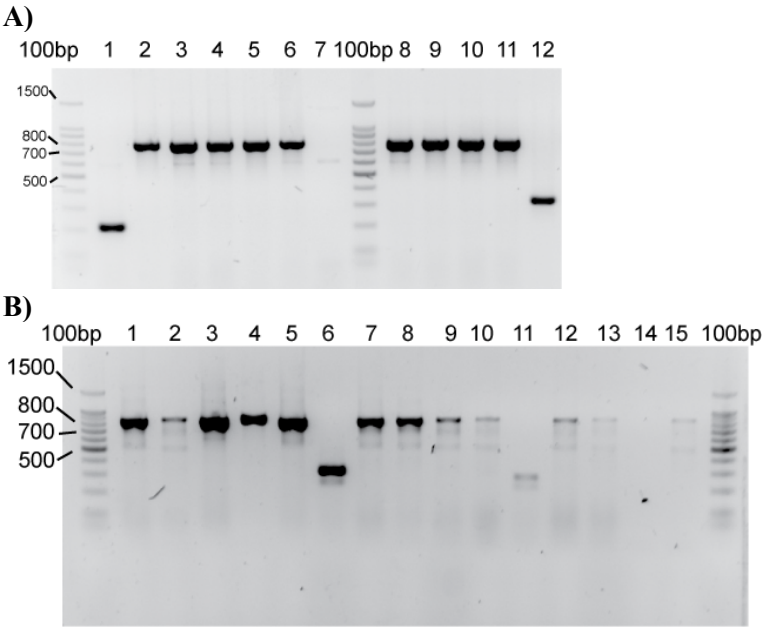

Figure 3.5. Screening of DH5α colonies of the two cloning in pET28a+. The 100bp molecular marker is indicated in the corresponding lanes and the arabic numbers on the lanes denote the different colonies.
*In gel **A** the screening of the cloning NcoI – XhoI is shown. The length of the expected fragment is of 749bp, thus the positive colonies are 2,3,4,5,6,8,9,10 and 11.*
*In gel **B** the screening of the cloning NdeI – XhoI are shown. The expected length of the fragment is of 806bp , thus the positive colonies are 1,2,3,4,5,7,8,9,10,12,13 and 15.*

A total of 9 colonies resulted positive for the cloning NcoI-XhoI (fig. 3.5 A) , while 12 for NdeI-XhoI (fig. 3.5 B). One colony for each cloning was grown in LB, the pET28a+ vector containing the cDNA of SOD2 was extracted and sequenced. The obtained sequence demonstrates the absence of sequence errors inserted by the DNA polymerase. The vectors obtained with the two cloning were called: pET28a+ SOD2 and pEt28a+ his-tag SOD2.

3.2 SOD2 wild-type expression and purification

3.2.1 SOD2 expression and purification

E.coli BL21 (DE3) cells were transformed with pET28a+ SOD2 and the protein expression was tested. Few colonies were inoculated in flasks with 50ml LB supplemented with kanamycin and, once the culture had reached the exponential phase of growth, different concentration of the inducer, IPTG (0.1mM, 0.25mM, 0.5mM and 1mM) were added. A sample of culture was taken before, during and after the overnight expression and was analyzed with SDS-PAGE to check the level of protein expression (fig. 3.6).

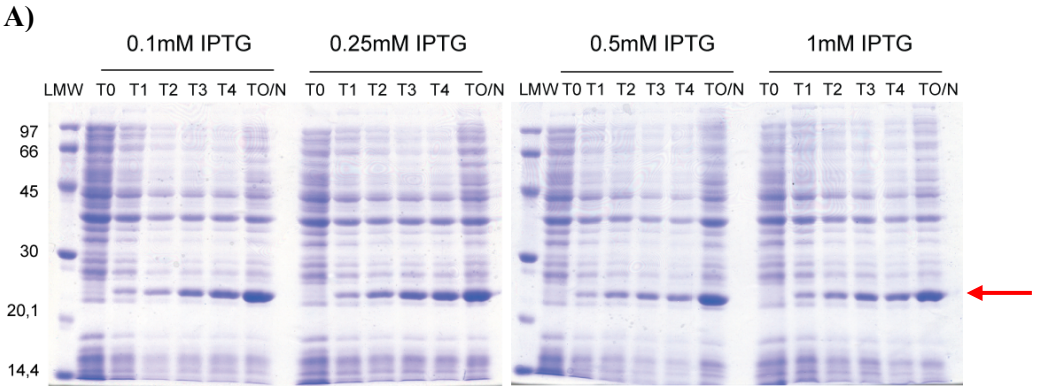

Figure 3.6: Time course of expression test of SOD2 using different concentrations of IPTG. The red arrow indicates SOD2 protein.
A) *SDS-PAGEs of the protein expression test. At the top of the gels the different concentrations of IPTG used for induction are indicated. The lane T0 corresponds to the culture before the IPTG induction while T1, T2, T3 and T4 are cultures 1,2,3 and 4 hours after the induction. O/N shows the situation after an overnight induction.*
B) *Growth curve of BL21 (DE3) cells after induction with 0,1mM IPTG.*

Manganese was supplied in the culture as previously reported in the literature, since induced cultures with no added manganese show lower superoxide dismutase activity and an increased fraction of insoluble SOD2 (Beck et al., 1988). As shown by the SDS-PAGE (fig. 3.6), the increase of IPTG did not lead to an increase of protein production, hence it was decided to use the lower IPTG concentration tested (0.1mM). In contrast, a time dependent effect is evident suggesting to induce over night the expression of protein.

To purify the protein the protocol of Beck and co-workers was used as starting point (Beck et al., 1988). Samples of the purification steps were analyzed on SDS-PAGE (fig. 3.7). The membrane disruption was obtained mechanically by sonication of the cells. Then, the supernatant was heated at 60°C for 40 minutes enabling the removing of the majority of the contaminant proteins. Other contaminants were eliminated with the first step of 45% ammonium sulphate precipitation. The second step of precipitation at 90% ammonium sulphate resulted in the precipitation of about the 90% of SOD2. The protein was resuspended in buffer, dialysed and loaded onto an anionic exchange column.

SOD2 did not bind to the anion exchanger, hence it eluted in the flow through, while other proteins were retained to the stationary phase.

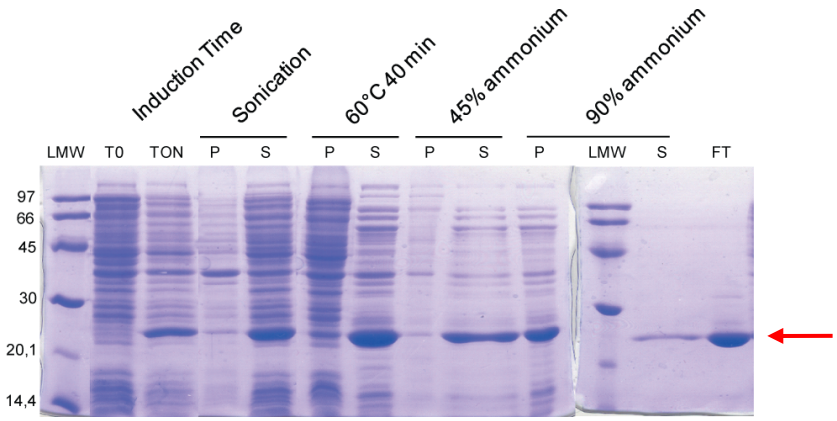

Figure 3.7. SDS-PAGE analysis of expression and purification of recombinant SOD2 (cloned without His-tag) from BL21 (DE3) cells.
The red arrow indicates SOD2 protein.
LMW: molecular weights markers. T0 and TON denote the crude extract obtained from E. coli cells before and after an overnight induction with IPTG 0.1 mM. P and S refer to the pellet and supernatant after sonication, after the step at 60°C, after precipitation with ammonium sulphate at 45% and 90 % saturation. FT is the flow through of the anionic exchange chromatography.

Escherichia coli genome encodes for three homodimeric superoxide dismutase enzymes, called FeSOD, MnSOD and Cu/ZnSOD. As suggested by their names, the first contains iron as cofactor, while the second manganese and the third copper and zinc. The copper zinc enzyme is localized in the periplasma whereas the other two are found in the cytoplasm (Benov et al., 1995; Carlioz et al., 1988; Takeda and Avila, 1986). Since the *coli*'s enzymes displays an identity percentage of about 40% in comparison with the human enzyme, it was necessary to verify if any of the *coli*'s SOD co-purify with the recombinant human enzyme (Parker and Blake, 1988). To this aim the purification protocol was applied to a culture of BL21(DE3) cells transformed with the empty vector. At the end of the purification, the flow though of the anionic exchange was loaded on a native-PAGE, which was stained with Coomassie revealing the presence of one protein band (fig. 3.8). Superoxide dismutase activity staining allowed to identify this protein as an *E.coli*'s superoxide dismutase (fig.3.8). Therefore, this protocol led to the co-purification of an endogenous *E. coli*'s SOD with the cloned human enzyme.

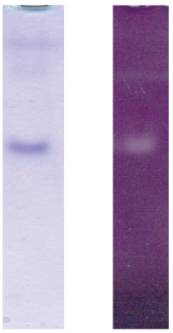

Figure 3.8. Native-PAGE after application of the purification protocol starting from E.coli BL21(DE3) cells transformed with pET28a+ empty vector.
The flow through from anionic exchange chromatography was loaded into a native-PAGE. The gel was stained with Coomassie brilliant blue (left) and for superoxide dismutase activity to demonstrate the presence of endogenous SOD.

One of the objectives of this thesis was to study the enzymatic activity of SOD2 after the incubation with dopamine-quinones. It was clear that the presence of another SOD enzyme could interfere such measurements. For this reason it was decided to set up a new protocol of purification using the pET28a+ his-tag SOD2 vector in order to set up an alternative method to avoid contamination with endogenous SOD.

3.2.2 His-tag SOD2 expression and purification

E.coli BL21 (DE3) cells were transformed with pET28a+ his-tag SOD2 and the protein expression was tested as for pET28a+ SOD2. Manganese concentration was the same and different IPTG concentration were used to induce the protein expression, which was monitored with SDS-PAGE (fig. 3.9). From the gel it was clear that the his-tag SOD2 protein presented a higher expression level in comparison with the protein without the tag. In particular, the highest expression level of the protein was reached 1-2 hours after induction but the bacteria continued to grown until an OD_{600} of 2.4, even more than with SOD2 without the His-tag. The expression conditions chosen were the same as for SOD2, namely 0.1mM IPTG for an overnight induction time.

A)

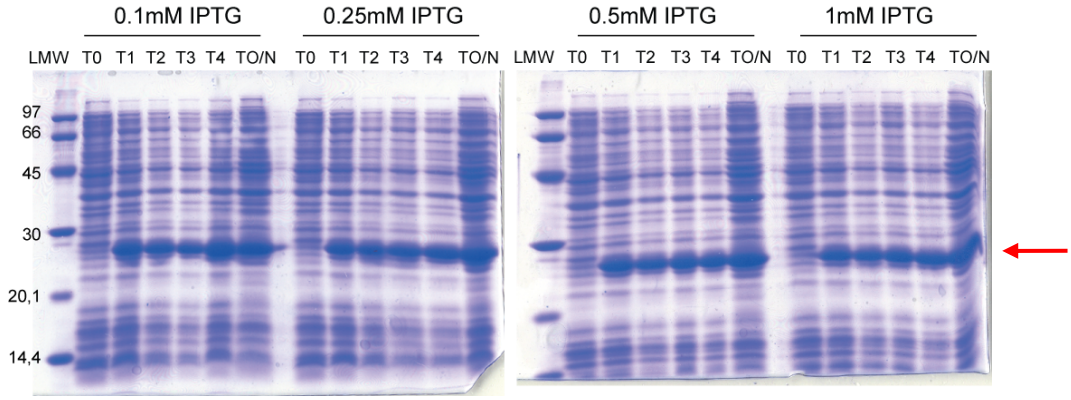

B)

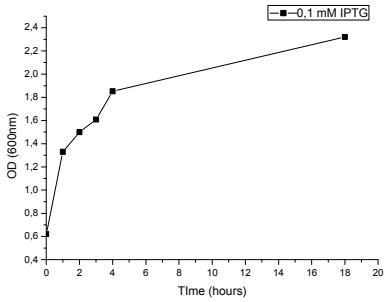

Figure 3.9. Time course of expression test of his-tag SOD2 using different concentrations of IPTG. *The red arrow indicates his-tag SOD2 protein.*
A) *SDS-PAGEs of the protein expression test. At the top of the gels the different concentrations of IPTG used for induction are indicated. The lane T0 corresponds to the culture before the IPTG induction while T1, T2, T3 and T4 are cultures 1,2,3 and 4 hours after the induction. O/N shows the situation after an overnight induction.*
B) *Growth curve of BL21 (DE3) cells after induction with 0,1mM IPTG.*

The sonication was used to disrupt the membrane cells and the protein was purified with an immobilizing ion affinity chromatography (IMAC) exploiting the presence of the histidine-tag, which has an high affinity for the metal ion bounded to the matrix of the column. This affinity interaction is the result of coordination of a nitrogen on the imidazole moiety of polyhistidine with a vacant coordination site on the metal. Thus, the protein bounded to the metals, while the other passed though without interacting with the stationary phase. The imidazole gradient was optimized to elute the protein: 0-500 mM imidazole in 20 minutes (fig.3.10).
As shown in fig.3.10 the protein elutes as a single peak but it was collected in two separated parts called 1 and 2 because the asymmetry of the peak lead to think that other proteins were present**.** This was confirmed as samples from each step of the purification were analyzed by SDS-PAGE (fig.3.11). The first part of the peak presented other proteins while the second one contained only the human recombinant enzyme, hence for the next step only the second part was used for the following purification step. Note that part of SOD2 protein was present as precipitate in the pellet after sonication, this was independent from the number of

sonication cycles. The reason was probably due to high expression level that causing the compartimentalization in inclusion bodies of bacteria cells.

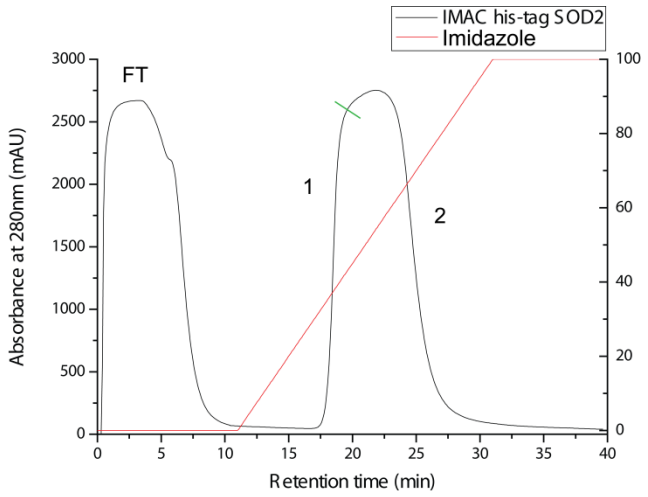

Figure 3.10. Immobilized Metal Affinity Column (IMAC) of his-tag SOD2.
The supernatant of after sonication of the crude extract was loaded into the IMAC The flow trough (FT) peak identify protein pools that are not retained in the column. The imidazole gradient (0-500mM in 20 minutes) used for the elution of SOD2 is shown in red. The protein elutes as a single peak. The green line divides the SOD2 peak in two part: the first part (1) contains also other proteins while the second one (2) contains the only the human recombinant enzyme.

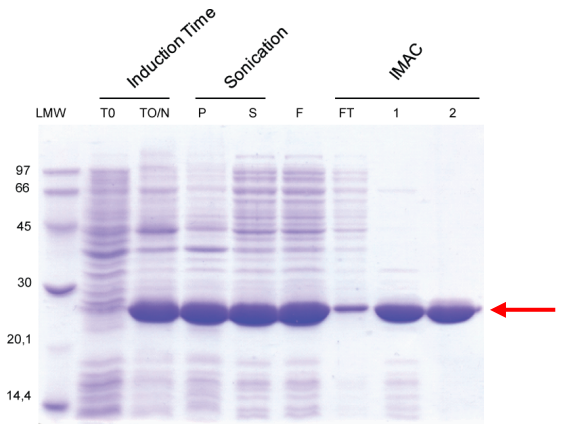

Figure 3.11. SDS-PAGE of wt SOD2 expression and purification.
The red arrow indicates His-tag SOD2 protein. First lane: molecular markers as indicated (LMW); T0: crude extract from cells before induction; TO/N: at the end of the overnight induction with 0,1mM IPTG; P and S: pellet and supernatant after sonication step; F: supernatant filtered with 0,22µm cut-off; FT: flow through from IMAC, 1 and 2: pool 1 and 2 of the elution peak obtained with imidazole gradient (see fig.3.10).

The next step was the removal of the His-tag. To this aim, a thrombin cleavage site is inserted in the vector between the tag and the N-terminal end of the protein. Different concentrations of thrombin protease were tested for different incubation times, analyzing the result on a SDS-PAGE silver stained (fig. 3.12).

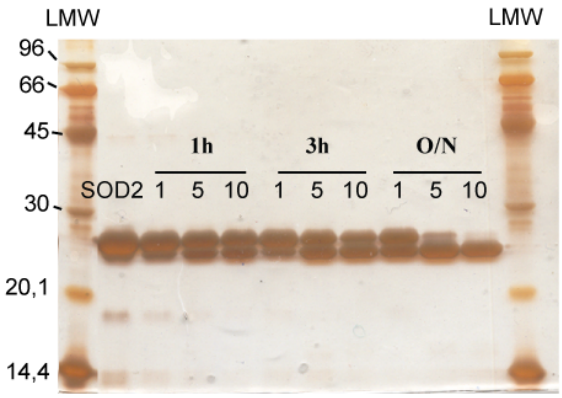

Figure 3.12. SDS-PAGE of the His-tag removal.
One mg of his-tag SOD2 purified by IMAC (see fig. 3.10 and 3.11) was incubated with different units of thrombine 1,5 or 10 (as indicated in the gel) and incubated for 1 hour (1h), 3 hours (3h) or overnight (O/N).

As shown by SDS-PAGE 1 mg protein had to be incubated overnight with 10 units of thrombin enzyme to cleavage the tag efficiently. The cleavage protocol was optimized increasing the incubation time up to 16 hours and decreasing the units of thrombin to 3 for 1 mg of protein. To remove the tag and the uncleaved SOD2, the protein was incubated with cobalt affinity gel, followed by removal of the resin by centrifugation. Cobalt affinity gel works like a IMAC column, hence the his-tag peptide and the uncleaved protein binds to cobalt bound to the beads of the gel.

The yield of human recombinant SOD2 attained with this optimized protocol was of 40-60 mg per liter of culture.

3.2.3 Protein characterization

The characterization of the purified protein is an important step for two reasons: the first one is to evaluate the quality of the produced protein; the second is to investigate if the purified recombinant protein has characteristics comparable to those reported in literature for the purified protein.

A precise molecular mass determination is an important tool to verify if post-translational modifications are present. Since the removal of the his-tag by thrombin leaved a sequence of 4 aminoacids (GSHM) upstream the cDNA of SOD2, the expected molecular weight calculated for a monomer of SOD2 was 22616,6 kDa. In this thesis the cysteine residue are referred as the 140 and the 196 on the basis of the crystal structure but actually the cysteine residues number are 144 and 200 because of these 4 aminoacid. The protein purified was analyzed by

RP-HPLC (fig. 3.13) revealing the presence of two peaks referred to as peak 1 and peak 2, which were collected and analyzed by mass spectrometry measurements in collaboration with Dr. Patrizia Polverino De Laureto (CRIBI, University of Padova). A protein with a molecular weight of 22616,32 kDa was identified in correspondence with the second peak corresponding to SOD2 in agreement with the expected molecular weight for human SOD2. A mass of 22613,90 kDa was present in the first peak corresponding to the expected protein mass less two Dalton.

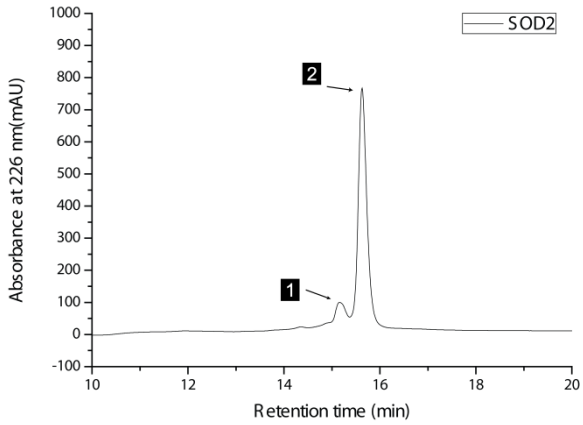

Figure 3.13. RP-HPCL of SOD2. *The protein eluted in two peaks (1,2), which were collected and analyzed with mass spectrometry identifying a molecular mass of 22613,90 kDa in the first peak corresponding to SOD2, while a mass of 22616,32 kDa in the second peak.*

The 2 Da difference of between the two species of SOD2 could correspond to two cysteine residues oxidized to form a disulphide bridge. In native conditions Cys140 and Cys196 present in the human SOD2 sequence do not form any disulphide bridge and its formation would be a problem for the purpose of this thesis that is to investigate the interaction of SOD2 with dopamine-quinones, that involve free cysteinyl residues. To answer to this question the cysteine residues were first reduced with tris(2-carboxyethyl)phosphine (TCEP) and then alkylated, hence blocked with iodoacetamide. The protein was analyzed with RP-HPLC, which still revealed the presence of the first peak with equal proportions. Since the peak with anomalous molecular weight account for the 7% of the protein present and does not involve modification of cysteines and it was not possible to separate the two isoforms with ion exchange chromatography, no further attempts were made to separate the two peaks under non denaturing conditions.

To quantify the protein concentration, the molar extinction coefficient was experimentally determined with the Edlehoch method, which is suggested to be the best method (Pace et al., 1995). The following extinction coefficient of 42846.2M^{-1} cm^{-1} referred to the monomer was determined. This value is very close to 40500M^{-1} cm^{-1}, which is the coefficient reported in literature for the monomer (Greenleaf et al., 2004).

The metal bound to the protein was quantified in collaboration with Prof. Carlo Barbante at the University of Venezia using a ICP-MS, which revealed that 90% of the monomers resulted metal loaded (fig. 3.14, table 3.1).

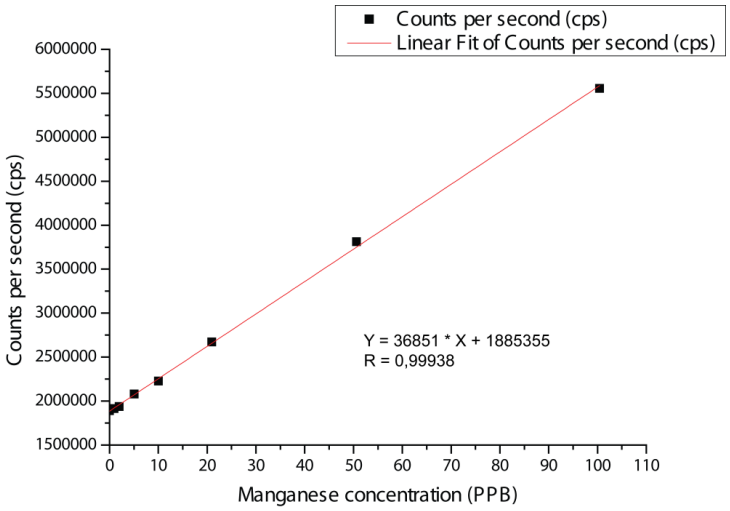

Figure 3.14. Manganese quantification of SOD2 with ICP. *The internal standard calibration with the linear fit is showed.*

		Standard deviation
intercept	1885355.88	17184.89
slope	36370.22	422.76
Manganese concentration (PPB)	51.84	0.02
Manganese concentration (µM)	94.35	0.04
Protein concentration (µM)	104	1
ratio Mn / monomero	0.9	

Table 3.2. Data obtained for ICP-MS measurements.

3.3 Covalent modification of SOD2 induced by dopamine-quinones (DAQs)

Once obtained and characterized the protein, it was possibly to study its interaction with DAQs. To this purpose the recombinant protein and dopamine

was incubated 1 hour at 25°C in the presence of tyrosinase. The addition of tyrosinase to the reaction mixture starts the enzymatic oxidation of dopamine to dopamine-quinones. The advantage of the oxidation reaction catalyzed by this enzyme is to avoid the production of radical species associated to the spontaneous oxidation of dopamine. A necessary control is to verify the direct reactivity of tyrosinase toward the tyrosine residues of SOD2. In this control no reaction of the protein incubated with tyrosinase was observed.

The interaction between SOD2 and DAQs and the nature of the adducts generated was studied with different experimental approaches. The first technique used was UV-visible spectroscopy.

3.3.1 UV-visible Spectroscopy

The oxidation of dopamine generates three quinone species, dopamine-o-quinone (DQ), aminochrome (AC) and indole-5,6- quinone (IQ), which are all potentially reactive in a cellular environment (see 1.2.2.5). This pathway can be followed by optical spectroscopy (fig. 3.15): dopamine, DQ and AC present characteristic UV–vis peaks with absorption maxima respectively at 280 dopamine, 390 (DQ) and 300/480 (AC) nm (Graham, 1978). The UV-vis characterization of IQ remains still elusive. During the tyrosine-mediated oxidation of DA in water solution both, DQ and AC, are visible but at physiological pH, corresponding to the conditions of the experiment, only AC is detectable in the optical spectra with no evidence for the presence of DQ because its cyclization is fast. The time evolution of AC can be easily followed; unfortunately, the quantitative analysis of the decay is hampered by the formation of a black precipitate, melanin, that induces light scattering.

Since dopamine-o-quinone (DQ) is the dopamine-quinone upstream aminochrome (AC), if the protein at ratio SOD2:dopamine 1:1 would interact completely with DQ, the two maxima of AC will not be visible after dopamine oxidation.

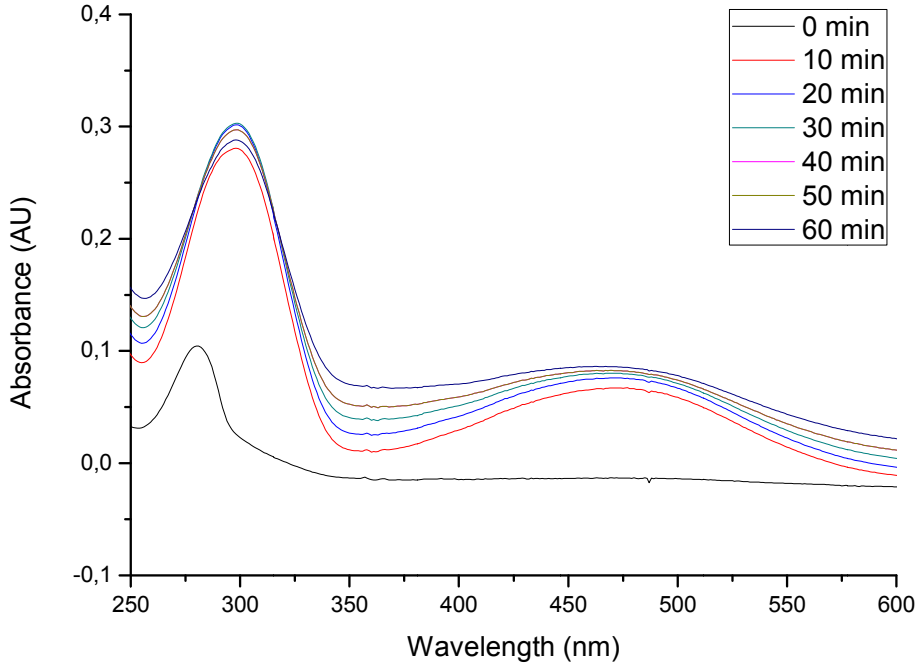

Figure 3.15. UV-visible spectra of dopamine oxidation in the presence of tyrosinase. *Dopamine presents an absorption maximum at 280 nm, upon oxidation two peaks at 300 nm and 475 nm appear corresponding to aminochrome formation.*

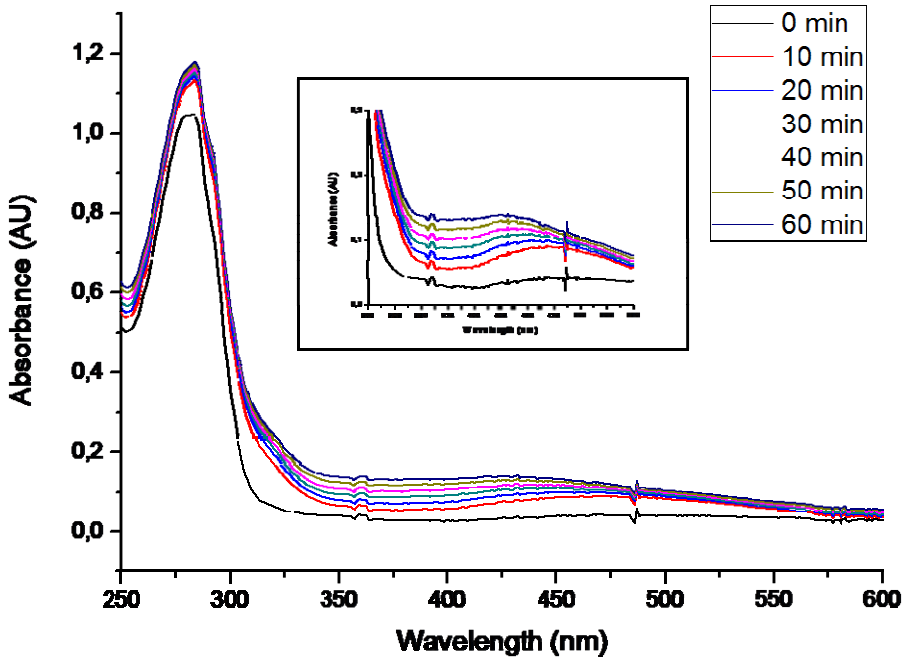

Figure 3.16. UV-visible spectra of dopamine oxidation in the presence of tyrosinase and SOD2 at ratio 1:1 (SOD2:dopamine). *The peak at around 430nm (enlarged in the inset) suggested a interaction of DAQ with SOD2. The formation of AC is visible at 475 nm and this indicates that, if there is an interaction of DAQs with SOD2, the DC would not interact completely with SOD2.*

The analysis of the interaction of DAQs with the protein kinetic (fig. 3.16) was not simple because it showed an increase of the absorbance around 475 nm, indicated the formation of AC. The peak at 300 nm was masked in this experiment by the absorption spectrum of protein, hence it was not possible to obtain informations. Interestingly a maximum peak appeared at around 430 nm that is not present in the kinetic of dopamine oxidation (fig.3.14), this suggested a possible interaction of SOD2 with a DAQ. Since this peak compared after the AC formation, this suggested that AC or a downstream DAQ could interact with the protein. However, this approach is not quantitative and did not allow to define which is the quinone interacting with the protein. In fact, the formation of AC did not allow to exclude that DQ interacts with SOD2, because this interaction could involve only a fraction of DQ. Since the UV-vis spectroscopy kinetics were not exhaustive to define both qualitatively and quantitatively the possible interaction of SOD2 with DAQs, mass spectrometry measurements were carried out after separation .a different approach was used: RP-HPLC and mass spectrometry.

3.3.2 Reversed-phase HPLC and mass spectrometry analysis

The interaction of SOD2 with DAQs lead to the formation of a covalent bond between the quinone and the SOD2. This could modify the superficial charges, hence the hydrophobicity of the protein. Therefore, RP-HPLC could be useful to separate the wild protein from the modified and to identify which DAQ interacts with the protein. SOD2 was incubated with dopamine and tyrosinase at ratio 1:1 for 1 hour at 25 °C, the reaction products were loaded on a C4 column and the chromatogram obtained was compared with that obtained with SOD2 alone (fig. 3.17). The formation of modified SOD2 is suggested by the onset of a protein peak (fig. 3.17, peak 4) with retention time intermediate between peak 1 and 2 of wild type SOD2 (already described in the section 3.2.3). This result, together with the change in the size of peaks 1 and 2, suggested a possible interaction between DAQs and the protein. The ratio SOD2:dopamine was increased from 1:1 to 1:5 to evaluate if such increase of dopamine would modified the distribution of species in the chromatographic profile (fig. 3.17). The chromatogram of the products obtained upon reaction of the SOD:DA 1:5 ratio confirmed a change. The higher retention time peak decreased (fig. 3.16, peak 7) while the one with lower retention time increased (peak 6). Moreover peak 4 observed at a ratio 1:1 is no longer evident and two new peaks at higher retention times appeared.

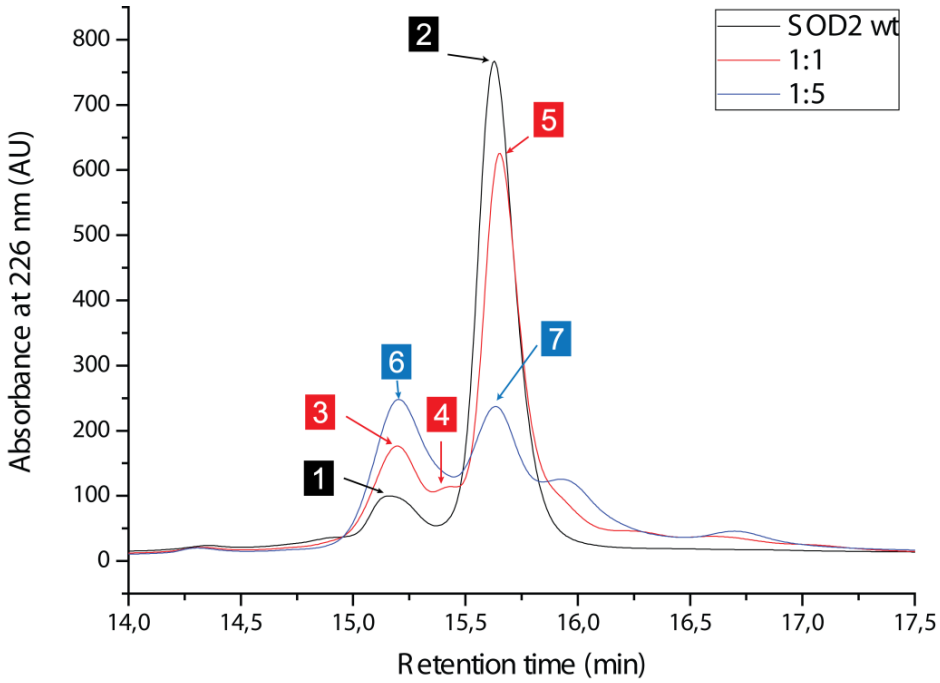

Figure 3.17. RP-HPLC chromatograms of SOD2 and the interaction of SOD2:dopamine at ratio1:1 and 1:5. *All the 7 peaks were numbered from 1 to 7. At ratio 1:1 the size of peak 3 increase with the respect of SOD2 and the peak 4 appeared. If dopamine was increased (ratio 1:5) the size of peak 6 increased further , the peak number 4 present at ratio 1:1 was not present,*

The UV spectra were recorded on the fraction upon elution from the column and analyzed to identify the presence of DAQs (fig. 3.18). Also in this case, SOD2 in the absence of dopamine was used as control (fig. 3.18 A) for experiments with SOD2 with dopamine at ratio 1:1 (fig. 3.18 B) and 1:5 (fig.3.18 C). Comparing the UV-spectra, it can be seen that the peaks 3,6,7 contain proteins with an absorption spectrum from 300 nm to 400, which was not present in the control. This was a further indication of a probably interaction of SOD2 with DAQs.

A)

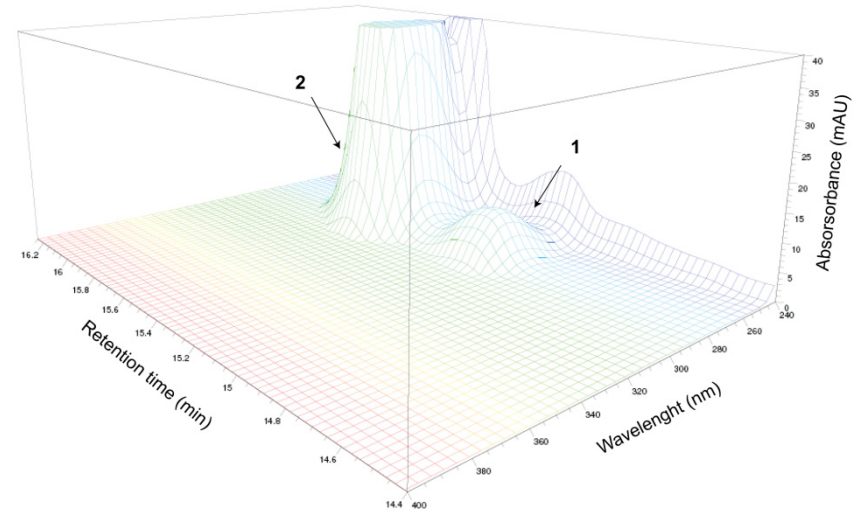

B)

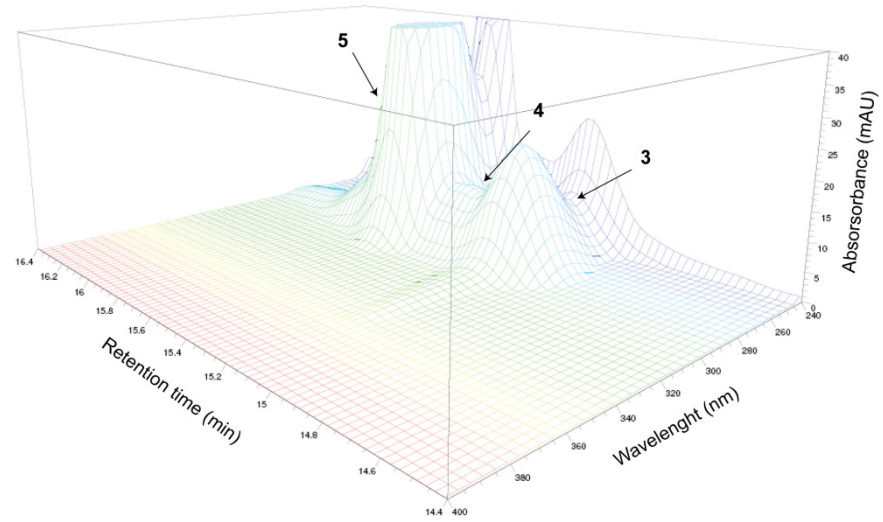

C)

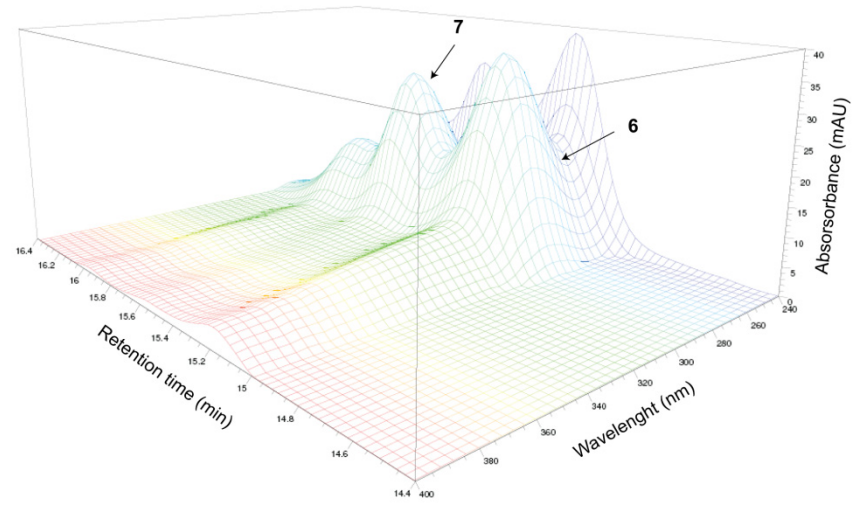

Figure 3.18 3D plots of the fractions of eluted from the C4 column during RP-HPLC, which show the UV-visible spectra. A) SOD2, B) 1:1 and C) 1:5.
The presence of DAQs can be supposed in the peak 3 of ratio 1:1 and peaks 6 and 7 and also in the small peak appeared at ratio 1:5.

To unambiguously identify if the protein was covalently modified after the interaction with DAQs, the solutions corresponding to individual peaks of RP-HPLC were collected and analyzed by mass spectrometry. The molecular weights of protein associated with the different peaks of RP-HPLC are summarized in (table 3.3).

	Peak	Molecular weight (Da)	Modification Mass (Da)
SOD2 wt	**1**	**22613.9±2**	
	2	**22616.3±2**	
1:1	**3**	**22614.1±2** **22758.2±2**	**+ 141.5**
	4	**22616.7±2** **22767.0±2**	**+ 150.3**
	5	**22616.2±2**	
1:2	**6**	**22758.8±2** **22904.1±2**	**+ 142.5** **+ 287.8**
	7	**22616.3±2** **22762.8±2**	**+ 146.5**

Table 3.3. Mass spectrometry analysis of each peak collected from RP-HPLC of SOD2, SOD2 after the interaction with DAQs, ratio SOD2:dopamine 1:1 and 1:5.
All the numbered peaks of RP-HPLC were collected and analyzed with mass spectrometry. The molecular weights found are reported in the table with the mass of the DAQs modifications.

The mass spectrometry analysis found new species upon the incubation with DAQs confirming that SOD2 was covalently modified by DAQs. The new species found were 5. However, variation of +141.5 Da, and +142.5 Da could be assigned probably to the formation of the same specie, within the instrument error. A great heterogeneity of reaction products can be expected on consideration that one cysteine residue of the protein could interact with different quinones, along the formation of IQ. Moreover the presence of specie +287.8 suggested also the interaction of both cysteine residues with one DAQ. The next step was to identify which DAQs interacted with SOD2. The molecular weight of each dopamine-quinone of dopamine oxidation is reported in table 3.4.

Dopamine-quinone	Molecular weight (Da)
Dopamine-o-quinone	150.15
Leukoaminochrome	151.16
Aminochrome	149.15
5,6-dihyroxyindole	149.15
Indole-5,6-quinone	147.13

Table 3.4. molecular weight of each dopamine-quinone

Since the interaction of a dopamine-quinone with a cysteine residue would lead to a loss of an hydrogen atom, one Dalton must be removed to each molecular weight reported in the table 3.4. The molecular mass obtained of the modified protein can now be compared with the expected molecular mass of different DAQs: the species +150.2 could correspond to the dopamine-o-quinone adduct and the +146.5 could be the indole-5,6-quinone adduct. The assignment of the other modifications (+142.5/141.5) to a DAQ was not possible because there is no DAQ with this molecular weight. Hence, the mass determined might be the result of a complex interaction, that is the sum of a subtraction/acquisition of molecules between DAQs and the protein that can not be analyzed in full details.

3.3.3 Gel electrophoresis characterization of the interaction of SOD2 with DAQs

Gel electrophoresis was applied to understand if the interaction of the protein with DAQs would change the electrophoretic pattern of SOD2. The investigation was extended to others ratio of SOD2:dopamine in addition to 1:1 and 1:5, namely 1:2 and 1:3 ratios in order to have a complete profile of the interaction phenomenon. First of all the reaction products of the different ratio were analyzed with SDS-PAGE, hence in denaturing conditions (fig. 3.19). The SDS-PAGE revealed that as the ratio with dopamine increased intensity of the bands corresponding to the monomers of SOD2 decreased with the appearing of aggregates resistant to the high temperature and SDS treatments. It is worth noting the appearance of a specie corresponding to a SOD2 covalent dimer, which decreased at ratio 1:3 and 1:5. Moreover at high ratio an increase of aggregates at high molecular weight, that could not enter in the resolving gel, was also observed.

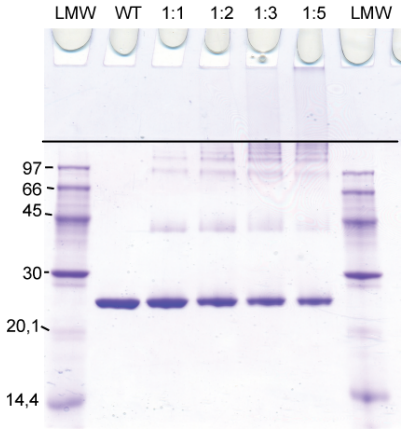

Figure 3.19. SDS-PAGE of SOD2 and the different ratio SOD2:dopamine 1:1, 1:2, 1:3 and 1:5.
LMW: molecular weight marker. The black line separates the stacking gel from the resolving gel.
The gel shows the presence of aggregates at high molecular weight as the ratio of SOD2:dopamine increases.

The reaction products separated with SDS-PAGE were then electroblotted on a nitrocellulose membrane to perform the quinone staining (fig. 3.20), which enables to detect quinones attached to proteins as blue/violet bands. This technique was applied to understand which of the SOD2 bands presents a covalently bound quinone. The staining showed that the dimers and the high molecular aggregates were positive, hence all presented at least one bound quinone. The bands corresponding to SOD2 and SOD2 incubated with tyrosinase as control appeared slightly colored probably due to remaining red ponceau background.

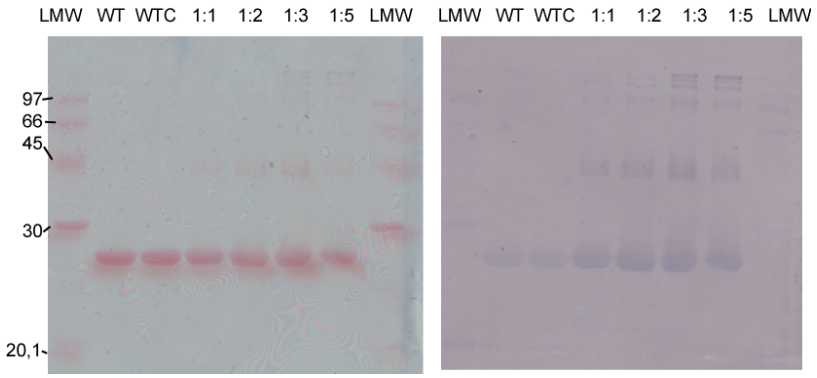

Figure 3.20. Quinone staining on nitrocellulose membrane
WT = wild-type, WTC = wild-type incubated with tyrosinase as control, 1:1, 1:2, 1:3 and 1:5 are different ratio of SOD2:dopamine.
In the left proteins have been stained with ponceau S and on the right panel the same membrane destained and assayed with quinone staining, which shows the presence of quinones.

The native structure of SOD2 after the covalent modifications induced by DAQs was investigated by native-PAGE (fig. 3.21), where proteins migrates on the basis of their quaternary structure and their isoelectric point. The native-PAGE showed that SOD2 and the protein incubated with tyrosinase migrated as a single band, while, after the interaction with DAQs, a pattern of several bands appeared. The pattern could be due to different combinations of one DAQ attached to the

cysteine 140 or 196 or two quinones attached to both residues of the monomer of the homotetrameric structure. Otherwise the reason could be a different DAQ bound to the monomers. Hence the different combinations will have different isoelectric points. Since mass spectrometry revealed different DAQs Moreover as the concentration of dopamine increased the intensity of the pattern decreased in concomitance with the increase of SOD2 species which did not enter in the gel, appearing as band on the top of the gel.

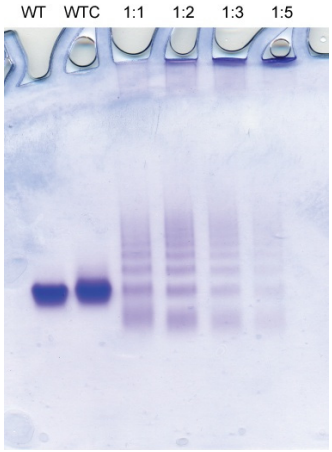

Figure 3.21. Native-PAGE of SOD2 and the different ratio SOD2:dopamine 1:1, 1:2, 1:3 and 1:5. *Wt indicates SOD2, whereas WTC the protein incubated with tyrosine as control. Upon the incubation of SOD2 with DAQs a complex pattern of different species appears.*

The nature of the species that did not enter in the gel and of the complex pattern present after the covalent modification of SOD2 by DAQs was investigated eluting the species from the native-PAGE and separating them in a SDS-PAGE. Silver staining was used to stain the proteins, because it is more sensitive with the respect of Comassie (fig. 3.22).

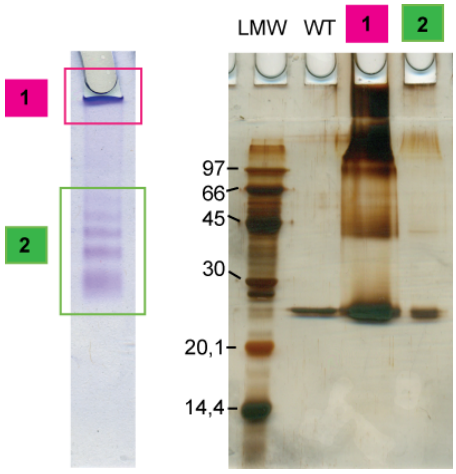

Figure 3.22. SDS-PAGE of Native-PAGE gel bands.
The portion 1 highlighted in pink of the Native-PAGE on the left was cut, the proteins were eluted from the gel and loaded in lane 1 of the SDS-PAGE.
The same procedure was applied for the portion number 2 in green and all the bands of the native-PAGE correspond to monomers of SOD2 with different isoelettric point.

This approach demonstrated that the species that did not enter in the gel correspond to covalent protein aggregates, even if a portion is not covalently as

demonstrated by the presence of monomer. Moreover, the complex band pattern migrating in the native gel can be resolved into monomers of SOD2.

To define the different isoelectric points of the various monomers species resulting from protein modification, 2 dimensional electrophoresis was applied. This method allows the separation of proteins by two dimensions: in the first the separation is performed by their isoelettric point, while in the second by their molecular weight. The 2 dimensional gel of SOD2 led to identification of two monomers of SOD2 with different isoelectric point: 8.3 and 8.5 (fig. 3.23 A). This pattern is compatible with the two peaks with the two peaks separated by RP-HPLC (fig 3.13). In fig. 3.23 B, the results obtained with SOD2 protein incubated with dopamine at ratio 1:1.

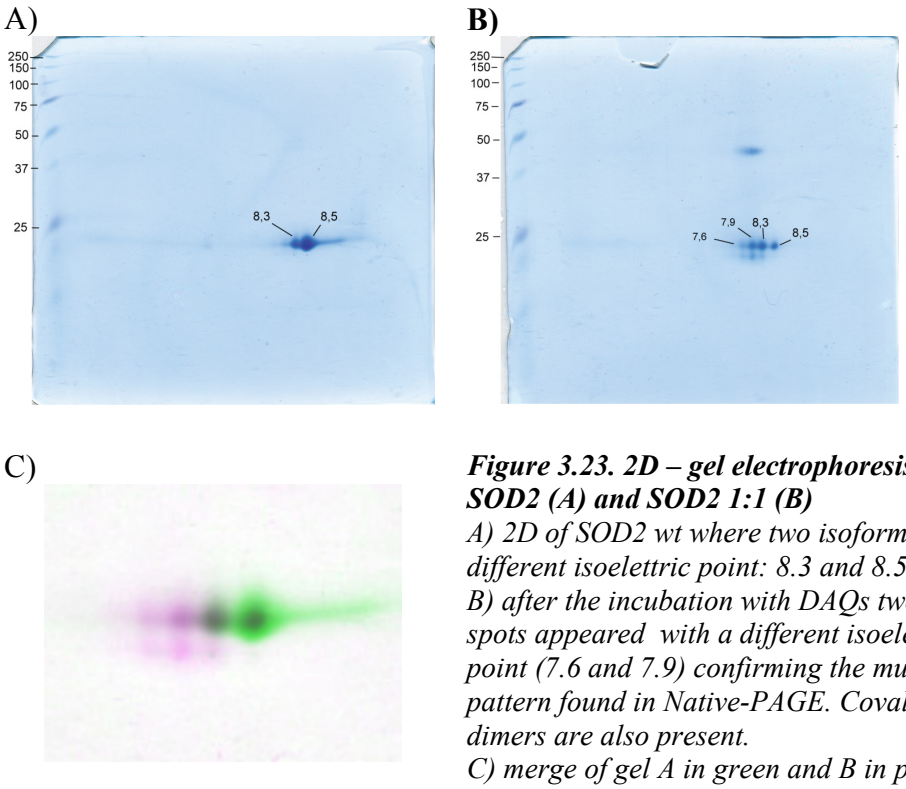

Figure 3.23. 2D – gel electrophoresis of SOD2 (A) and SOD2 1:1 (B)
A) 2D of SOD2 wt where two isoforms with different isoelettric point: 8.3 and 8.5;
B) after the incubation with DAQs two more spots appeared with a different isoelettric point (7.6 and 7.9) confirming the multiple pattern found in Native-PAGE. Covalent dimers are also present.
C) merge of gel A in green and B in pink.

This gel displayed the presence of covalent dimers of SOD2 and also of two more monomeric species with isoelectric point of 7.6 and 7.9 in comparison with the control. The presence of monomers with different isoelectric point confirmed the previous hypothesis that the complexity of the pattern present in native-PAGE was due to a combination of monomers with different charge due to the possible combinations of interaction between one o two quinones with one or two cysteine residues. Moreover in the 2D a second series of spot corresponding to isoelectric points 7.6, 7.9 and 8.3 migrated just below the other. The possible explanation might be a partial denaturation of proteins leading to a decrease of the molecular weight.

At this point it was interesting to understand if, after the covalent modification of SOD2 by DAQs, the protein was still active. A superoxide dismutase activity staining was performed on the native-PAGE, which enables to visualize *white* bands of SOD activity on a blue/violet background (fig. 3. 24). The activity staining demonstrated that all SOD2 species were still able to dismutate superoxide anions radicals but this method did not allow for quantifying precisely the enzymatic activity and for detecting small differences between the different protein species.

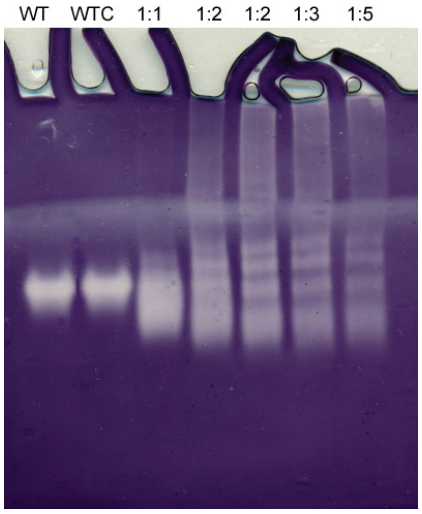

Figure 3.24. Superoxide dismutase activity staining on native-PAGE.
Wt indicates SOD2, whereas WTC the protein incubated with tyrosine as control. 1:1, 1:2, 1:3 and 1:5 are the different ratio of SOD2:dopamine.
All SOD2 species appear to be active.

3.3.4 Superoxide dismutase enzymatic activity

One of the goals of this project was to verify if covalent modifications induced by DAQs would cause an inhibition of the enzymatic activity failing to protect mitochondria from oxidative stress. Hence enzymatic assays were carried out on the wild-type SOD2 and on the protein after reaction with DAQ to quantify the enzymatic activity. The measurement of catalytic activity of SOD enzymes is complicated because their substrate is superoxide anion, a radical that is unstable and spontaneously dismutate. Hence it is necessary to produce the substrate in situ when the measurement is performed. It is also important to thoroughly control the experimental conditions to have reproducible data since the spontaneous dismutation of superoxide occurs at a rate that is very sensitive on solutions conditions, such as pH and temperature.

Two types of assays have been developed: indirect and direct. The first ones are based on a generator and a detector of superoxide. The generator produces superoxide anions, which react with the detector to a degree that depends on the amount of SOD present. Basically two system are used in the

indirect assays. The first one, with one enzymatic reaction generating superoxide anions and another component reacting in a measurable way with the radical (Crapo et al., 1978). The second one, in which a molecule, as pyrogallol, self-oxidize to generate superoxide anion that then further propagate the generation of down stream species (Misra and Fridovich, 1972, 1977; Puget and Michelson, 1976). The superoxide dismutase activity is then determined in terms of its ability to prevent generation of downstream species. With these kind of assays it is possible to quantify the enzymatic activity as enzymatic units. One enzymatic unit is normally defined as the amount of enzyme catalyzing the transformation of 1 μmol of substrate per minute. This definition of unit is not applicable to SOD given that the substrate is indirectly produced, hence a unit of SOD is defined as the protein amount which causes 50 % of inhibition of the reaction rate of the detector molecule. It is important to note that one unit of SOD determined with one assay will not correspond to a unit of SOD2 determined with another one. Hence it is possible to compare the activity of SOD2 of different samples only using the same assay in exactly the same conditions. Moreover, one problem of the indirect assaies is that any agent that inhibits superoxide anions generation appears as a false positive SOD activity.

The direct assays are based on the quantifiable generation of superoxide anions, in an acqueous solution. Hence the consumption of the substrate can be detected by the disappearance of its UV-spectroscopic signal, since superoxide anion absorb at 260nm, enabling the determination of kinetic parameters. This type of assay can be performed with a stopped and flow spectrophotometer. Alternatively the direct assays involve radiation chemistry, in particular two techniques are available: gamma radiolysis and pulse radiolysis. Among the two, pulse radiolysis is the best technique, but it requires an accelerator of particles that removes this technique from a routine laboratory capability (Klug et al., 1972; Marklund, 1976).

Many indirect assay assays have been proposed in literature, the first used in this thesis was luminonol-xanthine oxidase assay, an assay based on the inhibition by SOD of the light production from the system oxygen-hypoxanthine-xanthine oxidase-luminol. Xanthine oxidase reacts with hypoxanthine producing superoxide anions, which oxydize luminol producing chemiluminescence. This type of assay was rejected after many tests because the absence of linearity and reproducibility of the data as suggested in fig. 3.25. It was not possible to obtain a linear reproducible signal even without SOD.

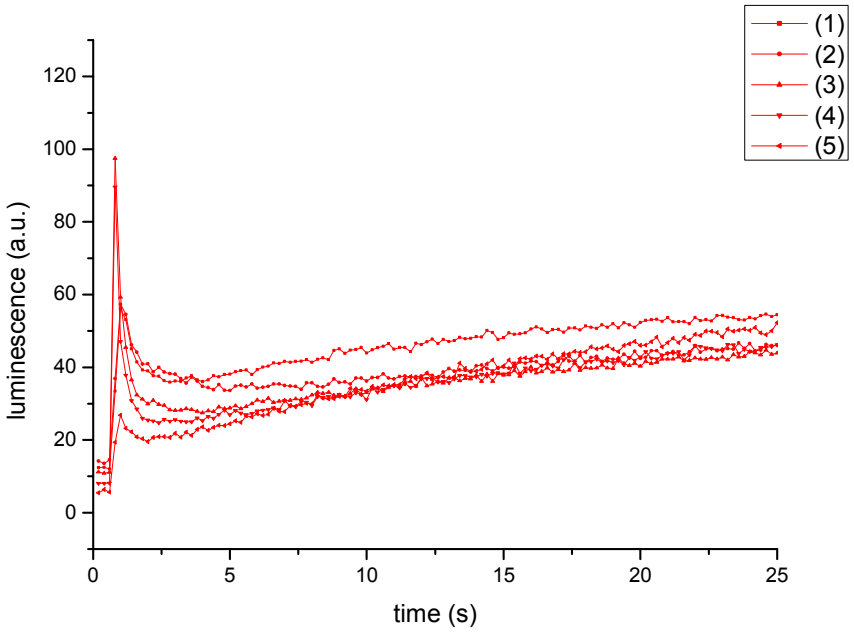

Figure 3.25. Luminol-xanthine oxidase assay. *Example of the luminescence measured 5 times in the same conditions without SOD. The luminescence is due to the interaction of luminol with superoxide anions produced upon the addition of hyphoxanthine to the system.*

Pyrogallol assay was the second assay tested since it was reported in literature as the best in terms of reproducibility, accuracy and simplicity (Keyhani and Keyhani, 2006). This assay is based on the auto-oxidation of pyrogallol occurring at alkaline pH producing superoxide anions. The mechanism of the auto-oxidation involves superoxide anion as a propagating species, which lead to the formation of purpurogallin, which can be followed at 420 nm. If the protien is present, there is an inhbition of the auto-oxydation of pyrogallol, hence of the purpurogallin formation. The setting phase was complex because the auto-oxidation of this molecule occurred also in the water solution, hence the first measurements were affected by this problem. This problem was overcame dissolving the pyrogallol in a tonometer under anaerobic conditions. The measurements obtained are consistent during one day experimental session but is not possible to compare it with those of another day because of the change of the slope of the pyrogallol auto-oxidation (fig. 3.26). We still do not know the reason of this change, there is a probably variable that we do not control. This is plausible, since the reaction involves radicals formation, which is affected by several factors.

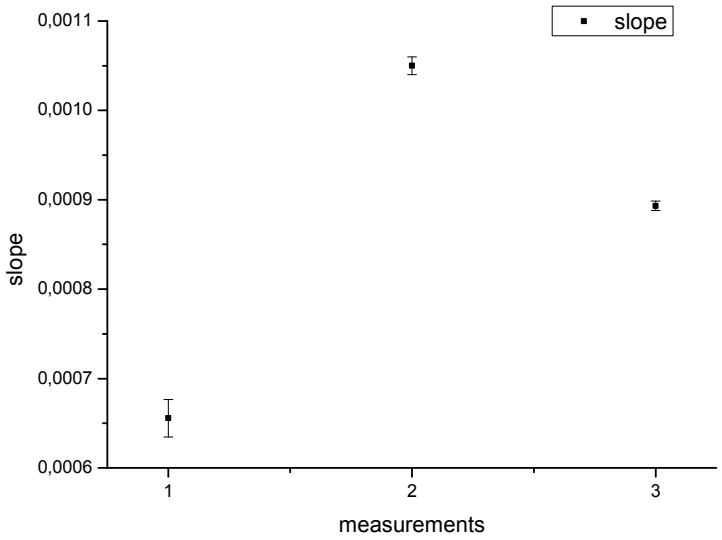

Figure 3.26. Pyrogallol auto-oxidation slopes measured in three different experimental session. *Each point is the average with standard deviation of 3 replicated measurements.*

This assay was applied to SOD2 and to the protein covalent modified by DAQs. Here another problem was encountered: the auto-oxidation of pyrogallol resulted to be affected by the presence of tyrosinase. The reason is thought to be due to the presence of contaminats in the tyrosinase preparation (it is a mushroom extract). To overcome this problem, both the activity measuments of SOD2 and the blanck auto-oxidation were performed in the presence of tyrosinase (fig. 3.27).In table 3.5 are reported the units of enzymatic activity.

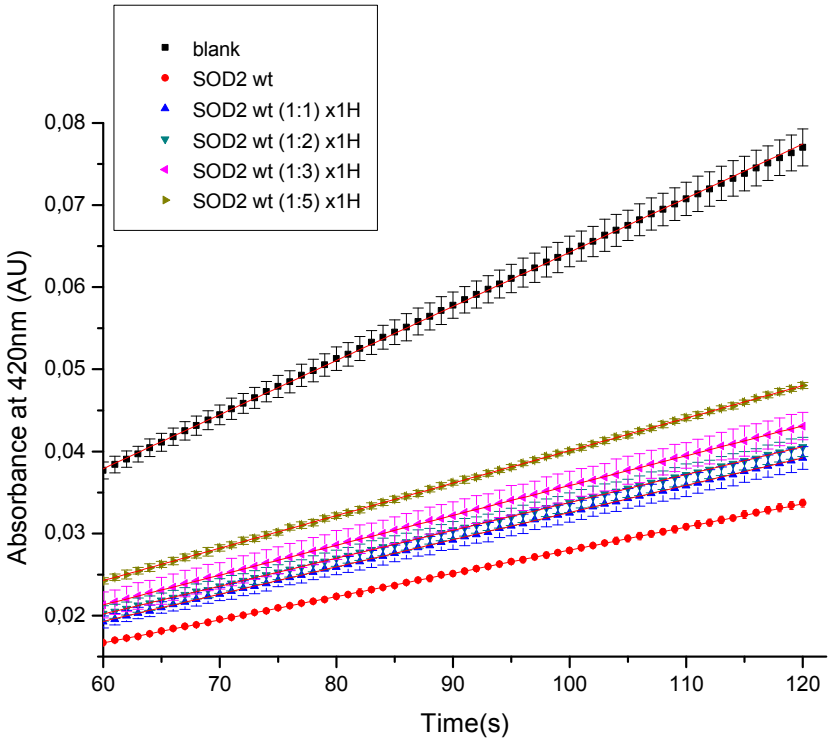

Figure 3.27. Pyrogallol assay of SOD2 and SOD2:dopamine 1:1, 1:2, 1:3 and 1:5.
The presence of SOD2 inhibits pyrogallol auto-oxidation. When covalent modified SOD2 by DAQs is added the percentage of inhibition decreases indicating that DAQs inhibits enzymatic activity of SOD2.

Reaction	Slope (AU/s) (*10^{-4})	% of inhibition	Activity (U)	Specific activity (U/mg) (*10^{5})
Blank	6.56± 0.2	-	-	-
SOD2	2.83 ± 0.06	56.8 ± 1.4	1.32 ± 0.05	4.39 ± 0.18
(1:1) x 1 h	3.31 ± 0.11	49.4 ± 1.7	0.98 ± 0.07	3.3 ± 0.2
(1:2) x1h	3.40 ± 0.07	48.2 ± 1.1	0.93 ± 0.04	3.10 ± 0.13
(1:3) x1h	3.63 ± 0.03	44.6 ± 0.4	0.80 ± 0.01	2.7± 0.4
(1:5) x1h	3.96 ± 0.07	39.6 ± 1.1	0.66 ± 0.03	2.19 ± 0.1

Table 3.5. Enzymatic activity data processed are reported. To note that units of SOD2 decrease as the increase of DAQs.

The covalent modifications of SOD2 by DAQs caused an increase of the pyrogallol auto-oxidation with respect to the wild-type demonstrating that DAQs inhibits the enzymatic activity of the protein. In fact the units of activity decreased when the enzyme concentration remained constant. This inhibition was proportional to DAQs concentration: as the ratio SOD2:dopamine increased, also the inhibition increased.

Once established that SOD2 activity was affected by DAQs, the issue become the mechanism of inhibition of DAQs. The question of the actual mechanism of inhibition can only be addressed by an evaluation of kinetic constants. To this aim the only suitable technique is a direct assay, hence it was necessary to generate superoxide anions directly.

Among the different direct assays, pulse radiolysis presents several advantages: it requires only water, oxygen and formate to generate superoxide anions.The timescale of superoxide anions generation is sub-microseconds allowing a large time window for measuring kinetic reactions (Abreu and Cabelli, 2010). As far as gamma radiolysis and pulse radiolysis are concerned, both the techniques consist in the irradiation of water causing its ionization and cleavage leading to the production of radical species. The irradiation is achieved in the first case with gamma rays (^{60}Co or ^{137}Cs as source of gamma rays); while in the second with a pulse of electrons. The difference between the two techniques is that in the case of gamma radiolysis there is a continual radiation of the water producing a steady-state flux of radicals; whereas with pulse radiolysis short burst of electrons in the time scale from nanoseconds to picoseconds are used. Thus, pulse radiolysis gives the possibility to study reaction kinetics and not the overall yield of dismutation.

Pulse radiolysis experiments were carried out in collaboration with Dr. Diane Cabelli at the Brookhaven National Laboratory (NY, USA), where I spent a period of my PhD. This technique enables the production of superoxide anions by pulsing electrons produced by a Van der Graaf accelerator directly in the SOD2 solution.

The proposed catalytic mechanism of SOD2 involving the reduction/oxidation of manganese is different from other SODs (see 1.2.2.7 for more details):

$$Mn^{3+}SOD(OH^-) + O_2^{\cdot -} + (H^+) \rightarrow Mn^{2+}SOD(H_2O) + O_2 \quad \mathbf{k1}$$

$$Mn^{2+}SOD(H_2O) + O_2^{\cdot -} + (H^+) \rightarrow M^{3+}SOD(H_2O) + H_2O_2 \quad \mathbf{k2}$$

$$Mn^{2+}SOD(H_2O) + O_2^{\cdot -} \rightarrow M^{3+}SOD(H_2O)\text{-}O_2^{2-} \quad \mathbf{k3}$$

$$Mn^{3+}SOD(H_2O)\text{-}O_2^{2-} + (H^+) \rightarrow Mn^{3+}SOD(OH^-) + H_2O_2 \quad \mathbf{k4}$$

Superoxide dismutase activity was measured with pulse radiolysis under two conditions: at high concentrations of protein, following the first disappearance of Mn^{3+} as decrease in intensity of the absorption band at 480nm (step 1). Then, after fully reduce the protein with hydrogen peroxide, the same absorption band is used to followed the reappearance of Mn^{3+} (step 2). The second condition, is at low

protein concentration, monitoring the disappearance of superoxide anions at 260 nm under catalytic conditions. Data are currently under processing.

3.4 Reactivity of SOD2 cysteines toward DAQs

The next step of my PhD project was to identify the site or sites of interaction of SOD2 with DAQs, Plausible candidates as reactive species are the two cysteine residues (cysteine 140 and 196 see fig. 1.21) present in the sequence of human SOD2, as expected from the nucleophilic reactivity of –SH groups. The first approach used was the limited proteolysis before and after the covalent modification of DAQs to indentify the peptides whose physico-chemical properties are modified for the presence of covalently bound quinones.

3.4.1 Limited proteolysis

Among the different endopeptidases available, trypsin was chosen because of its ability to cleave the polypeptide chain at the carboxyl side of lysine or arginine residues present in the sequence of human SOD2 in the same regions of cysteines, allowing to obtain short peptides, which can be easily identified. However, this enzyme proved to be not able to proteolyze SOD2 even under partially denaturing conditions (2M Urea or 2M guanidinium chloride). Therefore, it was necessary to use pepsin, a different endopeptidase that has the disadvantage of having a scarse specificity of cleavage. The enzyme tends to cleave preferentially between aromatic aminoacids. SOD2 was proteolyzed with pepsin and the reaction products were separated with a C18 column RP-HPLC (fig. 3.29 A). As control the protein before the proteolysis was loaded on the C18 column (fig. 3.28). Limited proteolysis was performed after treatment of SOD2 at ratio SOD2:dopamine 1:1 (fig. 3.29 B). The peaks obtained were collected and analyzed by mass spectrometry in collaboration with Dr. Patrizia Polverino De Laureto (table 3.6).

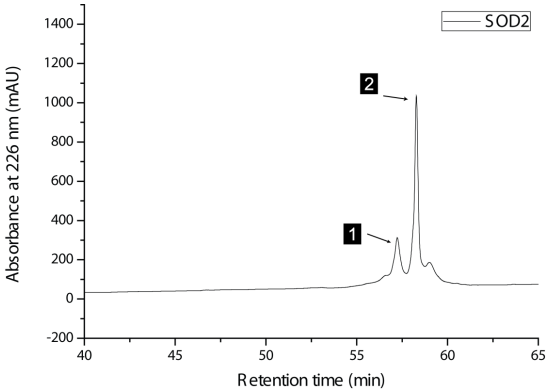

Figure 3.28. RP-HPLC of SOD2 using a C18 column.
In the chromatogram the two peaks numbered with 1 and 2 were collected and analyzed with mass spectrometry.

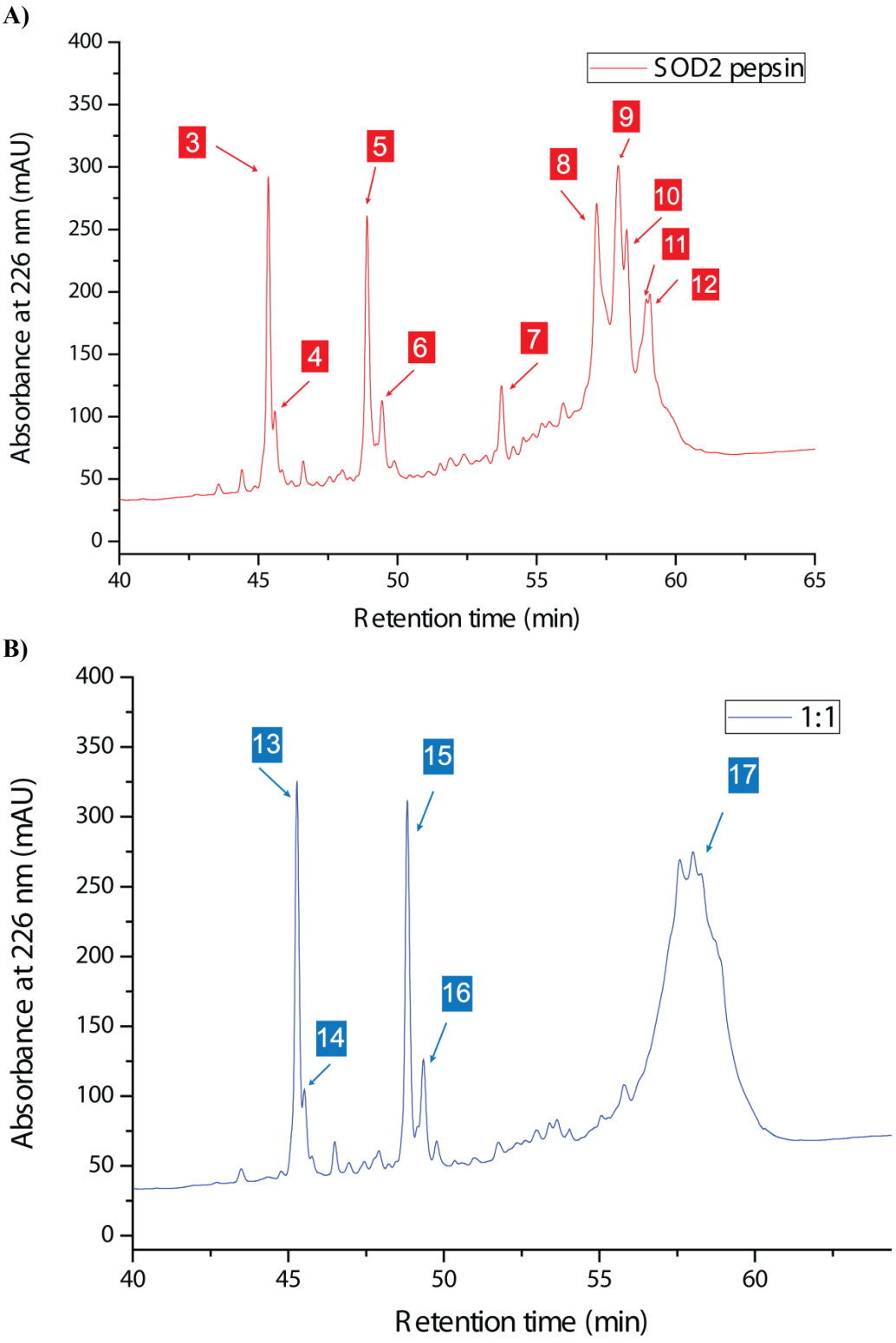

Figure 3.29. RP-HPLC of SOD2 after proteolysis with pepsin. A): SOD2 B):SOD2 after the incubation with dopamine at ratio 1:1.
The various peaks numbered 3-17 were collected and analyzed with mass spectrometry.

	Peak	Molecular weight (Da)	Predicted Peptides (Da)
SOD2 wt	**1**	22613.7±2	-
	2	22616.3±2	-
Proteolyzed SOD2	**3**	6862.1±2	-4-57 (6862.6) 68-131 (6862.6)
	4	6862.2±2	-4-57 (6862.6) 68-131 (6862.6)
		4786.2±2	-1-38 (4786.3) 50-95 (4785.3) 51-96 (4785.3) 87-130 (4786.4)
	5	8978.9±2	24-105 (8978.9) 67-150 (8978.9) 69-152 (8978.0) 71-153 (8977.0) 89-169 (8977.2)
	6	10930.2±2 10858.9±2	29-129 (10926.2) 30-130 (10926.2)
	7	4936.4±2 4835.7±2	160-198 (4934.5) 108-153 (4835.4)
	8	22613.6±2	-
	9	13653.2±2	12-136 (13653.3) 28-154 (13653.3)
	10	22616±2	-
	11	15773.4±2	7-151 (15772.6) 8-152 (15772.6) 17-161 (15773.8) 29-172 (15772.7) 46-188 (15773.8) 58-198 (15771.9)
	12	13657.3±2	78-198 (13655.56)
Proteolyzed 1:1	**13**	6862.3±2	-4-57 (6862.64) 68-131 (6862.64)
	14	4786.05±2	-1-38 (4786.3) 50-95 (4785.3) 51-96 (4785.3) 87-130 (4786.4)
		6862.05±2	-4-57 (6862.6) 68-131 (6862.6)
	15	8978.7±2	24-105 (8978.9) 67-150 (8978.9) 69-152 (8978.0) 71-153 (8977.0) 89-169 (8977.2)
	16	10929.9±2 10860.2±2	29-129 (10926.2) 30-130 (10926.2)
	17	22742.6±2 22904.2±2	

Table 3.6. Molecular weight of the peptide obtained from limited proteolysis of SOD2 and SOD2:dopamine 1:1 and predicted peptides. *The 4 aminoacids (GSHM) leaved after the thrombin cleavage are referred as -1,-2,-3 and -4.*

The results of fig. 3.29 show that there are no differences in the first part of the chromatogram (form 40 to 50 minutes) between SOD2 and SOD2 treated with

dopamine. More interesting was the second part of the chromatogram (from 50 to 60 minutes) where the peak number 7 is absent after covalent modifications of DAQs and the peak 8,9,10,11,12 appeared as a single broad peak numbered as 17. The absence of peak number 7 was promising, meaning that the peptide/s of this peak was modified by DAQs changing the retention time. The identification of each peptide by mass spectrometry analysis was difficult because of the poor specificity in pepsin cleavage, hence one peptide mass could correspond to many possible protein peptide as shown in table 3.6. The two molecular weights found in the peak 7 could correspond to two peptide: 112-157 and 164-202, both carrying one cysteinyl residue. The effective presence of both peptides was demonstrated by cleavage of this peak with trypsin, RP-HPLC separation of the peptides obtained, mass spectrometry of peaks and tandem MS/MS. Since both the peptides were absent after DAQs incubation, the retention time was changed due to a possible DAQ modification on the cysteine of both peptides. Therefore, limited proteolysis suggested that both cysteine residues could be targets of quinones. In the second part of the chromatograms of SOD2:dopamine 1:1 sample (peak 17) it was not possible to identify the peaks corresponding to the modified peptides probably as a consequence of the low chromatographic resolution. However, it was possible to identified the mass corresponding to the uncleaved protein with one and two bound DAQs molecules.

On the basis of these results, it was decided to use another approach: to individually mutate the cysteine residues of the protein into alanines, a non-polar amminoacid to avoid the introduction of charges. The approach will allow to single out the reactivity of each cysteine residue.

3.4.2 Site directed mutagenesis of cysteine residues of human SOD2

Site direct mutagenesis was applied to cysteine 140 using the cDNA of pET28a+ his-tag SOD2 as template and one primer containing the nucleotidic substitution which enabled to obtain the specific mutation C140A. The same procedure was applied unsuccessfully for the mutation of the cysteine 196. Therefore, another variant of site direct mutagenesis PCR was used, which is based on the use of two complementary primers instead of one. The use of two primers enabled to obtain also the C196A mutant. The double mutant C140A/C196A was obtained starting from the single mutant C140A as template and using the two primers previously used to obtaining the C196A. The double mutant will be used as negative control.

Once obtained the cDNA of His-tag SOD2 mutants, a test of protein expression was performed exploiting the conditions used for the wild-type his-tag SOD2 expression, that is 0.1mM IPTG in the presence of manganese chloride (fig. 3.30).

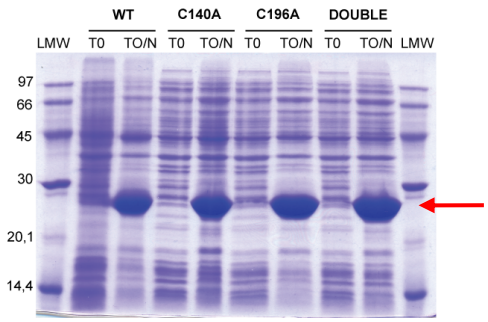

Figure 3.30. SDS-PAGE of expression of SOD2 cysteine mutants.
The red arrows indicates SOD2. LMW are the molecular weight. The lane T0 corresponds to the culture before the IPTG induction and O/N shows the situation after an overnight induction. The expression of the three mutants (C140A, C196A and C140A/C196A) were induced with 0,1mM IPTG as the wt protein.

Once verified that the expression of the mutants was comparable with that of the wild-type protein, the mutants were purified applying the same protocol optimized for the wild-type (fig. 3.31).

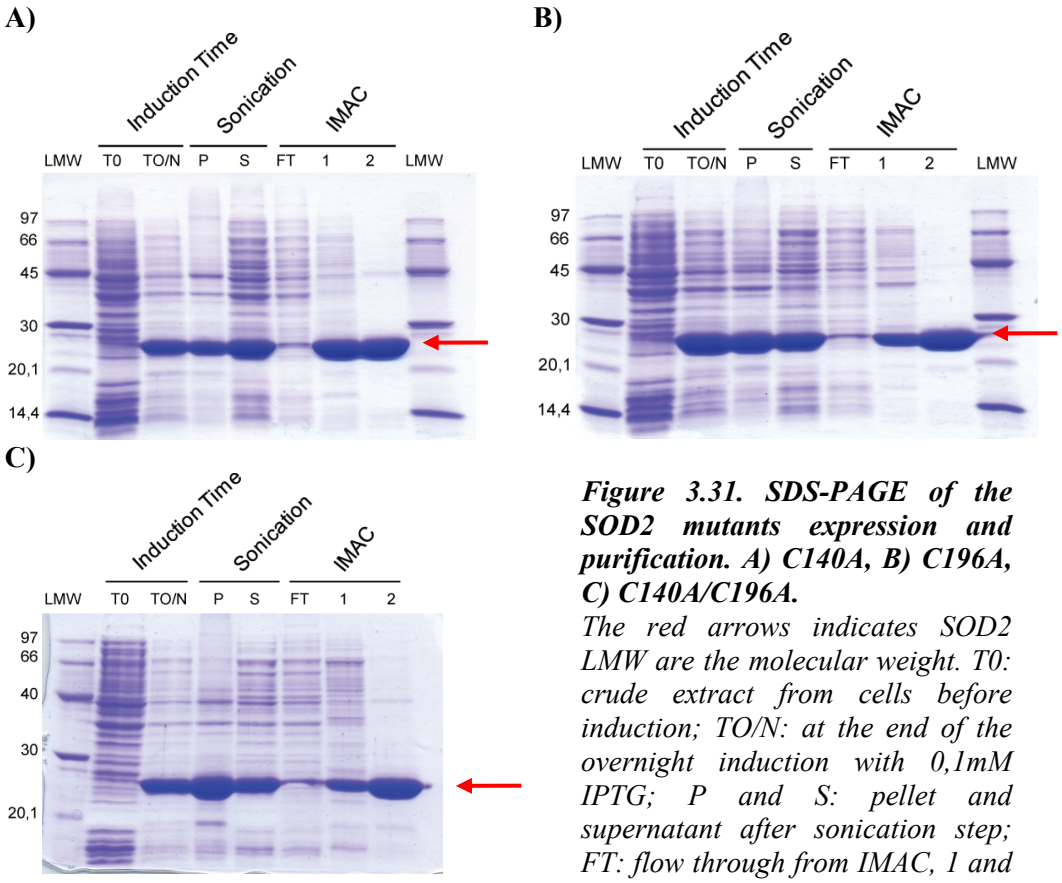

Figure 3.31. SDS-PAGE of the SOD2 mutants expression and purification. A) C140A, B) C196A, C) C140A/C196A.
The red arrows indicates SOD2 LMW are the molecular weight. T0: crude extract from cells before induction; TO/N: at the end of the overnight induction with 0,1mM IPTG; P and S: pellet and supernatant after sonication step; FT: flow through from IMAC, 1 and 2: pool 1 and 2 of the elution peak obtained with imidazole gradient (0-500mM).

The yield of cysteine mutants obtained was of 40-60 mg per liter of culture as for the wild-type protein.

The mutants were loaded on a C4 column RP-HPLC (fig.3.32), the peaks were collected and analyzed by mass spectrometry in collaboration with Dr. Patrizia Polverino De Laureto. The RP-HPLC chromatograms revealed the presence of two peaks as for the wild-type and the molecular mass measurements confirmed the 2 Dalton difference between the two peaks. The expected molecular weight for the single mutants were 22584.6 and the observed value was 22585.01±2 for the C140A while 22585.3±2 for the C196A. The expected mass for the double mutant was 22552.51 and the observed 22553.2±2

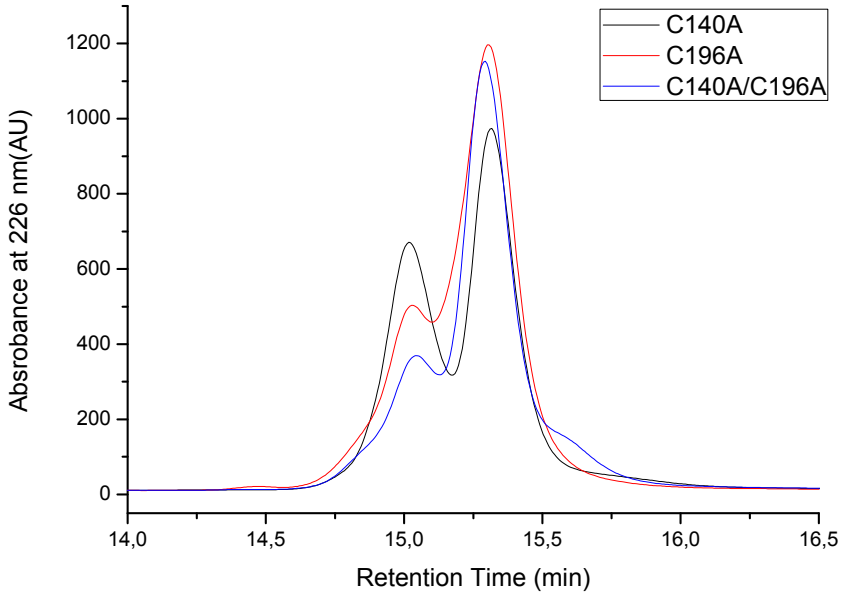

Figure 3.32. RP-HPLC of the SOD2 mutants.

The quantification of the metal loading was performed with ICP-MS in collaboration with Prof. Carlo Barbante (University of Venezia). The results obtained are summarized in table 3.7. The ICP-MS measurements revealed that the metal loading of the monomers of C140A was 97%, that of C196A was 90% and that of the C140A/C196A was 96%.

A)

		Standard deviation
intercept	767380,26	41280,98
slope	35666,51	1012,52
Manganese concentration (PPB)	21,52	0,09
Manganese concentration (µM)	39,16	0,17
Protein concentration (µM)	40	1
Ratio Mn/ monomero	0.97	0,03

B)

		Standard deviation
intercept	1195346,07	24777,80
slope	38167,77	603,76
Manganese concentration (PPB)	31,32	0,04
Manganese concentration (µM)	57,00	0,07
Protein concentration (µM)	63	1
Ratio Mn/ monomero	0.9	0,02

C)

		Standard deviation
intercept	1392856,54	103319,79
slope	42113,04	2780,96
Manganese concentration (PPB)	33,07	0,26
Manganese concentration (µM)	58	0,48
Protein concentration (µM)	60,20	1
Ratio Mn/ monomero	0,96	0,02

Table 3.7. Data obtained form ICP-MS analysis of the mutants: C140A (A), C196A (B), C140A/C196A (C).

3.4.3 Interaction of SOD2 cysteine mutants with DAQs

Once obtained the three mutants, they were incubated with dopamine. Since the single mutant has only a cysteine possibly interacting with DAQs, in contrast to the wild-type SOD2, the mutants were incubated with half the concentration of dopamine as in previous experiments to compare the reactivity. Thus, the used mutant:dopamine ratio were 1:0.5, 1:1, 1:1.5, 1:2.5, the reaction mixture being incubated 1 hour at 25°C. The obtained reaction products were analyzed on SDS-PAGE and Native-PAGE (fig. 3.34). Gel electrophoresis revealed that the pattern

obtained for the mutant C140A resembled that of the wild-type protein after modification by DAQs. The difference between the two proteins was the lower amount of aggregated material that appeared with C140A SOD2 in comparison with the wild-type as shown by the native-PAGE (fig. 3.34). In the case of C196A and C140A/C196A SOD2, the covalent dimers were absent but aggregates at high molecular weight were present, although in a small degree.

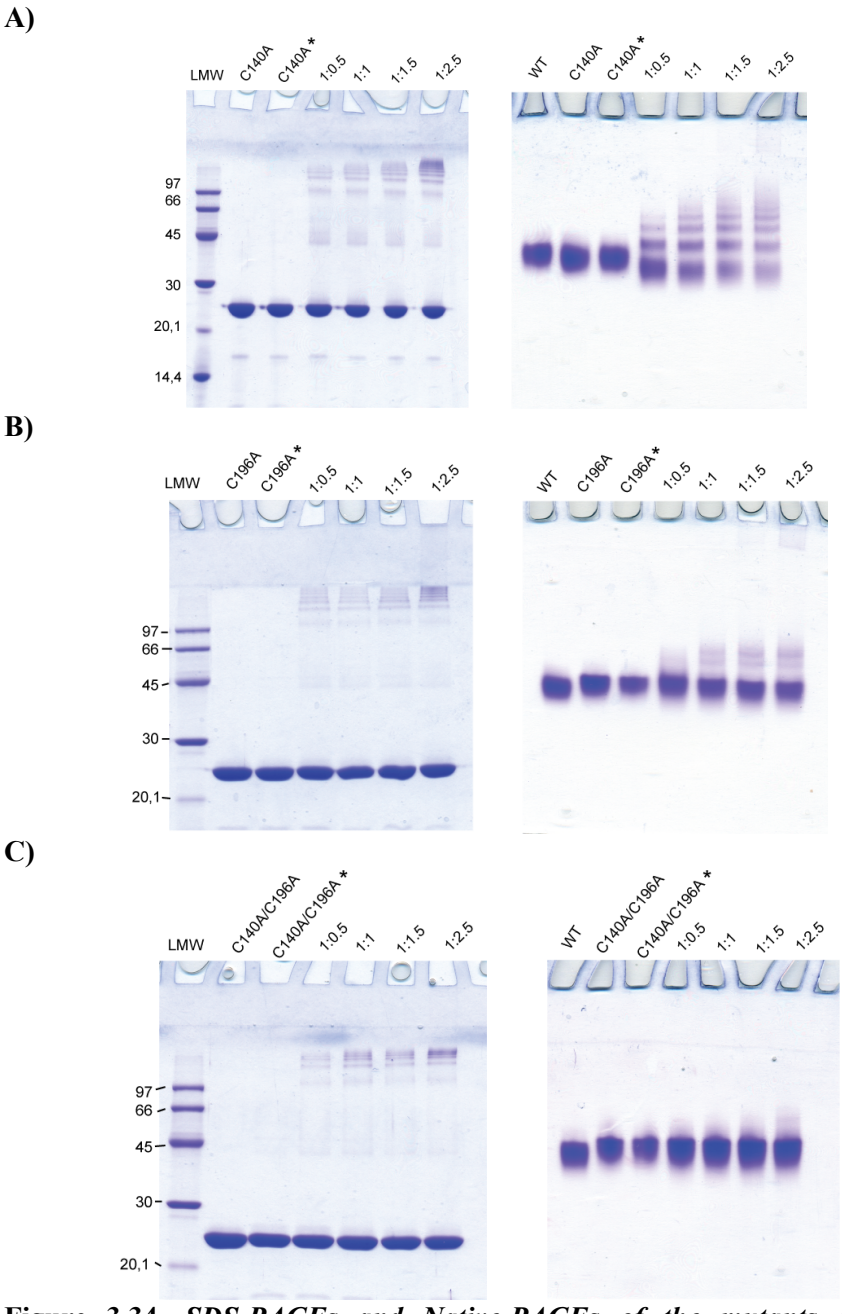

Figure 3.34. ***SDS-PAGEs and Native-PAGEs of the mutants after the incubation with different ratio of mutant:dopamine.***
*Left panes: SDS-PAGE; right panels Native-PAGE of: the mutant C140A (panels A) where it can be seen that after the dopamine incubation, the pattern obtained is comparable with that of the wild-type; the mutant C196A (panels B); the double mutant (panels C). The lanes where * is added to the mutant definition refer to the mutant alone incubated with tyrosinase as control.*

To verify the presence of DAQs bound to the mutants quinone staining was performed (fig. 3.35).

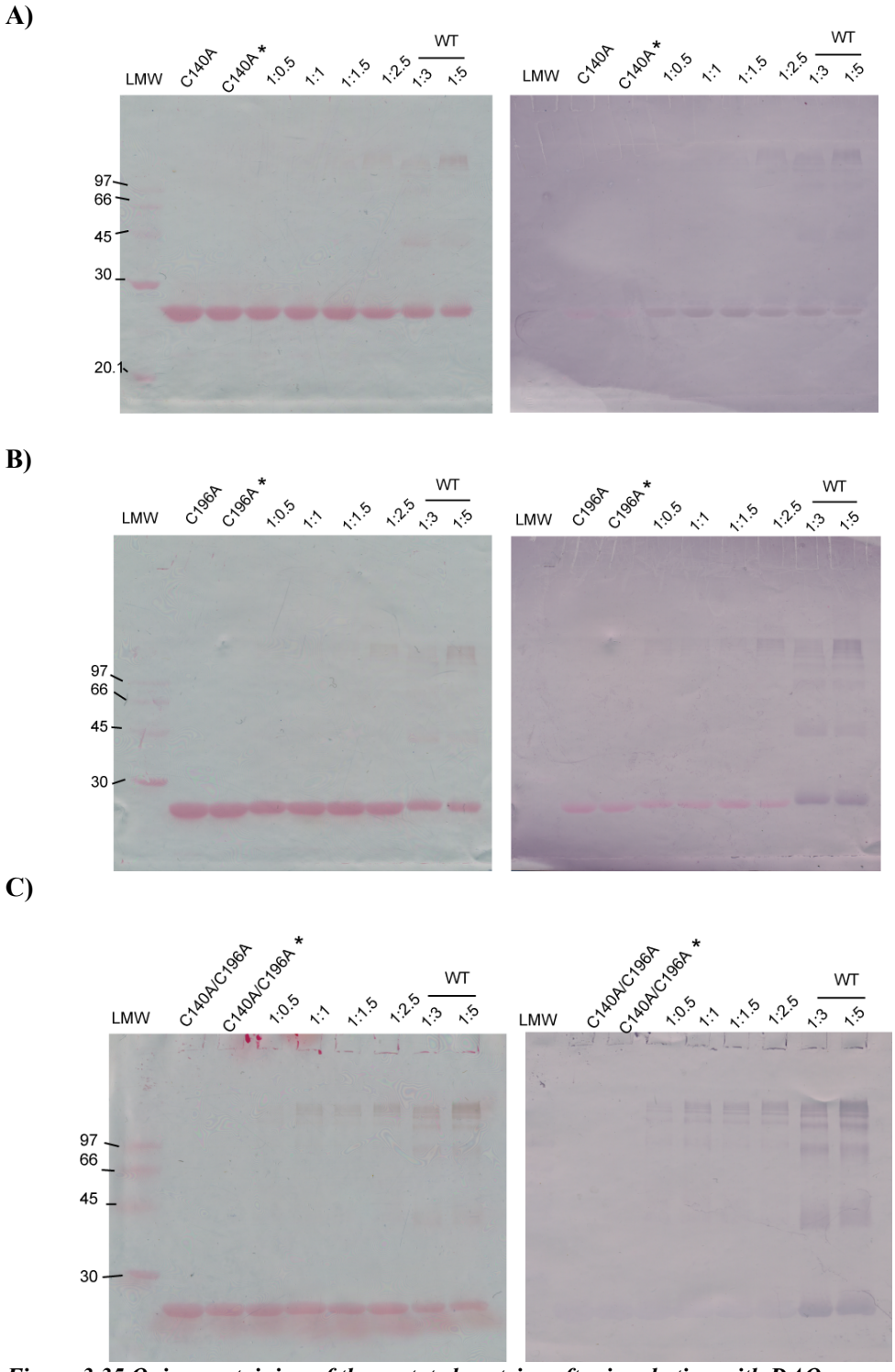

Figure 3.35 Quinone staining of the mutated proteins after incubation with DAQs.
A) mutant C140A, B) mutant C196A, C) C140A/C196A. *Left panels: nitrocellulose membrane stained with ponceau red; right panel: the same membrane stained for quinone proteins identification. As positive control in the last two lanes of every gel the wild-type protein incubated with dopamine at ratio 1:3 and 1:5 was loaded. The C196A (B) and the double mutant (C) do not display reactivity with DAQs on the monomer, while the aggregates seems to be positive to the staining. The lanes where * is added to the mutant definition refer to the mutant alone incubated with tyrosinase as control.*

The reactions products were electroblotted on a nitrocellulose membrane after SDS-PAGE separation, membranes were stained with red ponceau to demonstrate the presence of proteins and after the ponceau destaining, proteins were stained with a quinone detection protocol. Positive quinone proteins will result blue/violet. As positive controls, the reaction products of wild-type SOD2 incubated with dopamine at ratio 1:3 and 1:5 were loaded in each SDS-PAGE. In the case of mutant C196A red proteins bands can be seen of after quinone staining because traces of ponceau red staining were left. This approach revealed that the reactive mutant was the C140A, hence the cysteine 196 was the DAQs target. In the membrane of the other two mutants, aggregates appeared to be slightly violet/blue suggesting protein aggregation with melanin.

The reaction products of the three mutants incubated with dopamine were separated by RP-HPLC and the collected peaks were analyzed by mass spectrometry. The observed molecular masses demonstrated a covalent modification of the mutant C140A: a molecular weight of 22733.7±2 (+150 Da), 22730.9±2 (+146 Da) and 22889.4±2 (+ 305 Da) were found. The other mutants did not show any DAQs modifications. Hence the indication was that the cysteine residue 196 was the target of DAQs. To confirm this, another approach was used: radioactivity. SOD2 and the mutants were incubated in the presence of ^{14}[C]-labelled-dopamine, the reaction products were separated on SDS-PAGEs, the gels were dried up and exposed for autoradiography (fig. 3.36).

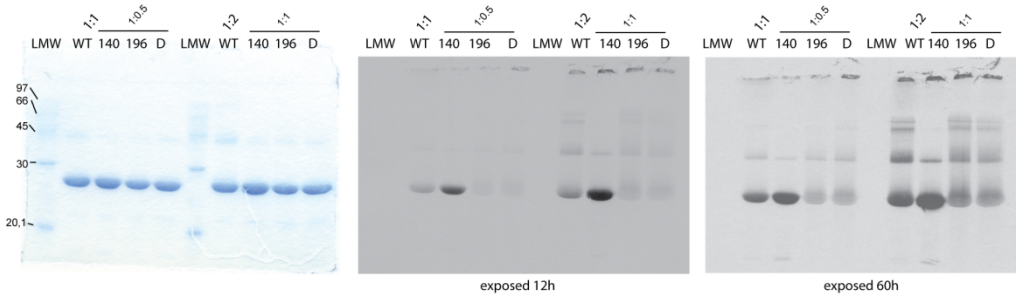

Figure 3.36. SDS-PAGEs and autoradiography of the wild-type and mutated proteins incubated with different ratio of ^{14}[C]***-labeled –dopamine.*** *WT = wild-type, 140 = C140A mutant, 196 = C196A mutant, D = double mutant; 1:0.5, 1:1 and 1:2 indicate the different ratio between protein and dopamine. The radioactivity is incorporated by the wild-type and C140A mutant. Thus, the cysteine 196 is the DAQs target.*

The autoradiography, after 12 and 60 hours of exposition showed that the radioactivity was incorporated by the wild-type and by the mutant C140A, in this last case even with more intensity, confirming the reactivity of cysteine 196. The C140A mutant exhibited the presence of the covalent dimer but aggregates were

absent. After 60 hours of exposition radioactivity was incorporated by the C196A and by the double mutants but the signal was saturated in the wild-type and the C140A mutant. The radioactivity incorporated in the C196A and the double mutant after the overexposition might indicate that also the cysteine 140 or other nucleophilic amino acid residues could be reactive towards DAQs, although to a lesser extent not detectable by mass spectrometry and quinone staining.

The reason for the incorporation of more radioactivity in the mutant C140A than in the wild-type was probably due to the ratio of protein:dopamine and the quantity of C14-labelled dopamine added. In the case of SOD2 wild-type ratio 1:1 50% C14-labelled dopamine and 50% of cold dopamine where added to the protein, while in the mutants 1:0.5 the C14-labelled dopamine was 100% (the same percentages were applied for ratio 1:2 of the wild-type and 1:1 for the mutants) to compare the results. However, if the C14-labelled dopamine added to the mutant C140A at ratio 1:0.5 would react 100% with the cysteine residue 196, the incorporated radioactivity will be higher than that of the wild-type ratio 1:1 because only 50% of total dopamine would react. Hence, the same experiment was performed with the addition of 50% C14-labelled dopamine and 50% dopamine using the same ratio 1:1 for the wild-type and the mutants (fig.3.37) confirming our idea. Moreover, the radioactivity of the other two mutants was localized to the aggregates confirming the results of quinone staining. Furthermore in the SDS-PAGE was loaded also SOD2 incubated with dopamine in absence of tyrosinase for 1hour, autoradiography showed a slightly reactivity. This suggests that SOD2 could be a target of DAQs in cells where the dopamine oxidation is not mediated by tyrosinase.

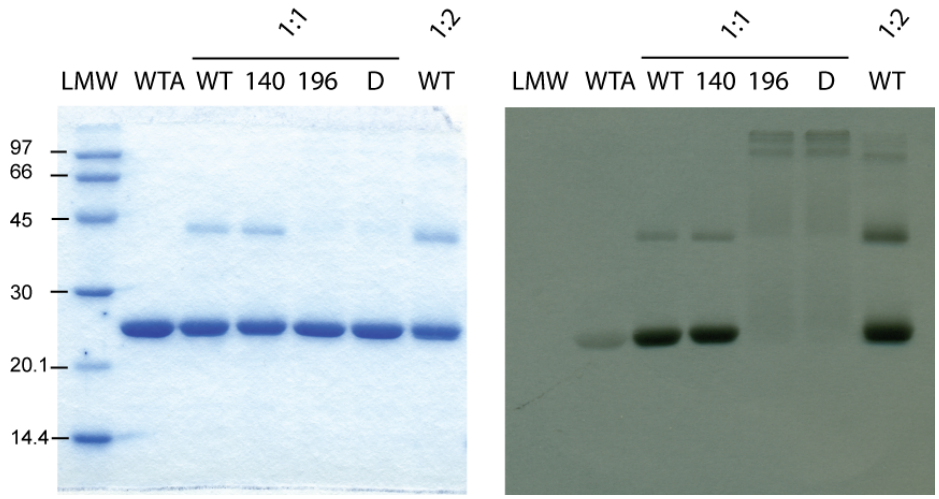

Figure 3.37. ***SDS-PAGEs and autoradiography of the wild-type and mutated proteins incubated with different ratio of C-14-labeled–dopamine.*** *WTA= SOD2 incubated with dopamine but not tyrosinase, WT = wild-type, 140 = C140A mutant, 196 = C196A mutant, D = double mutant; 1:1 and 1:2 indicate the different ratio between protein and dopamine.*

The enzymatic activity of the mutants C140A, C196A and of the double mutant (as control) after the incubation with dopamine was tested with pyrogallol assay (fig. 3.38, 3.39 and 3.40). The measurements on the C140A mutant after DAQs covalent modification resulted in the inhibition of the enzymatic activity, which is proportional with the increase of dopamine. At ratio 1:0,5 the units of activity decreased from 0.67 to 0.46 and decreased to 0.41 at ratio 1:1 and then adding more dopamine the units decreased to 0.24 (table 3.8). On the contrary, the C196A and the double mutant did not show any significant decrease of the activity even in the presence of dopamine (table 3.9 and table 3.10). In figure 3.41 the specific activity are plot.

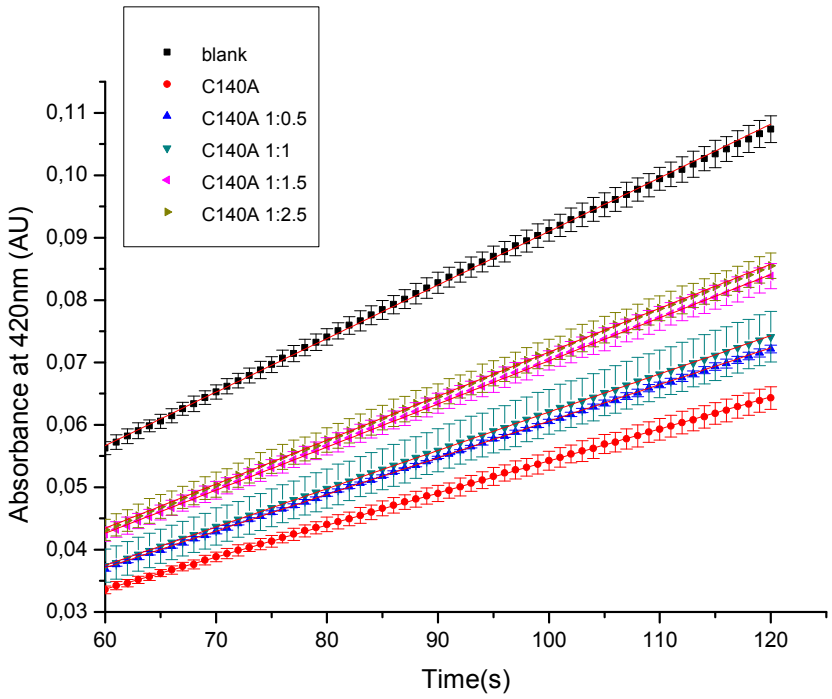

Figure 3.38. Pyrogallol activity assay on the C140A mutant. *1:0.5; 1:1; 1:1.5; 1:2.5 indicate the ratio between the mutant and the dopamine.*

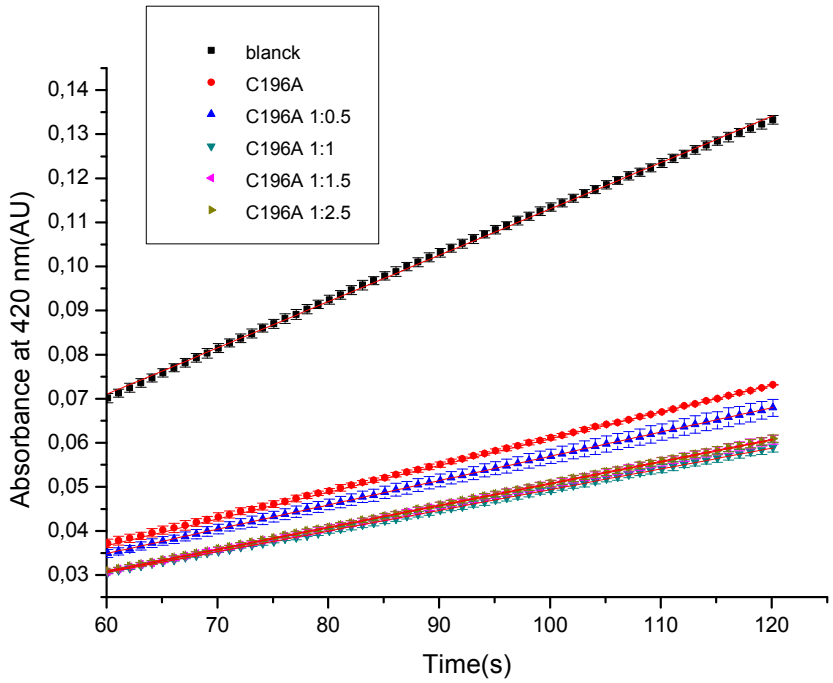

Figure 3.39. Pyrogallol activity assay on double mutant C196. *1:0.5; 1:1; 1:1.5; 1:2.5 indicate the ratio between the mutant and the dopamine.*

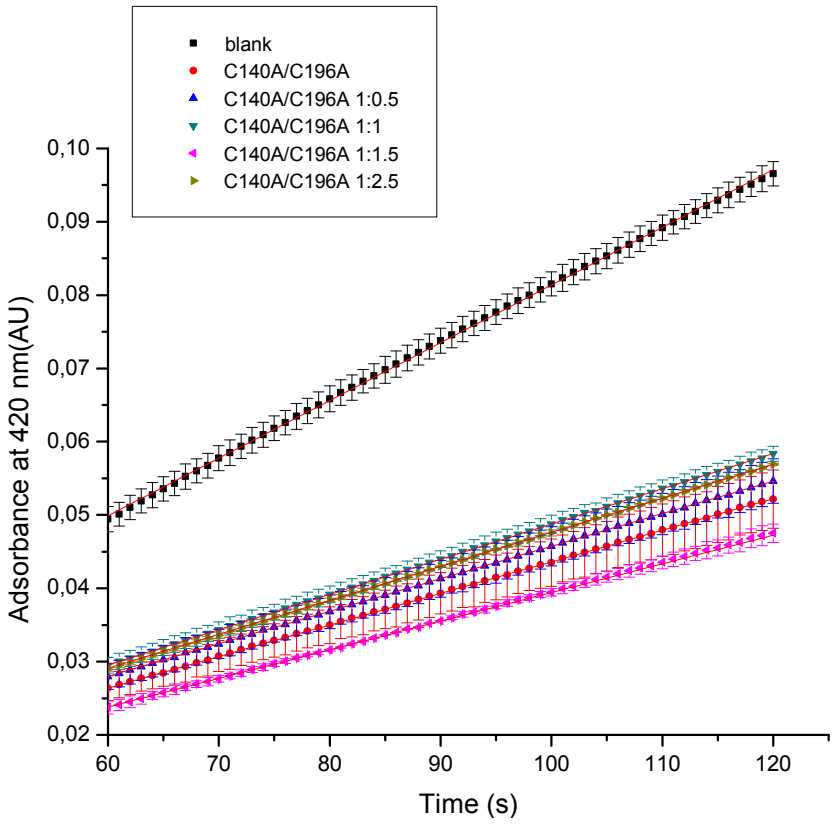

Figure 3.40. Pyrogallol activity assay on double mutant C140A/C196. *1:0.5; 1:1; 1:1.5; 1:2.5 indicate the ratio between the mutant and the dopamine.*

Reaction	Slope (AU/s) (*10 $^{-4}$)	% of inhibition	Activity (U)	Specific activity (U/mg) (*10^5)
Blank	8,53± 0.19	0	-	-
C140A	5.12 ± 0.23	39.9 ± 2.6	0.67 ± 0.07	2.2 ± 0.24
C140A 1:0.5	5.86 ± 0.16	31.3 ± 1.9	0.46 ± 0.04	1.52 ± 0.13
C140A 1:1	6.04 ± 0.23	29.2 ± 2.6	0.41 ± 0.05	1.38 ± 0.17
C140A 1:1.5	6.88 ± 0.23	19.3 ± 2.7	0.24 ± 0.04	0.80 ± 0.14
C140A 1:2.5	6.87 ± 0.27	19.4 ± 3.2	0.24 ± 0.05	0.81 ± 0.17

Table 3.7. ***Enzymatic activity data relative to the C140A mutant.***
To note that units of SOD2 decrease upon increasing of DAQs.

Reaction	Slope (AU/s) (*10 $^{-4}$)	% of inhibition	Activity (U)	Specific activity (U/mg) (*10^5)
Blank	10.5 ± 0.1			
C196A	5.99 ± 0.14	42.98 ± 1.39	0.75± 0.04	2.51 ± 0.14
C196A 1:0.5	5.5 ± 0.20	47.61 ± 1.92	0.91 ± 0.07	3.03 ± 0.23
C196A 1:1	4.7 ± 0.14	55.09 ± 1.07	1.23 ± 0.06	4.09 ± 0.21
C196A 1:1.5	5.14 ± 0.11	51.05 ± 1.29	1.04 ± 0.04	3.48 ± 0.15
C196A 1:2.5	49.8 ± 0.08	52.57 ± 0.82	1.11 ± 0.04	3.46 ± 0.12

Table 3.8. ***Enzymatic activity data relative to the C196A mutant .***
The enzymatic activity does not change significantly after the incubation with DAQs.

Reaction	Slope (AU/s) (*10 $^{-4}$)	% of inhibition	Activity (U)	Specific activity (U/mg) (*10^5)
Blank	7,87 ± 0.09			
C140A/C196A	4,36 ± 0.31	43.46 ± 4.85	0.81± 0.88	2.70 ± 0.41
C140A/C196A 1:0.5	4,43 ± 0.21	42.76 ± 3.14	0.78 ± 0.08	2.59 ± 0.27
C140A/C196A 1:1	4,80 ± 0.09	39.52 ± 1.07	0.64 ± 0.03	2.13 ± 0.11
C140A/C196A 1:1.5	3,97 ± 0.35	49.62 ± 4.4	0.99 ± 0.17	3.31 ± 0.58
C140A/C196A 1:2.5	4,65 ± 0.35	40.98 ± 0.45	0.69 ± 0.01	2.31 ± 0.04

Table 3.9. ***Enzymatic activity data relative to the double mutant are reported.***
To note that the enzymatic activity does not change significantly.

Kinetic parameters were assayed for the three mutants with pulse radiolysis at high and low protein concentrations. Data are currently under processing.

3.5 Structural modifications induced by DAQs on SOD2

Covalent modifications of DAQs on cysteine 196 of human SOD2 caused an inhibition of the enzymatic activity, thus the next step was to correlate such effect to structural changes at protein level. This study was carried out at the level of secondary structure by far-UV circular dichroism (fig. 3.41). The far-UV spectra showed that the secondary structure content remained essentially unaltered. It was interesting to note that while the lineshape was unaltered, the overall intensity of the spectra decreased upon increasing of the dopamine ratio. The decreased of the signal can be quantified as 3-4% for ratio 1:1 and 1:2 and 10% for the ratio 1:3. This loss of signal could be explained with protein aggregation seen in SDS-PAGE and in native-PAGE.

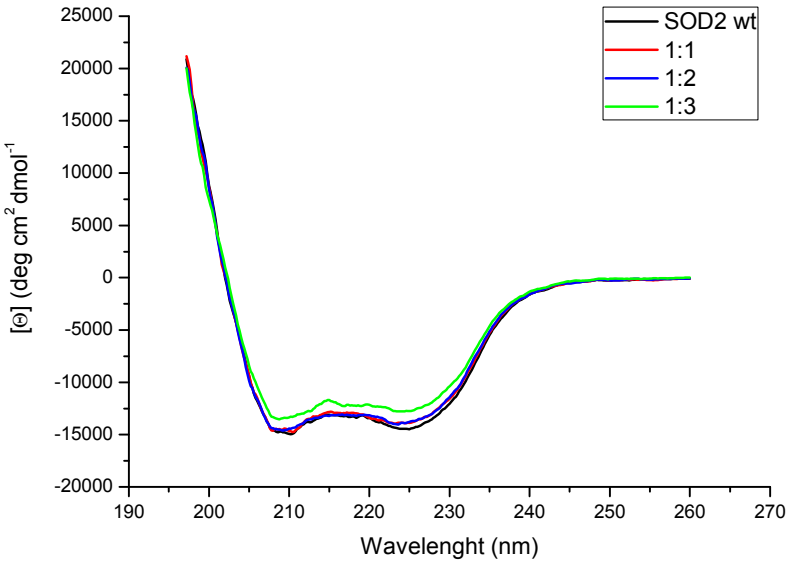

Figure 3.41. Far-UV circular dichroism spectra of SOD2 wild-type and the protein incubated with dopamine at different ratio (1:1, 1:2 and 1:3). *The spectra show that there is no change in the overall structure of protein after the covalent modifications. However, there is a loss of signal (3-4% for ratio 1:1 and 1:2, while 10% for ratio 1:3).*

Near-UV circular dichroism was applied to investigate if the tertiary structure of the protein was subjected to changes (fig.3.42). Upon the interaction with DAQs,

the near-UV spectra revealed a possible change in the tertiary structure of the protein. In particular it could be seen an increase of the intensity of the signal, especially in the region of phenylalanine residues. The spectra displayed a small shift of the peak maximum, from 294.4 to 293.4 nm, corresponding to the region of tryptophan residues. The shift indicated that the covalent modification of the cysteine 196 could perturb directly or indirectly one or more of the six tryptophan residues of the protein.

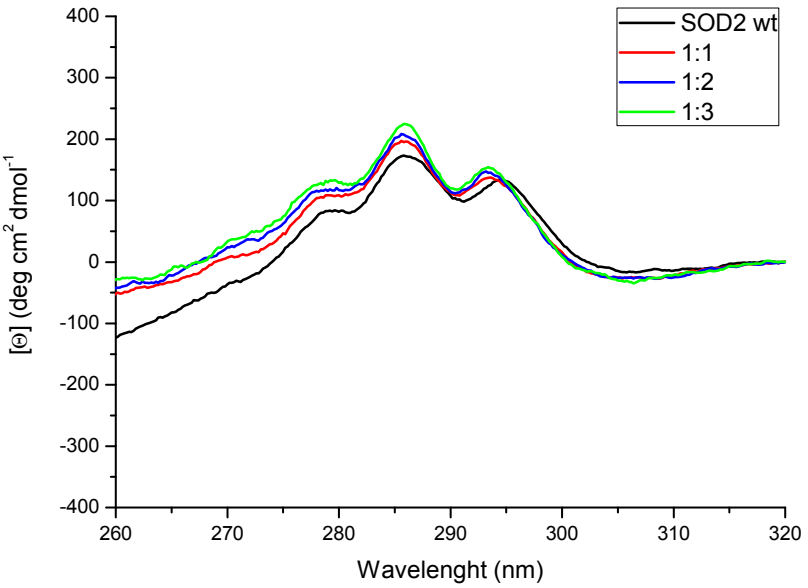

Figure 3.42. Near UV Circular dichroism spectra of the wild-type and the wild-type incubated with different ratio of dopamine (1:1, 1:2 and 1:3).
The spectra display the increase of the intensity of the signal and a shift of the spectrum in the region of tryptophans after DAQs incubation.

A different level of investigation was to study the active site of the protein, as the active site of SOD2 involves manganese, changes in the metal coordination can be investigated with EPR. Since the 9 GHz Mn(II) EPR, present at the university, is not particularly sensitive to changes in the environment or better is too complex to be interpreted, it was decided to perform high magnetic-field high-frequency EPR (HFEPR), which gives the possibility to obtain highly resolved and detailed Mn(II) spectra (reviewed by Tabares et al., 2010).

The 285 GHz Mn(II) HFEPR spectra were recorded in collaboration with Dr. Leandro Tabares at CEA Saclay (Gif-sur-Yvette, France) (fig.3.43). The HFEPR spectra of the mutant C140A and C196A (fig. 3.42 A) were superimposable to that of the wild-type, demonstrating that these mutations do not change the active site structure. When dopamine is added to the wild-type, the lineshape of the spectrum changed, however it is hard to reconsile the observed differences with

the differences in coordination geometry of the manganese in the active site. Of the two mutants, only the C196A reproduced the small change observed in the lineshape of the spectrum upon treatment with DAQs. This result was not expected, since the DAQ modified cysteine is Cys 196, hence it is necessary to further explore the HFEPR spectra on the C196A mutant to unravel this appearent contradiction. It should be mentioned that the possibility remains the difference in coordination geometry related to the change in the enzymatic activity could be below to the detection level of the spectroscopic method .

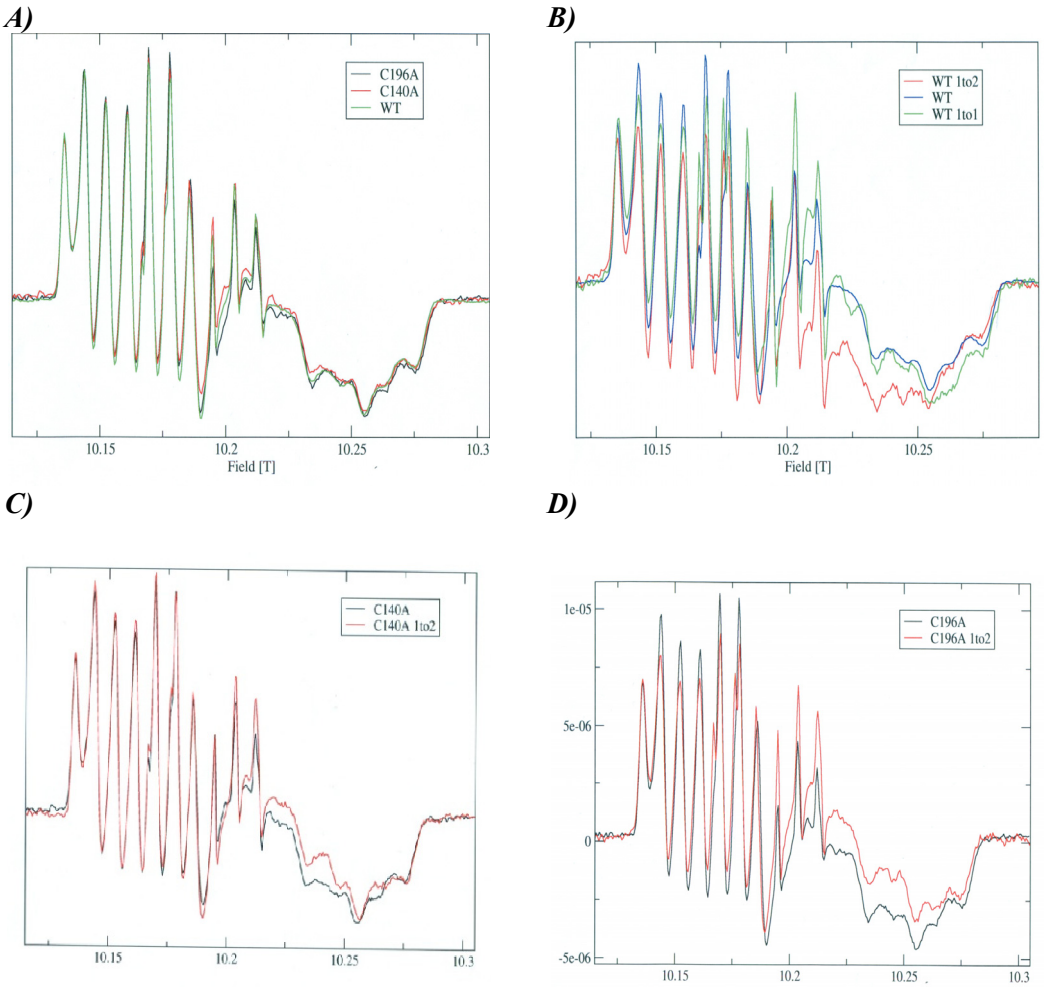

Figure 3.42. HFEPR-SPECTRA of SOD2, the mutants and the proteins incubated with dopamine.

A) spectra of the wild-type and the two mutant C140A and C196A showing that the cysteine mutation do not changes the active site;

B) spectra of the wild-type displaying that the covalent modifications induced by DAQs affect the manganese coordination;

C) and D) spectra of the mutant C140A (C) and C196A (D) with and without dopamine at ratio 1:1 where it is visible that the geometry of the active site is unchanged in the C140A while in the C196A differences are evident.

3.6 Protein crystallization optimization

Two features are important in considering the possibility to crystallize a protein: the purity of the sample and the homogeneity of the protein molecules to be crystallized. The purity of the sample was achieved by the optimized purification protocol. The potential problem was the homogeneity, since the interaction with DAQs led to different reaction products and aggregated forms. Consequentially, the aim was to optimize the reaction with DAQs to maximize the formation of one single reaction product.

SOD2 was incubated with dopamine at ratio 1:1 and dopamine was added each hour for 5 hours, every hour an aliquot was taken and the reaction products were separated by RP-HPLC (fig.3.43). The chromatograms showed that the peak corresponding to the wild SOD2 decreased with the rise of the peak assigned to the modified SOD2. The peaks were collected and analyzed by mass spectrometry in collaboration with Dr. Patrizia Polverino De Laureto. At the end of the reaction the species observed in the peak of the modified protein were two: +22758.5 ± 2 Da (+142 Da) and 22905.9 ± 2 (+289 Da).

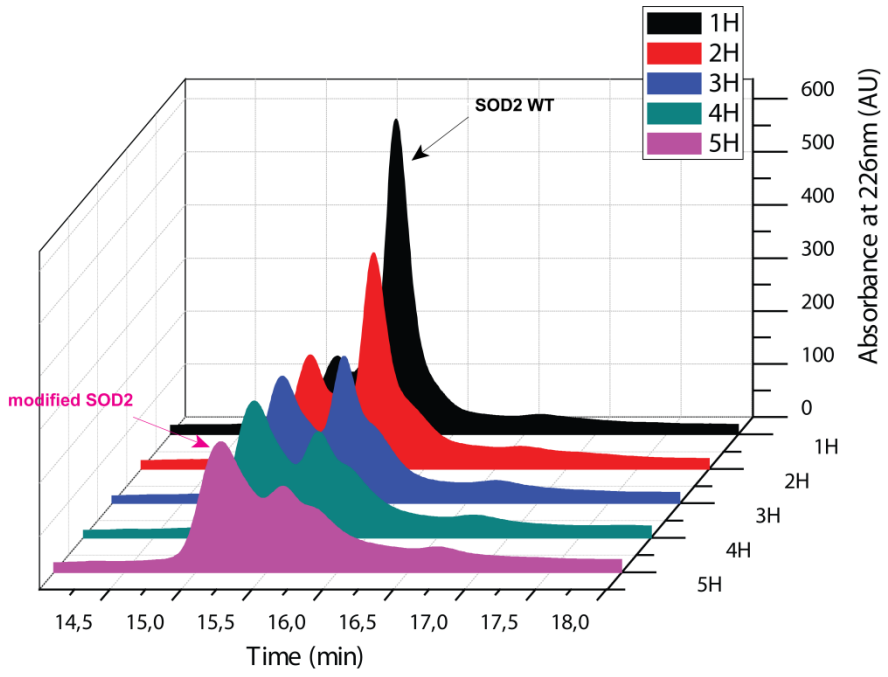

Figure 3.43. RP-HPLC time course over 5 hours of the SOD2 modification by DAQs at ratio 1:1 with the addition of dopamine every hour. *The peak corresponding to unmodified SOD2 decrease and increase the peak of the modified protein over the time.*

The reaction products obtained after every hour of reaction were evaluated by SDS-PAGE and native-PAGE (fig. 3.44), which revealed the presence of

aggregates mainly in the last two hours of incubation. Now, we are trying to crystallize the protein in collaboration with Dr. Stefano Capaldi (University of Verona). We decided to test the crystallization of the reaction product after 4 hour of incubation time with dopamine, because it represents a good compromise between the aggregated protein and the amount of modified SOD2.

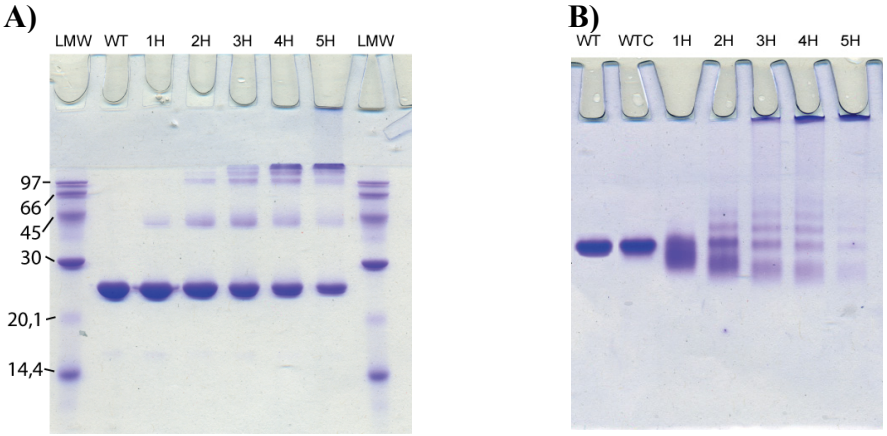

Figura 3.44. SDS-PAGE (A) and native-PAGE (B) showing time course of the SOD2 modification by DAQs at ratio 1:1 with the addition of dopamine every hour for 5 hours. *1H, 2H, 3H, 4H and 5H indicate 1,2,3,4, and 5 hours after the incubation with dopamine. WTC stands for wild-type incubated 5 hours with tyrosinase as control.*

The crystal structure of the modified SOD2 will provide information about the changes induced by DAQs, hence will be useful to understand the inhibition of the dismutase activity.

.

4. Discussion and conclusion

The work of this thesis was addressed to study the molecular mechanisms of aetiopathogenesis of PD. Evidence from literature suggests that mitochondrial dysfunction and oxidative stress play a central role in the aetiopathogenesis of this disease. The loss of dopaminergic neurons in substantia nigra pars compacta, suggests that dopamine could have an important role in the disease (Thomas et al., 2007). In particular, reactive dopamine derivatives such as dopamine-quinones (DAQs) are suggested to contribute to dopaminergic neurotoxicity. A molecular mechanism proposed to rationalize their toxicity points to the competence of DAQs to form adducts with cysteine residues exposed at the surface of proteins, leading to modification of their functional properties. (Sulzer D. et al., 2000).
The reaction toward cysteines has very little, if any, specificity for the several available protein targets. Therefore, several purported protein targets have been described in the literature, such tyrosine hydroxylase, parkin and α-synuclein (Bisaglia et al., 2010b; Kuhn et al., 1999; LaVoie et al., 2005).

This thesis is aimed to show the potential role of SOD2 in the pathogenesis of PD. This enzyme that catalyze the dismutation of superoxide anions to molecular oxygen and hydrogen peroxide in mitochondria, is particularly relevant as DAQs target, since its important role as mitochondrial scavenger. Since oxidative stress is implicated in PD and superoxide dismutase 2 is a vital enzyme (the inactivation of this gene by homologous recombination turns to be lethal in mice due myocardial injury and neurodegeneration (Lebovitz et al., 1996; Li et al., 1995)), several group of reseach studied the possible involvement of this enzyme in PD using different approaches. The first was to measure the enzymatic activity of SOD2 in substantia nigra of PD brain patients obtaining contrasting results (Marttila et al., 1988; Poirier et al., 1994; Saggu et al., 1989; Shimoda-Matsubayashi et al., 1997). Another approach consisted in analyzing a possible correlation between the polimorphism A-9V (in the mitochondrial targeting sequence) and the PD and once again the results were contrasting (Farin et al., 2001; Grasbon-Frodl et al., 1999; Shimoda-Matsubayashi et al., 1996). However a possible direct involvement of SOD2 in PD was suggested in the increase of vulnerability of hemizygous mice deficient in SOD2 ($SOD2^{+/-}$), which have a 50% decrease of enzymatic activity, treated with MPTP (Andreassen et al., 2001). The vulnerability to MPTP decreased if SOD2 was overexpressed (Klivenyi et al., 1998).

SOD2 presents two cysteinyl residues per monomer that are potentially reactive toward DAQs. The aim of this thesis was first to establish if SOD2 is a target of DAQs. Second, to quantify the magnitude of DAQs modification of cysteine residues and eventually unravel the molecular mechanism through which such modification affects enzymatic activity.

The first part of the project was to clone the cDNA of SOD2 and protein production. The second part was focused on the study of the interaction between SOD2 and DAQs *in vitro* using different biochemical and biophysical techniques. The protein could be cloned and purified in good yield to perform biochemical studies. In order to stimulate the quinone production, the reactive derivatives of dopamine were obtained by reaction with tyrosinase. Control experiments allowed to exclude any effect of tyrosinase on SOD2. Mass spectrometry analysis revealed the presence of new species upon the interaction of the protein with DAQs: +141.53, +142.55, +146.53, +150.26 and +287.81 Dalton. The +150.26 Da was associated to the dopamine-o-quinone and +146.53 Da to indole5,6-quinone. The presence of +287.81 Da was assigned to the covalent modification of both cysteine residue 140 and the 196 of the same monomer. The +141.53 and +142.55 could not be assigned to any DAQ, they are likely to result from a more complex interaction. SDS-PAGE, Native-PAGE and 2D-PAGE revealed the presence of aggregates and tetramers with different isoeletric point due to the statistical combination of monomers with different DAQs modifications. One monomer with one type of modification can dimerize with another monomer with a different DAQ bounded, then this dimer would associate with another dimer with potentially other modifications leading to the complex pattern seen in Native-PAGE. In 2D- electrophoresis, modified SOD2 monomers exhibit a more acidic isoelectric point as compared to the native protein. This change in isoelectric point can not be rationalized in a simple way. The reaction of SOD2 with DAQ is expected to result in the gain of one amino group contributed by the bound quinone, resulting in a shift of the isoelectric point to higher values. Since SOD2 has been suggested to retain its quaternary structure in 8M urea{Matsuda, 1990 #2032} a possible interpretation of the apparent discrepancy in variations in isoelectric point is that the covalently bound quinone induces a perturbation increasing the overall exposure of negative charges contributed by acidic aminoacids.

The functional effects of the covalent modification were investigated by activity assays. The study of the enzymatic activity of SOD was not simple because of the unstable nature of the protein substrate: the superoxide anion. The protein activity was measured using first an indirect assay based on pyrogallol auto-oxidation. By this protocol the enzymatic activity resulted to be inhibited

upon interaction with DAQs. However, the indirect assay did not allow to determine the kinetic parameters of the dismutation. Direct assay using pulse radiolysis was performed in collaboration with Dr. Diane Cabelli to obtain such kinetic parameters. Data are currently under processing.

The third part was focused on the identification of which cysteine was the primary target of DAQs. Limited proteolysis did not allow to pin down the exact residue but suggested both cysteine as potentially target. More success was obtained with the cysteine mutants. The C140A, C196A and C140A/C196A mutants produced allowed using autoradiography, quinone-staining, native-PAGE, SDS-PAGE and mass spectrometry to demonstrate that cysteine 196 is the primary target.. The higher reactivity of the cysteine 196 can be expected because in the crystallographic structure of SOD2 this residue results to be exposed to the solvent in comparison with the cysteine 140, which appears to be buried in the protein fold (fig.4.1 .

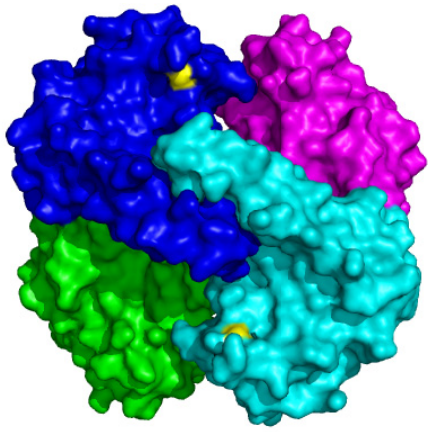

Figure 4.1. Quaternary structure of SOD2, the cysteine residue are yellow and correspond to the 196 residue of two monomers.

In agreement, Matsuda and co-workers showed that only the cysteine 196 can be titrated in the native enzyme using the method of Ellman (Matsuda et al., 1990). However, in our autoradiography experiments radioactivity was visible also in correspondence with the electrophoretic band relative to the C196A mutant thus is not possible to exclude that C140 reacts with DAQs, although with lower yield. However, since radioactivity was relievable also in the lane of C196A mutant after overexposure, it was not possible exclude that the cysteine 140 might react with DAQs in a small percentage, hence it would be a secondary target of DAQs. As an alternative, most plausible, DAQs would react with another nucleophilic residue (tyrosine, lysine or metionine) of the protein to a lesser extent as would be suggested by the presence of radioactivity also in the lane of the double cysteine mutant. Moreover, the latter possibility was demonstrated by the presence of the

+290 Dalton after the incubation of the C140A with dopamine indicating a second site of DAQs interaction different of the cysteine residue 140. In this regard, α-synuclein, which has no cysteine residues, is a DAQs target (Bisaglia et al. 2010b).

The following step was to correlate the structural modifications induced by DAQs t with the inhibition of enzymatic activity. Far-UV CD spectra displayed a decrease of the signal intensity upon the interaction with DAQs and near-UV CD spectra suggested a small change in the tertiary structure. The shift in the Trp residue(s) in the near-UV CD spectra suggest that a change on the spatial orientation of Trp residue(s) could take place. In order to correlate this structural change with the decrease of activity it is worth noting that tryptophan 161, which forms one hydrophobic side of the active site cavity, is implicated in the catalysis: mutations involving this residue induce structural changes in adjacent residues (Gln 143 and Tyr 34) involved in the hydrogen-bonded network causing a decrease of the enzymatic activity (Cabelli et al., 1999; Hearn et al., 2001). Moreover, the Trp 123 forms a hydrogen bond with the carboxamide of Gln 143 (involved in the hydrogen-bonded network), its replacement causes a decrease of catalytic activity probably due to a electrostatic effect (Greenleaf et al., 2004). Hence, a perturbation of the spatial location of tryptophan 161 or 123 in the DAQ-modified SOD2 could explain a decrease of the enzymatic activity observed in this work. In alternative, the structural change could involve other residues modifying the chemical environment of the Trp amino acids causing a change in the shift. This general perturbation would affect the hydrogen-bonded network, which is fundamental for the catalytic activity, hence the inhibition of the activity. These structural changes, however, do not alter the structure of the Mn complex, as suggested by the constant lineshape of HFEPR spectra of the protein before and after reaction with DAQs but do not exclude the possibility of an alteration affecting the hydrogen bond network. HFEPR spectra revealed a decrease of signal intensity suggesting protei precipitation. Now, we are working on the cystallization of the modified protien in order to elucidate this aspect.

Alternatively, the covalent modification would change the protein the redox potential affecting catalysis. The redox potential of SOD2 is normally 393±29mV at pH 7.8, hence is placed between that of the oxidation of superoxide to oxygen (-160mV) and the reduction of superoxide to hydrogen peroxide (+850mV), and the catalysis is thermodynamically favored (Leveque et al., 2001). Another alternative interpretation of the reduced enzymatic activity is based on the possibility that the DAQ modification could interfere sterically or electrostatically with the negatively charged superoxide affecting the binding rate of substrate to the enzyme. With this hypothesis, the activity inhibition would

result from the same effects brought about the nitration of tyrosine 34 In literature it is described that this post-translational modification inactivates the enzymatic activity of SOD2.. The crystal structure of the nitrated enzyme does not show any significant conformational changes (Quint et al., 2006), yet molecular dynamics simulations showed that the presence of the nitrated group blocks the migration of superoxide anion, due to an electrostatic and steric repulsion, increasing the free energy profile for substrate access to the metal center (Moreno et al., 2010). It would be interesting to study if tyrosine 34 nitration occurs in PD dopaminergic neurons as another possible pathway affecting the enzymatic catalysis of SOD2.

In this thesis a new perspective for the involvement of SOD2 with PD is suggested: SOD2 would be covalently modified by DAQs in mitochondria leading to a decrease of its enzymatic activity, hence an increase of superoxide anions in mitochondria. In PD mitochondria are particularly exposed to oxidative stress due to the complex I deficiency (Mann et al., 1994). The loss of function of the enzyme responsible for superoxide scavenging would exacerbate oxidative stress causing mitochondrial dysfunction, and, ultimately, the neuron cell death. To support the hypothesis of SOD2 modification by DAQs in mitochondria, one important issue is whether DAQ, that are formed in the cytosol, do enter into these organelles. Two lines of evidence support this hypothesys. One is based on the incorporation of radioactivity inside mitochondria incubated with C14-labeled DAQs demonstrated in our laboratory (Arduini et al. 2008 PhD thesis). The second is based on a proteomic study showing thatSOD2 interacts with DAQs in rat brain mitochondria incubated with C14-labelad dopamine and tyrosinase for 15 minutes (Van Laar et al., 2008; Van Laar et al., 2009). Currently we are working on a human dopaminergic cell line to demonstrate that this pathway could be possible in a cell model. Next step would be to probe the possibility to use superoxide dismutase mimetics, small molecules that mimic superoxide dismutase activity, to increase survival of cells exposed to dopamine or pesticides as model of PD. The ultimate aim is to use such molecules as a therapy to prevent or at least slow down the dopaminergic neuron loss.

Appendix 1

Nucleotic and aminoacid sequence of superoxide dismutase 2:

```
atgggcagcagccatcatcatcatcacagcagcggcctggtgccgcgcggcagccat
 M  G  S  S  H  H  H  H  H  H  S  S  G  L  V  P  R  G  S  H
atgaagcacagcctccccgacctgccctacgactacggcgccctggaacctcacatcaac
 M  K  H  S  L  P  D  L  P  Y  D  Y  G  A  L  E  P  H  I  N
gcgcagatcatgcagctgcaccacagcaagcaccacgcggcctacgtgaacaacctgaac
 A  Q  I  M  Q  L  H  H  S  K  H  H  A  A  Y  V  N  N  L  N
gtcaccgaggagaagtaccaggaggcgttggccaagggagatgttacagcccagatagct
 V  T  E  E  K  Y  Q  E  A  L  A  K  G  D  V  T  A  Q  I  A
cttcagcctgcactgaagttcaatggtggtggtcatatcaatcatagcattttctggaca
 L  Q  P  A  L  K  F  N  G  G  G  H  I  N  H  S  I  F  W  T
aacctcagccctaacggtggtggagaacccaaaggggagttgctggaagccatcaaacgt
 N  L  S  P  N  G  G  G  E  P  K  G  E  L  L  E  A  I  K  R
gactttggttcctttgacaagtttaaggagaagctgacggctgcatctgttggtgtccaa
 D  F  G  S  F  D  K  F  K  E  K  L  T  A  A  S  V  G  V  Q
ggctcaggttggggttggcttggtttcaataaggaacggggacacttacaaattgctgct
 G  S  G  W  G  W  L  G  F  N  K  E  R  G  H  L  Q  I  A  A
tgtccaaatcaggatccactgcaaggaacaacaggccttattccactgctggggattgat
 C  P  N  Q  D  P  L  Q  G  T  T  G  L  I  P  L  L  G  I  D
gtgtgggagcacgcttactaccttcagtataaaaatgtcaggcctgattatctaaaagct
 V  W  E  H  A  Y  Y  L  Q  Y  K  N  V  R  P  D  Y  L  K  A
atttggaatgtaatcaactgggagaatgtaactgaaagatacatggcttgcaaaaagtaa
 I  W  N  V  I  N  W  E  N  V  T  E  R  Y  M  A  C  K  K  -
```

The histidine tag is highlighted in red. Cys residue (140 and 196) are marked in green. In pink are depicted the 4 aminoacids, which remained after the thrombin cleaveage. In this thesis this 4 aminoacid are numbered as position -1,-2,-3,-4.

Appendix 2

1. Culture media

Luria Bertani broth (LB):

1% bacto-triptone
0,5% bacto-yeast extract
0,5% NaCl
pH 7.5 with NaOH

The culture media is sterilized by autoclaving. In order to obtain LB agar plates 1,5% of agar is added before autoclaving. Antibiotic is added if necessary (Kanamycin (sulfate) 30 mg/ml).

Super Optimal Broth (SOB):
2% bacto-triptone
0,5% bacto-yeast extract
2,5 mM KCl
10 mM MgCl2
10 mM MgSO4
10 mM glucosio
The culture media is sterilized by autoclaving.

Super Optimal broth with Catabolic repressor (SOC):
SOB with the addition of 20 mM glucose filtered 0,22µm.

2. Bacteria strains of *Escherichia coli*

DH5α
Genotype: *lac*ZΔM15, *rec*A1, *end*A1, *gyr*A96, *thi*-1, *hsd*R17(r_k -, m_k+), *sup*E44, *rel*A1, *deo*R, Δ(*lac*ZYA-*arg*F)U169.
The strain has been used for the cloning.

BL21 (DE3)
Genotype: F^-, *omp*T, *hsd*SB (r_B, m_B), *gal dcm* (DE3).
The strain has been used for the expression and purification of proteins due to the presence of lambda DE3 lysogen.

References

Abou-Sleiman, P.M., Muqit, M.M., and Wood, N.W. (2006). Expanding insights of mitochondrial dysfunction in Parkinson's disease. Nat Rev Neurosci *7*, 207-219.

Abreu, I.A., and Cabelli, D.E. (2010). Superoxide dismutases-a review of the metal-associated mechanistic variations. Biochim Biophys Acta *1804*, 263-274.

Amatore, C., and Arbault, S. (2007). Electrochemical Methods for Neuroscience (Boca raton (FL), CRC Press).

Andersen, J.K. (2004). Oxidative stress in neurodegeneration: cause or consequence? Nat Med *10 Suppl*, S18-25.

Andreassen, O.A., Ferrante, R.J., Dedeoglu, A., Albers, D.W., Klivenyi, P., Carlson, E.J., Epstein, C.J., and Beal, M.F. (2001). Mice with a partial deficiency of manganese superoxide dismutase show increased vulnerability to the mitochondrial toxins malonate, 3-nitropropionic acid, and MPTP. Exp Neurol *167*, 189-195.

Antonyuk, S.V., Strange, R.W., Marklund, S.L., and Hasnain, S.S. (2009). The structure of human extracellular copper-zinc superoxide dismutase at 1.7 A resolution: insights into heparin and collagen binding. J Mol Biol *388*, 310-326.

Arduini, I. (2008). Toxic effects of the oxidized products of the neurotransmitter dopamine on mitochondria and their implications in Parkinson disease. PhD thesis (Padova).

Asanuma, M., Miyazaki, I., and Ogawa, N. (2003). Dopamine- or L-DOPA-induced neurotoxicity: the role of dopamine quinone formation and tyrosinase in a model of Parkinson's disease. Neurotox Res *5*, 165-176.

Ascherio, A., Zhang, S.M., Hernan, M.A., Kawachi, I., Colditz, G.A., Speizer, F.E., and Willett, W.C. (2001). Prospective study of caffeine consumption and risk of Parkinson's disease in men and women. Ann Neurol *50*, 56-63.

Auluck, P.K., Caraveo, G., and Lindquist, S. (2010). alpha-Synuclein: membrane interactions and toxicity in Parkinson's disease. Annu Rev Cell Dev Biol *26*, 211-233.

Banci, L., Bertini, I., Boca, M., Girotto, S., Martinelli, M., Valentine, J.S., and Vieru, M. (2008). SOD1 and amyotrophic lateral sclerosis: mutations and oligomerization. PLoS One *3*, e1677.

Barker, J.E., Heales, S.J., Cassidy, A., Bolanos, J.P., Land, J.M., and Clark, J.B. (1996). Depletion of brain glutathione results in a decrease of glutathione reductase activity; an enzyme susceptible to oxidative damage. Brain Res *716*, 118-122.

Beck, Y., Bartfeld, D., Yavin, Z., Levanon, A., Gorecki, M., and Hartman, J.R. (1988). Efficient Production of Active Human Manganese Superoxide Dismutase in Escherichia Coli. Nature Biotechnology *6*, 930-935.

Beilina, A., Van Der Brug, M., Ahmad, R., Kesavapany, S., Miller, D.W., Petsko, G.A., and Cookson, M.R. (2005). Mutations in PTEN-induced putative kinase 1 associated with recessive parkinsonism have differential effects on protein stability. Proc Natl Acad Sci U S A *102*, 5703-5708.

Benov, L., Chang, L.Y., Day, B., and Fridovich, I. (1995). Copper, zinc superoxide dismutase in Escherichia coli: periplasmic localization. Arch Biochem Biophys *319*, 508-511.

Berg, D., Youdim, M.B., and Riederer, P. (2004). Redox imbalance. Cell Tissue Res *318*, 201-213.

Berlett, B.S., and Stadtman, E.R. (1997). Protein oxidation in aging, disease, and oxidative stress. J Biol Chem *272*, 20313-20316.

Berman, S.B., and Hastings, T.G. (1999). Dopamine oxidation alters mitochondrial respiration and induces permeability transition in brain mitochondria: implications for Parkinson's disease. J Neurochem *73*, 1127-1137.

Bisaglia, M., Mammi, S., and Bubacco, L. (2007). Kinetic and structural analysis of the early oxidation products of dopamine: analysis of the interactions with alpha-synuclein. J Biol Chem *282*, 15597-15605.

Bisaglia, M., Soriano, M.E., Arduini, I., Mammi, S., and Bubacco, L. (2010a). Molecular characterization of dopamine-derived quinones reactivity toward NADH and glutathione: implications for mitochondrial dysfunction in Parkinson disease. Biochim Biophys Acta *1802*, 699-706.

Bisaglia, M., Tosatto, L., Munari, F., Tessari, I., de Laureto, P.P., Mammi, S., and Bubacco, L. (2010b). Dopamine quinones interact with alpha-synuclein to form unstructured adducts. Biochem Biophys Res Commun *394*, 424-428.

Block, M.L., Zecca, L., and Hong, J.S. (2007). Microglia-mediated neurotoxicity: uncovering the molecular mechanisms. Nat Rev Neurosci *8*, 57-69.

Bonifati, V., Rizzu, P., van Baren, M.J., Schaap, O., Breedveld, G.J., Krieger, E., Dekker, M.C., Squitieri, F., Ibanez, P., Joosse, M.*, et al.* (2003). Mutations in the DJ-1 gene associated with autosomal recessive early-onset parkinsonism. Science *299*, 256-259.

Borgstahl, G.E., Parge, H.E., Hickey, M.J., Beyer, W.F., Jr., Hallewell, R.A., and Tainer, J.A. (1992). The structure of human mitochondrial manganese superoxide dismutase reveals a novel tetrameric interface of two 4-helix bundles. Cell *71*, 107-118.

Borgstahl, G.E., Parge, H.E., Hickey, M.J., Johnson, M.J., Boissinot, M., Hallewell, R.A., Lepock, J.R., Cabelli, D.E., and Tainer, J.A. (1996). Human mitochondrial manganese superoxide dismutase polymorphic variant Ile58Thr

reduces activity by destabilizing the tetrameric interface. Biochemistry *35*, 4287-4297.

Braak, H., Ghebremedhin, E., Rub, U., Bratzke, H., and Del Tredici, K. (2004). Stages in the development of Parkinson's disease-related pathology. Cell Tissue Res *318*, 121-134.

Bull, C., Niederhoffer, E.C., Yoshida, T., and Fee, J.A. (1991). Kinetic studies of superoxide dismutases: properties of the manganese-containing protein from Thermus thermophilus. Journal of the American Chemical Society *113*, 4069-4076

Cabelli, D.E., Guan, Y., Leveque, V., Hearn, A.S., Tainer, J.A., Nick, H.S., and Silverman, D.N. (1999). Role of tryptophan 161 in catalysis by human manganese superoxide dismutase. Biochemistry *38*, 11686-11692.

Canet-Aviles, R.M., Wilson, M.A., Miller, D.W., Ahmad, R., McLendon, C., Bandyopadhyay, S., Baptista, M.J., Ringe, D., Petsko, G.A., and Cookson, M.R. (2004). The Parkinson's disease protein DJ-1 is neuroprotective due to cysteine-sulfinic acid-driven mitochondrial localization. Proc Natl Acad Sci U S A *101*, 9103-9108.

Carlioz, A., Ludwig, M.L., Stallings, W.C., Fee, J.A., Steinman, H.M., and Touati, D. (1988). Iron superoxide dismutase. Nucleotide sequence of the gene from Escherichia coli K12 and correlations with crystal structures. J Biol Chem *263*, 1555-1562.

Chaudhuri, K.R., Healy, D.G., and Schapira, A.H. (2006). Non-motor symptoms of Parkinson's disease: diagnosis and management. Lancet Neurol *5*, 235-245.

Cooke, M.S., Evans, M.D., Dizdaroglu, M., and Lunec, J. (2003). Oxidative DNA damage: mechanisms, mutation, and disease. FASEB J *17*, 1195-1214.

Cookson, M.R. (2010). DJ-1, PINK1, and their effects on mitochondrial pathways. Mov Disord *25 Suppl 1*, S44-48.

Cookson, M.R., and Bandmann, O. (2010). Parkinson's disease: insights from pathways. Hum Mol Genet *19*, R21-27.

Costa, J., Lunet, N., Santos, C., Santos, J., and Vaz-Carneiro, A. (2010). Caffeine exposure and the risk of Parkinson's disease: a systematic review and meta-analysis of observational studies. J Alzheimers Dis *20 Suppl 1*, S221-238.

Crapo, J.D., McCord, J.M., and Fridovich, I. (1978). Preparation and assay of superoxide dismutases. Methods Enzymol *53*, 382-393.

Dale Purves, G.J.A., David Fitzpatrick, Lawrence C Katz, Anthony-Samuel LaMantia, James O McNamara, and S Mark Williams. (2001). Neuroscience (Sinauer Associates).

Danielson, S.R., and Andersen, J.K. (2008). Oxidative and nitrative protein modifications in Parkinson's disease. Free Radic Biol Med *44*, 1787-1794.

Dauer, W., and Przedborski, S. (2003). Parkinson's disease: mechanisms and models. Neuron *39*, 889-909.

Dawson, T.M., and Dawson, V.L. (2003). Molecular pathways of neurodegeneration in Parkinson's disease. Science *302*, 819-822.

Di Fonzo, A., Chien, H.F., Socal, M., Giraudo, S., Tassorelli, C., Iliceto, G., Fabbrini, G., Marconi, R., Fincati, E., Abbruzzese, G.*, et al.* (2007). ATP13A2 missense mutations in juvenile parkinsonism and young onset Parkinson disease. Neurology *68*, 1557-1562.

Eric R. Kandel, J.H.S., Thomas M. Jessell (2000). Principles of Neural Science, Fourth Edition edn (The McGraw-Hill Companies, Inc).

Ermak, G., and Davies, K.J. (2002). Calcium and oxidative stress: from cell signaling to cell death. Mol Immunol *38*, 713-721.

Farin, F.M., Hitosis, Y., Hallagan, S.E., Kushleika, J., Woods, J.S., Janssen, P.S., Smith-Weller, T., Franklin, G.M., Swanson, P.D., and Checkoway, H. (2001). Genetic polymorphisms of superoxide dismutase in Parkinson's disease. Mov Disord *16*, 705-707.

Farrer, M.J. (2006). Genetics of Parkinson disease: paradigm shifts and future prospects. Nat Rev Genet *7*, 306-318.

Funayama, M., Hasegawa, K., Kowa, H., Saito, M., Tsuji, S., and Obata, F. (2002). A new locus for Parkinson's disease (PARK8) maps to chromosome 12p11.2-q13.1. Ann Neurol *51*, 296-301.

Gasser, T., Muller-Myhsok, B., Wszolek, Z.K., Oehlmann, R., Calne, D.B., Bonifati, V., Bereznai, B., Fabrizio, E., Vieregge, P., and Horstmann, R.D. (1998). A susceptibility locus for Parkinson's disease maps to chromosome 2p13. Nat Genet *18*, 262-265.

Goedert, M. (2001). Alpha-synuclein and neurodegenerative diseases. Nat Rev Neurosci *2*, 492-501.

Graham, D.G. (1978). Oxidative pathways for catecholamines in the genesis of neuromelanin and cytotoxic quinones. Mol Pharmacol *14*, 633-643.

Grasbon-Frodl, E.M., Kosel, S., Riess, O., Muller, U., Mehraein, P., and Graeber, M.B. (1999). Analysis of mitochondrial targeting sequence and coding region polymorphisms of the manganese superoxide dismutase gene in German Parkinson disease patients. Biochem Biophys Res Commun *255*, 749-752.

Greenamyre, J.T., Sherer, T.B., Betarbet, R., and Panov, A.V. (2001). Complex I and Parkinson's disease. IUBMB Life *52*, 135-141.

Greenleaf, W.B., Perry, J.J., Hearn, A.S., Cabelli, D.E., Lepock, J.R., Stroupe, M.E., Tainer, J.A., Nick, H.S., and Silverman, D.N. (2004). Role of hydrogen bonding in the active site of human manganese superoxide dismutase. Biochemistry *43*, 7038-7045.

Gros-Louis, F., Gaspar, C., and Rouleau, G.A. (2006). Genetics of familial and sporadic amyotrophic lateral sclerosis. Biochim Biophys Acta *1762*, 956-972.

Hastings, T.G. (1995). Enzymatic oxidation of dopamine: the role of prostaglandin H synthase. J Neurochem *64*, 919-924.

Hastings, T.G. (2009). The role of dopamine oxidation in mitochondrial dysfunction: implications for Parkinson's disease. J Bioenerg Biomembr *41*, 469-472.

Healy, D.G., Abou-Sleiman, P.M., and Wood, N.W. (2004). Genetic causes of Parkinson's disease: UCHL-1. Cell Tissue Res *318*, 189-194.

Hearn, A.S., Stroupe, M.E., Cabelli, D.E., Lepock, J.R., Tainer, J.A., Nick, H.S., and Silverman, D.N. (2001). Kinetic analysis of product inhibition in human manganese superoxide dismutase. Biochemistry *40*, 12051-12058.

Henchcliffe, C., and Beal, M.F. (2008). Mitochondrial biology and oxidative stress in Parkinson disease pathogenesis. Nat Clin Pract Neurol *4*, 600-609.

Hicks, A.A., Petursson, H., Jonsson, T., Stefansson, H., Johannsdottir, H.S., Sainz, J., Frigge, M.L., Kong, A., Gulcher, J.R., Stefansson, K.*, et al.* (2002). A susceptibility gene for late-onset idiopathic Parkinson's disease. Ann Neurol *52*, 549-555.

Hirsch, E.C., and Hunot, S. (2009). Neuroinflammation in Parkinson's disease: a target for neuroprotection? Lancet Neurol *8*, 382-397.

Hsu, J.L., Hsieh, Y., Tu, C., O'Connor, D., Nick, H.S., and Silverman, D.N. (1996). Catalytic properties of human manganese superoxide dismutase. J Biol Chem *271*, 17687-17691.

Hutter, C.M., Samii, A., Factor, S.A., Nutt, J.G., Higgins, D.S., Bird, T.D., Griffith, A., Roberts, J.W., Leis, B.C., Montimurro, J.S.*, et al.* (2008). Lack of evidence for an association between UCHL1 S18Y and Parkinson's disease. Eur J Neurol *15*, 134-139.

Ischiropoulos, H., and Beckman, J.S. (2003). Oxidative stress and nitration in neurodegeneration: cause, effect, or association? J Clin Invest *111*, 163-169.

Jenner, P. (2003). Oxidative stress in Parkinson's disease. Ann Neurol *53 Suppl 3*, S26-36; discussion S36-28.

Keyhani, E., and Keyhani, J. (2006). Comparative study of superoxide dismutase activity assays in Crocus sativus L. corms. Prikl Biokhim Mikrobiol *42*, 111-116.

Kim, Y., Park, J., Kim, S., Song, S., Kwon, S.K., Lee, S.H., Kitada, T., Kim, J.M., and Chung, J. (2008). PINK1 controls mitochondrial localization of Parkin through direct phosphorylation. Biochem Biophys Res Commun *377*, 975-980.

Kitada, T., Asakawa, S., Hattori, N., Matsumine, H., Yamamura, Y., Minoshima, S., Yokochi, M., Mizuno, Y., and Shimizu, N. (1998). Mutations in the parkin gene cause autosomal recessive juvenile parkinsonism. Nature *392*, 605-608.

Klivenyi, P., St Clair, D., Wermer, M., Yen, H.C., Oberley, T., Yang, L., and Flint Beal, M. (1998). Manganese superoxide dismutase overexpression attenuates MPTP toxicity. Neurobiol Dis *5*, 253-258.

Klug, D., Rabani, J., and Fridovich, I. (1972). A direct demonstration of the catalytic action of superoxide dismutase through the use of pulse radiolysis. J Biol Chem *247*, 4839-4842.

Kopin, I.J. (1987). MPTP: an industrial chemical and contaminant of illicit narcotics stimulates a new era in research on Parkinson's disease. Environ Health Perspect *75*, 45-51.

Kruger, R., Kuhn, W., Muller, T., Woitalla, D., Graeber, M., Kosel, S., Przuntek, H., Epplen, J.T., Schols, L., and Riess, O. (1998). Ala30Pro mutation in the gene encoding alpha-synuclein in Parkinson's disease. Nat Genet *18*, 106-108.

Kuhn, D.M., Arthur, R.E., Jr., Thomas, D.M., and Elferink, L.A. (1999). Tyrosine hydroxylase is inactivated by catechol-quinones and converted to a redox-cycling quinoprotein: possible relevance to Parkinson's disease. J Neurochem *73*, 1309-1317.

Latourelle, J.C., Sun, M., Lew, M.F., Suchowersky, O., Klein, C., Golbe, L.I., Mark, M.H., Growdon, J.H., Wooten, G.F., Watts, R.L.*, et al.* (2008). The Gly2019Ser mutation in LRRK2 is not fully penetrant in familial Parkinson's disease: the GenePD study. BMC Med *6*, 32.

Lautier, C., Goldwurm, S., Durr, A., Giovannone, B., Tsiaras, W.G., Pezzoli, G., Brice, A., and Smith, R.J. (2008). Mutations in the GIGYF2 (TNRC15) gene at the PARK11 locus in familial Parkinson disease. Am J Hum Genet *82*, 822-833.

LaVoie, M.J., and Hastings, T.G. (1999). Peroxynitrite- and nitrite-induced oxidation of dopamine: implications for nitric oxide in dopaminergic cell loss. J Neurochem *73*, 2546-2554.

LaVoie, M.J., Ostaszewski, B.L., Weihofen, A., Schlossmacher, M.G., and Selkoe, D.J. (2005). Dopamine covalently modifies and functionally inactivates parkin. Nat Med *11*, 1214-1221.

Lebovitz, R.M., Zhang, H., Vogel, H., Cartwright, J., Jr., Dionne, L., Lu, N., Huang, S., and Matzuk, M.M. (1996). Neurodegeneration, myocardial injury, and perinatal death in mitochondrial superoxide dismutase-deficient mice. Proc Natl Acad Sci U S A *93*, 9782-9787.

Lees, A.J. (2009). The Parkinson chimera. Neurology *72*, S2-11.

Leroy, E., Boyer, R., Auburger, G., Leube, B., Ulm, G., Mezey, E., Harta, G., Brownstein, M.J., Jonnalagada, S., Chernova, T.*, et al.* (1998). The ubiquitin pathway in Parkinson's disease. Nature *395*, 451-452.

Lev, N., Roncevic, D., Ickowicz, D., Melamed, E., and Offen, D. (2006). Role of DJ-1 in Parkinson's disease. J Mol Neurosci *29*, 215-225.

Leveque, V.J., Vance, C.K., Nick, H.S., and Silverman, D.N. (2001). Redox properties of human manganese superoxide dismutase and active-site mutants. Biochemistry *40*, 10586-10591.

Li, Y., Huang, T.T., Carlson, E.J., Melov, S., Ursell, P.C., Olson, J.L., Noble, L.J., Yoshimura, M.P., Berger, C., Chan, P.H.*, et al.* (1995). Dilated cardiomyopathy and neonatal lethality in mutant mice lacking manganese superoxide dismutase. Nat Genet *11*, 376-381.

Lincoln, S., Vaughan, J., Wood, N., Baker, M., Adamson, J., Gwinn-Hardy, K., Lynch, T., Hardy, J., and Farrer, M. (1999). Low frequency of pathogenic mutations in the ubiquitin carboxy-terminal hydrolase gene in familial Parkinson's disease. Neuroreport *10*, 427-429.

Lotharius, J., and Brundin, P. (2002). Pathogenesis of Parkinson's disease: dopamine, vesicles and alpha-synuclein. Nat Rev Neurosci *3*, 932-942.

Luoma, P., Melberg, A., Rinne, J.O., Kaukonen, J.A., Nupponen, N.N., Chalmers, R.M., Oldfors, A., Rautakorpi, I., Peltonen, L., Majamaa, K.*, et al.* (2004). Parkinsonism, premature menopause, and mitochondrial DNA polymerase gamma mutations: clinical and molecular genetic study. Lancet *364*, 875-882.

Mann, V.M., Cooper, J.M., Daniel, S.E., Srai, K., Jenner, P., Marsden, C.D., and Schapira, A.H. (1994). Complex I, iron, and ferritin in Parkinson's disease substantia nigra. Ann Neurol *36*, 876-881.

Marklund, S. (1976). Spectrophotometric study of spontaneous disproportionation of superoxide anion radical and sensitive direct assay for superoxide dismutase. J Biol Chem *251*, 7504-7507.

Marklund, S.L., Holme, E., and Hellner, L. (1982). Superoxide dismutase in extracellular fluids. Clin Chim Acta *126*, 41-51.

Marttila, R.J., Lorentz, H., and Rinne, U.K. (1988). Oxygen toxicity protecting enzymes in Parkinson's disease. Increase of superoxide dismutase-like activity in the substantia nigra and basal nucleus. J Neurol Sci *86*, 321-331.

Mata, I.F., Wedemeyer, W.J., Farrer, M.J., Taylor, J.P., and Gallo, K.A. (2006). LRRK2 in Parkinson's disease: protein domains and functional insights. Trends Neurosci *29*, 286-293.

Matsuda, Y., Higashiyama, S., Kijima, Y., Suzuki, K., Kawano, K., Akiyama, M., Kawata, S., Tarui, S., Deutsch, H.F., and Taniguchi, N. (1990). Human liver manganese superoxide dismutase. Purification and crystallization, subunit association and sulfhydryl reactivity. Eur J Biochem *194*, 713-720.

McGeer, P.L., Itagaki, S., Boyes, B.E., and McGeer, E.G. (1988). Reactive microglia are positive for HLA-DR in the substantia nigra of Parkinson's and Alzheimer's disease brains. Neurology *38*, 1285-1291.

Misra, H.P., and Fridovich, I. (1972). The role of superoxide anion in the autoxidation of epinephrine and a simple assay for superoxide dismutase. J Biol Chem *247*, 3170-3175.

Misra, H.P., and Fridovich, I. (1977). Superoxide dismutase: a photochemical augmentation assay. Arch Biochem Biophys *181*, 308-312.

Moreno, D.M., Marti, M.A., De Biase, P.M., Estrin, D.A., Demicheli, V., Radi, R., and Boechi, L. (2010). Exploring the molecular basis of human manganese superoxide dismutase inactivation mediated by tyrosine 34 nitration. Arch Biochem Biophys.

Nagakubo, D., Taira, T., Kitaura, H., Ikeda, M., Tamai, K., Iguchi-Ariga, S.M., and Ariga, H. (1997). DJ-1, a novel oncogene which transforms mouse NIH3T3 cells in cooperation with ras. Biochem Biophys Res Commun *231*, 509-513.

Navarro, A., and Boveris, A. (2009). Brain mitochondrial dysfunction and oxidative damage in Parkinson's disease. J Bioenerg Biomembr *41*, 517-521.

Nuti, A., Ceravolo, R., Dell'Agnello, G., Gambaccini, G., Bellini, G., Kiferle, L., Rossi, C., Logi, C., and Bonuccelli, U. (2004). Environmental factors and Parkinson's disease: a case-control study in the Tuscany region of Italy. Parkinsonism Relat Disord *10*, 481-485.

Obeso, J.A., Rodriguez-Oroz, M.C., Goetz, C.G., Marin, C., Kordower, J.H., Rodriguez, M., Hirsch, E.C., Farrer, M., Schapira, A.H., and Halliday, G. (2010). Missing pieces in the Parkinson's disease puzzle. Nat Med *16*, 653-661.

Olsen, D.A., Petersen, S.V., Oury, T.D., Valnickova, Z., Thogersen, I.B., Kristensen, T., Bowler, R.P., Crapo, J.D., and Enghild, J.J. (2004). The intracellular proteolytic processing of extracellular superoxide dismutase (EC-SOD) is a two-step event. J Biol Chem *279*, 22152-22157.

Olzmann, J.A., Brown, K., Wilkinson, K.D., Rees, H.D., Huai, Q., Ke, H., Levey, A.I., Li, L., and Chin, L.S. (2004). Familial Parkinson's disease-associated L166P mutation disrupts DJ-1 protein folding and function. J Biol Chem *279*, 8506-8515.

Oury, T.D., Chang, L.Y., Marklund, S.L., Day, B.J., and Crapo, J.D. (1994). Immunocytochemical localization of extracellular superoxide dismutase in human lung. Lab Invest *70*, 889-898.

Pace, C.N., Vajdos, F., Fee, L., Grimsley, G., and Gray, T. (1995). How to measure and predict the molar absorption coefficient of a protein. Protein Sci *4*, 2411-2423.

Paisan-Ruiz, C., Jain, S., Evans, E.W., Gilks, W.P., Simon, J., van der Brug, M., Lopez de Munain, A., Aparicio, S., Gil, A.M., Khan, N.*, et al.* (2004). Cloning of the gene containing mutations that cause PARK8-linked Parkinson's disease. Neuron *44*, 595-600.

Pankratz, N., Nichols, W.C., Uniacke, S.K., Halter, C., Murrell, J., Rudolph, A., Shults, C.W., Conneally, P.M., and Foroud, T. (2003a). Genome-wide linkage

analysis and evidence of gene-by-gene interactions in a sample of 362 multiplex Parkinson disease families. Hum Mol Genet *12*, 2599-2608.

Pankratz, N., Nichols, W.C., Uniacke, S.K., Halter, C., Rudolph, A., Shults, C., Conneally, P.M., and Foroud, T. (2003b). Significant linkage of Parkinson disease to chromosome 2q36-37. Am J Hum Genet *72*, 1053-1057.

Parker, M.W., and Blake, C.C. (1988). Iron- and manganese-containing superoxide dismutases can be distinguished by analysis of their primary structures. FEBS Lett *229*, 377-382.

Parkinson, J. (1817). An Essay on the Shaking Palsy, Vol London:
Neely & Jones (Sherwood).

Paz, M.A., Fluckiger, R., Boak, A., Kagan, H.M., and Gallop, P.M. (1991). Specific detection of quinoproteins by redox-cycling staining. J Biol Chem *266*, 689-692.

Perry, J.J., Shin, D.S., Getzoff, E.D., and Tainer, J.A. (2010). The structural biochemistry of the superoxide dismutases. Biochim Biophys Acta *1804*, 245-262.

Petersen, S.V., Oury, T.D., Valnickova, Z., Thogersen, I.B., Hojrup, P., Crapo, J.D., and Enghild, J.J. (2003). The dual nature of human extracellular superoxide dismutase: one sequence and two structures. Proc Natl Acad Sci U S A *100*, 13875-13880.

Petersen, S.V., Valnickova, Z., Oury, T.D., Crapo, J.D., Chr Nielsen, N., and Enghild, J.J. (2007). The subunit composition of human extracellular superoxide dismutase (EC-SOD) regulates enzymatic activity. BMC Biochem *8*, 19.

Poirier, J., Dea, D., Baccichet, A., and Thiffault, C. (1994). Superoxide dismutase expression in Parkinson's disease. Ann N Y Acad Sci *738*, 116-120.

Polymeropoulos, M.H., Lavedan, C., Leroy, E., Ide, S.E., Dehejia, A., Dutra, A., Pike, B., Root, H., Rubenstein, J., Boyer, R.*, et al.* (1997). Mutation in the alpha-synuclein gene identified in families with Parkinson's disease. Science *276*, 2045-2047.

Powers, K.M., Kay, D.M., Factor, S.A., Zabetian, C.P., Higgins, D.S., Samii, A., Nutt, J.G., Griffith, A., Leis, B., Roberts, J.W.*, et al.* (2008). Combined effects of smoking, coffee, and NSAIDs on Parkinson's disease risk. Mov Disord *23*, 88-95.

Puget, K., and Michelson, A.M. (1976). Oxidation of luminol by the xanthine oxidase system in presence of carbonate anions. Photochem Photobiol *24*, 499-501.

Quint, P., Reutzel, R., Mikulski, R., McKenna, R., and Silverman, D.N. (2006). Crystal structure of nitrated human manganese superoxide dismutase: mechanism of inactivation. Free Radic Biol Med *40*, 453-458.

Ragland, M., Hutter, C., Zabetian, C., and Edwards, K. (2009). Association between the ubiquitin carboxyl-terminal esterase L1 gene (UCHL1) S18Y variant

and Parkinson's Disease: a HuGE review and meta-analysis. Am J Epidemiol *170*, 1344-1357.

Reynolds, M.R., Berry, R.W., and Binder, L.I. (2007). Nitration in neurodegeneration: deciphering the "Hows" "nYs". Biochemistry *46*, 7325-7336.

Ritz, B., Ascherio, A., Checkoway, H., Marder, K.S., Nelson, L.M., Rocca, W.A., Ross, G.W., Strickland, D., Van Den Eeden, S.K., and Gorell, J. (2007). Pooled analysis of tobacco use and risk of Parkinson disease. Arch Neurol *64*, 990-997.

Robinson, P.A. (2008). Protein stability and aggregation in Parkinson's disease. Biochem J *413*, 1-13.

Rosenberg, A.H., Lade, B.N., Chui, D.S., Lin, S.W., Dunn, J.J., and Studier, F.W. (1987). Vectors for selective expression of cloned DNAs by T7 RNA polymerase. Gene *56*, 125-135.

Ross, G.W., Abbott, R.D., Petrovitch, H., Morens, D.M., Grandinetti, A., Tung, K.H., Tanner, C.M., Masaki, K.H., Blanchette, P.L., Curb, J.D.*, et al.* (2000). Association of coffee and caffeine intake with the risk of Parkinson disease. JAMA *283*, 2674-2679.

Ross, O.A., Soto, A.I., Vilarino-Guell, C., Heckman, M.G., Diehl, N.N., Hulihan, M.M., Aasly, J.O., Sando, S., Gibson, J.M., Lynch, T.*, et al.* (2008). Genetic variation of Omi/HtrA2 and Parkinson's disease. Parkinsonism Relat Disord *14*, 539-543.

Saggu, H., Cooksey, J., Dexter, D., Wells, F.R., Lees, A., Jenner, P., and Marsden, C.D. (1989). A selective increase in particulate superoxide dismutase activity in parkinsonian substantia nigra. J Neurochem *53*, 692-697.

Schapira, A.H. (2008). Mitochondria in the aetiology and pathogenesis of Parkinson's disease. Lancet Neurol *7*, 97-109.

Schapira, A.H. (2009). Neurobiology and treatment of Parkinson's disease. Trends Pharmacol Sci *30*, 41-47.

Schapira, A.H., Cooper, J.M., Dexter, D., Clark, J.B., Jenner, P., and Marsden, C.D. (1990). Mitochondrial complex I deficiency in Parkinson's disease. J Neurochem *54*, 823-827.

Schapira, A.H., Cooper, J.M., Dexter, D., Jenner, P., Clark, J.B., and Marsden, C.D. (1989). Mitochondrial complex I deficiency in Parkinson's disease. Lancet *1*, 1269.

Shaw, B.F., and Valentine, J.S. (2007). How do ALS-associated mutations in superoxide dismutase 1 promote aggregation of the protein? Trends Biochem Sci *32*, 78-85.

Shen, J., and Cookson, M.R. (2004). Mitochondria and dopamine: new insights into recessive parkinsonism. Neuron *43*, 301-304.

Shendelman, S., Jonason, A., Martinat, C., Leete, T., and Abeliovich, A. (2004). DJ-1 is a redox-dependent molecular chaperone that inhibits alpha-synuclein aggregate formation. PLoS Biol *2*, e362.

Shimoda-Matsubayashi, S., Hattori, T., Matsumine, H., Shinohara, A., Yoritaka, A., Mori, H., Kondo, T., Chiba, M., and Mizuno, Y. (1997). Mn SOD activity and protein in a patient with chromosome 6-linked autosomal recessive parkinsonism in comparison with Parkinson's disease and control. Neurology *49*, 1257-1262.

Shimoda-Matsubayashi, S., Matsumine, H., Kobayashi, T., Nakagawa-Hattori, Y., Shimizu, Y., and Mizuno, Y. (1996). Structural dimorphism in the mitochondrial targeting sequence in the human manganese superoxide dismutase gene. A predictive evidence for conformational change to influence mitochondrial transport and a study of allelic association in Parkinson's disease. Biochem Biophys Res Commun *226*, 561-565.

Shimura, H., Hattori, N., Kubo, S., Mizuno, Y., Asakawa, S., Minoshima, S., Shimizu, N., Iwai, K., Chiba, T., Tanaka, K.*, et al.* (2000). Familial Parkinson disease gene product, parkin, is a ubiquitin-protein ligase. Nat Genet *25*, 302-305.

Shin, J.H., Dawson, V.L., and Dawson, T.M. (2009). SnapShot: pathogenesis of Parkinson's disease. Cell *139*, 440 e441-442.

Shults, C.W. (2006). Lewy bodies. Proc Natl Acad Sci U S A *103*, 1661-1668.

Smeyne, R.J., and Jackson-Lewis, V. (2005). The MPTP model of Parkinson's disease. Brain Res Mol Brain Res *134*, 57-66.

Spillantini, M.G., Schmidt, M.L., Lee, V.M., Trojanowski, J.Q., Jakes, R., and Goedert, M. (1997). Alpha-synuclein in Lewy bodies. Nature *388*, 839-840.

Strauss, K.M., Martins, L.M., Plun-Favreau, H., Marx, F.P., Kautzmann, S., Berg, D., Gasser, T., Wszolek, Z., Muller, T., Bornemann, A.*, et al.* (2005). Loss of function mutations in the gene encoding Omi/HtrA2 in Parkinson's disease. Hum Mol Genet *14*, 2099-2111.

Studier, F.W., and Moffatt, B.A. (1986). Use of bacteriophage T7 RNA polymerase to direct selective high-level expression of cloned genes. J Mol Biol *189*, 113-130.

Studier, F.W., Rosenberg, A.H., Dunn, J.J., and Dubendorff, J.W. (1990). Use of T7 RNA polymerase to direct expression of cloned genes. Methods Enzymol *185*, 60-89.

Sulzer, D., and Zecca, L. (2000). Intraneuronal dopamine-quinone synthesis: a review. Neurotox Res *1*, 181-195.

Sutton, A., Khoury, H., Prip-Buus, C., Cepanec, C., Pessayre, D., and Degoul, F. (2003). The Ala16Val genetic dimorphism modulates the import of human manganese superoxide dismutase into rat liver mitochondria. Pharmacogenetics *13*, 145-157.

Tabares, L.C., Gatjens, J., and Un, S. (2010). Understanding the influence of the protein environment on the Mn(II) centers in Superoxide Dismutases using High-Field Electron Paramagnetic Resonance. Biochim Biophys Acta *1804*, 308-317.

Takeda, Y., and Avila, H. (1986). Structure and gene expression of the *E. coli* Mn-superoxide dismutase gene. Nucleic Acids Res *14*, 4577-4589.

Tanaka, K., Suzuki, T., Hattori, N., and Mizuno, Y. (2004). Ubiquitin, proteasome and parkin. Biochim Biophys Acta *1695*, 235-247.

Thomas, B., and Beal, M.F. (2007). Parkinson's disease. Hum Mol Genet *16 Spec No. 2*, R183-194.

Ton, T.G., Heckbert, S.R., Longstreth, W.T., Jr., Rossing, M.A., Kukull, W.A., Franklin, G.M., Swanson, P.D., Smith-Weller, T., and Checkoway, H. (2006). Nonsteroidal anti-inflammatory drugs and risk of Parkinson's disease. Mov Disord *21*, 964-969.

Tsang, A.H., and Chung, K.K. (2009). Oxidative and nitrosative stress in Parkinson's disease. Biochim Biophys Acta *1792*, 643-650.

Tse, D.C., McCreery, R.L., and Adams, R.N. (1976). Potential oxidative pathways of brain catecholamines. J Med Chem *19*, 37-40.

Valente, E.M., Abou-Sleiman, P.M., Caputo, V., Muqit, M.M., Harvey, K., Gispert, S., Ali, Z., Del Turco, D., Bentivoglio, A.R., Healy, D.G.*, et al.* (2004). Hereditary early-onset Parkinson's disease caused by mutations in PINK1. Science *304*, 1158-1160.

Valentine, J.S., Doucette, P.A., and Zittin Potter, S. (2005). Copper-zinc superoxide dismutase and amyotrophic lateral sclerosis. Annu Rev Biochem *74*, 563-593.

Vallone, D., Picetti, R., and Borrelli, E. (2000). Structure and function of dopamine receptors. Neurosci Biobehav Rev *24*, 125-132.

Van Laar, V.S., Dukes, A.A., Cascio, M., and Hastings, T.G. (2008). Proteomic analysis of rat brain mitochondria following exposure to dopamine quinone: implications for Parkinson disease. Neurobiol Dis *29*, 477-489.

Van Laar, V.S., Mishizen, A.J., Cascio, M., and Hastings, T.G. (2009). Proteomic identification of dopamine-conjugated proteins from isolated rat brain mitochondria and SH-SY5Y cells. Neurobiol Dis *34*, 487-500.

Vilarino-Guell, C., Soto, A.I., Lincoln, S.J., Ben Yahmed, S., Kefi, M., Heckman, M.G., Hulihan, M.M., Chai, H., Diehl, N.N., Amouri, R.*, et al.* (2009). ATP13A2 variability in Parkinson disease. Hum Mutat *30*, 406-410.

Wahner, A.D., Bronstein, J.M., Bordelon, Y.M., and Ritz, B. (2007). Nonsteroidal anti-inflammatory drugs may protect against Parkinson disease. Neurology *69*, 1836-1842.

Weihofen, A., Ostaszewski, B., Minami, Y., and Selkoe, D.J. (2008). Pink1 Parkinson mutations, the Cdc37/Hsp90 chaperones and Parkin all influence the maturation or subcellular distribution of Pink1. Hum Mol Genet *17*, 602-616.

Whitton, P.S. (2007). Inflammation as a causative factor in the aetiology of Parkinson's disease. Br J Pharmacol *150*, 963-976.

Wispe, J.R., Clark, J.C., Burhans, M.S., Kropp, K.E., Korfhagen, T.R., and Whitsett, J.A. (1989). Synthesis and processing of the precursor for human mangano-superoxide dismutase. Biochim Biophys Acta *994*, 30-36.

Xie, W., Wan, O.W., and Chung, K.K. (2010). New insights into the role of mitochondrial dysfunction and protein aggregation in Parkinson's disease. Biochim Biophys Acta *1802*, 935-941.

Xu, Y., Stokes, A.H., Roskoski, R., Jr., and Vrana, K.E. (1998). Dopamine, in the presence of tyrosinase, covalently modifies and inactivates tyrosine hydroxylase. J Neurosci Res *54*, 691-697.

Yang, Y.X., Wood, N.W., and Latchman, D.S. (2009). Molecular basis of Parkinson's disease. Neuroreport *20*, 150-156.

Zarranz, J.J., Alegre, J., Gomez-Esteban, J.C., Lezcano, E., Ros, R., Ampuero, I., Vidal, L., Hoenicka, J., Rodriguez, O., Atares, B.*, et al.* (2004). The new mutation, E46K, of alpha-synuclein causes Parkinson and Lewy body dementia. Ann Neurol *55*, 164-173.

Zecca, L., Zucca, F.A., Albertini, A., Rizzio, E., and Fariello, R.G. (2006). A proposed dual role of neuromelanin in the pathogenesis of Parkinson's disease. Neurology *67*, S8-11.

Zelko, I.N., Mariani, T.J., and Folz, R.J. (2002). Superoxide dismutase multigene family: a comparison of the CuZn-SOD (SOD1), Mn-SOD (SOD2), and EC-SOD (SOD3) gene structures, evolution, and expression. Free Radic Biol Med *33*, 337-349.

Zimprich, A., Biskup, S., Leitner, P., Lichtner, P., Farrer, M., Lincoln, S., Kachergus, J., Hulihan, M., Uitti, R.J., Calne, D.B.*, et al.* (2004). Mutations in LRRK2 cause autosomal-dominant parkinsonism with pleomorphic pathology. Neuron *44*, 601-607.

Zucca, F.A., Giaveri, G., Gallorini, M., Albertini, A., Toscani, M., Pezzoli, G., Lucius, R., Wilms, H., Sulzer, D., Ito, S.*, et al.* (2004). The neuromelanin of human substantia nigra: physiological and pathogenic aspects. Pigment Cell Res *17*, 610-617.